7

Oblique Incidence

7.1 Oblique Incidence and Snel's Laws

With some redefinitions, the formalism of transfer matrices and wave impedances for normal incidence translates almost verbatim to the case of oblique incidence.

By separating the fields into *transverse* and longitudinal components with respect to the direction the dielectrics are stacked (the z-direction), we show that the transverse components satisfy the identical transfer matrix relationships as in the case of normal incidence, provided we replace the media impedances η by the *transverse impedances* η_T defined below.

Fig. 7.1.1 depicts plane waves incident from both sides onto a planar interface separating two media ϵ, ϵ'. Both cases of parallel and perpendicular polarizations are shown.

In *parallel* polarization, also known as p-polarization, π-polarization, or TM polarization, the electric fields lie *on the plane* of incidence and the magnetic fields are

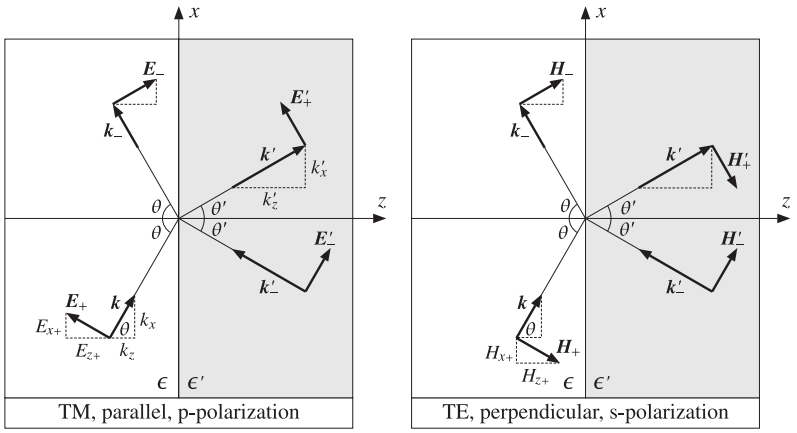

Fig. 7.1.1 Oblique incidence for TM- and TE-polarized waves.

perpendicular to that plane (along the y-direction) and *transverse* to the z-direction.

In *perpendicular* polarization, also known as s-polarization,[†] σ-polarization, or TE polarization, the electric fields are perpendicular to the plane of incidence (along the y-direction) and *transverse* to the z-direction, and the magnetic fields lie on that plane.

The figure shows the angles of incidence and reflection to be the same on either side. This is Snel's law[†] of reflection and is a consequence of the boundary conditions.

The figure also implies that the two planes of incidence and two planes of reflection all coincide with the xz-plane. This is also a consequence of the boundary conditions.

Starting with arbitrary wavevectors $\boldsymbol{k}_\pm = \hat{\mathbf{x}}\, k_{x\pm} + \hat{\mathbf{y}}\, k_{y\pm} + \hat{\mathbf{z}}\, k_{z\pm}$ and similarly for $\boldsymbol{k}'_\pm$, the incident and reflected electric fields at the two sides will have the general forms:

$$\boldsymbol{E}_+ e^{-j\boldsymbol{k}_+\cdot\boldsymbol{r}}, \quad \boldsymbol{E}_- e^{-j\boldsymbol{k}_-\cdot\boldsymbol{r}}, \quad \boldsymbol{E}'_+ e^{-j\boldsymbol{k}'_+\cdot\boldsymbol{r}}, \quad \boldsymbol{E}'_- e^{-j\boldsymbol{k}'_-\cdot\boldsymbol{r}}$$

The boundary conditions state that the net *transverse* (tangential) component of the electric field must be continuous across the interface. Assuming that the interface is at $z = 0$, we can write this condition in a form that applies to both polarizations:

$$\boldsymbol{E}_{T+} e^{-j\boldsymbol{k}_+\cdot\boldsymbol{r}} + \boldsymbol{E}_{T-} e^{-j\boldsymbol{k}_-\cdot\boldsymbol{r}} = \boldsymbol{E}'_{T+} e^{-j\boldsymbol{k}'_+\cdot\boldsymbol{r}} + \boldsymbol{E}'_{T-} e^{-j\boldsymbol{k}'_-\cdot\boldsymbol{r}}, \qquad \text{at} \quad z = 0 \tag{7.1.1}$$

where the subscript T denotes the transverse (with respect to z) part of a vector, that is, $\boldsymbol{E}_T = \hat{\mathbf{z}} \times (\boldsymbol{E} \times \hat{\mathbf{z}}) = \boldsymbol{E} - \hat{\mathbf{z}}\, E_z$. Setting $z = 0$ in the propagation phase factors, we obtain:

$$\boldsymbol{E}_{T+} e^{-j(k_{x+}x + k_{y+}y)} + \boldsymbol{E}_{T-} e^{-j(k_{x-}x + k_{y-}y)} = \boldsymbol{E}'_{T+} e^{-j(k'_{x+}x + k'_{y+}y)} + \boldsymbol{E}'_{T-} e^{-j(k'_{x-}x + k'_{y-}y)} \tag{7.1.2}$$

For the two sides to match at *all* points on the interface, the phase factors must be equal to each other for all x and y:

$$e^{-j(k_{x+}x + k_{y+}y)} = e^{-j(k_{x-}x + k_{y-}y)} = e^{-j(k'_{x+}x + k'_{y+}y)} = e^{-j(k'_{x-}x + k'_{y-}y)} \qquad \text{(phase matching)}$$

and this requires the x- and y-components of the wave vectors to be equal:

$$\begin{aligned} k_{x+} &= k_{x-} = k'_{x+} = k'_{x-} \\ k_{y+} &= k_{y-} = k'_{y+} = k'_{y-} \end{aligned} \tag{7.1.3}$$

If the left plane of incidence is the xz-plane, so that $k_{y+} = 0$, then all y-components of the wavevectors will be zero, implying that all planes of incidence and reflection will coincide with the xz-plane. In terms of the incident and reflected angles $\theta_\pm, \theta'_\pm$, the conditions on the x-components read:

$$k \sin\theta_+ = k \sin\theta_- = k' \sin\theta'_+ = k' \sin\theta'_- \tag{7.1.4}$$

These imply *Snel's law of reflection*:

$$\boxed{\begin{aligned} \theta_+ &= \theta_- \equiv \theta \\ \theta'_+ &= \theta'_- \equiv \theta' \end{aligned}} \qquad \text{(Snel's law of reflection)} \tag{7.1.5}$$

[†] from the German word *senkrecht* for perpendicular.

[†] named after Willebrord Snel, b.1580, almost universally misspelled as Snell.

And also *Snel's law of refraction*, that is, $k\sin\theta = k'\sin\theta'$. Setting $k = nk_0$, $k' = n'k_0$, and $k_0 = \omega/c_0$, we have:

$$\boxed{n\sin\theta = n'\sin\theta'} \quad \Rightarrow \quad \boxed{\frac{\sin\theta}{\sin\theta'} = \frac{n'}{n}} \qquad \text{(Snel's law of refraction)} \tag{7.1.6}$$

It follows that the wave vectors shown in Fig. 7.1.1 will be explicitly:

$$\begin{aligned} \boldsymbol{k} = \boldsymbol{k}_+ &= k_x\hat{\mathbf{x}} + k_z\hat{\mathbf{z}} = k\sin\theta\,\hat{\mathbf{x}} + k\cos\theta\,\hat{\mathbf{z}} \\ \boldsymbol{k}_- &= k_x\hat{\mathbf{x}} - k_z\hat{\mathbf{z}} = k\sin\theta\,\hat{\mathbf{x}} - k\cos\theta\,\hat{\mathbf{z}} \\ \boldsymbol{k}' = \boldsymbol{k}'_+ &= k'_x\hat{\mathbf{x}} + k'_z\hat{\mathbf{z}} = k'\sin\theta'\,\hat{\mathbf{x}} + k'\cos\theta'\,\hat{\mathbf{z}} \\ \boldsymbol{k}'_- &= k'_x\hat{\mathbf{x}} - k'_z\hat{\mathbf{z}} = k'\sin\theta'\,\hat{\mathbf{x}} - k'\cos\theta'\,\hat{\mathbf{z}} \end{aligned} \tag{7.1.7}$$

The net transverse electric fields at arbitrary locations on either side of the interface are given by Eq. (7.1.1). Using Eq. (7.1.7), we have:

$$\begin{aligned} \boldsymbol{E}_T(x,z) &= \boldsymbol{E}_{T+}e^{-j\boldsymbol{k}_+\cdot\boldsymbol{r}} + \boldsymbol{E}_{T-}e^{-j\boldsymbol{k}_-\cdot\boldsymbol{r}} = \big(\boldsymbol{E}_{T+}e^{-jk_zz} + \boldsymbol{E}_{T-}e^{jk_zz}\big)e^{-jk_xx} \\ \boldsymbol{E}'_T(x,z) &= \boldsymbol{E}'_{T+}e^{-j\boldsymbol{k}'_+\cdot\boldsymbol{r}} + \boldsymbol{E}'_{T-}e^{-j\boldsymbol{k}'_-\cdot\boldsymbol{r}} = \big(\boldsymbol{E}'_{T+}e^{-jk'_zz} + \boldsymbol{E}'_{T-}e^{jk'_zz}\big)e^{-jk'_xx} \end{aligned} \tag{7.1.8}$$

In analyzing multilayer dielectrics stacked along the z-direction, the phase factor $e^{-jk_xx} = e^{-jk'_xx}$ will be common at all interfaces, and therefore, we can ignore it and restore it at the end of the calculations, if so desired. Thus, we write Eq. (7.1.8) as:

$$\begin{aligned} \boldsymbol{E}_T(z) &= \boldsymbol{E}_{T+}e^{-jk_zz} + \boldsymbol{E}_{T-}e^{jk_zz} \\ \boldsymbol{E}'_T(z) &= \boldsymbol{E}'_{T+}e^{-jk'_zz} + \boldsymbol{E}'_{T-}e^{jk'_zz} \end{aligned} \tag{7.1.9}$$

In the next section, we work out explicit expressions for Eq. (7.1.9)

7.2 Transverse Impedance

The transverse components of the electric fields are defined differently in the two polarization cases. We recall from Sec. 2.10 that an obliquely-moving wave will have, in general, both TM and TE components. For example, according to Eq. (2.10.9), the wave incident on the interface from the left will be given by:

$$\begin{aligned} \boldsymbol{E}_+(\boldsymbol{r}) &= \big[(\hat{\mathbf{x}}\cos\theta - \hat{\mathbf{z}}\sin\theta)A_+ + \hat{\mathbf{y}}B_+\big]e^{-j\boldsymbol{k}_+\cdot\boldsymbol{r}} \\ \boldsymbol{H}_+(\boldsymbol{r}) &= \frac{1}{\eta}\big[\hat{\mathbf{y}}A_+ - (\hat{\mathbf{x}}\cos\theta - \hat{\mathbf{z}}\sin\theta)B_+\big]e^{-j\boldsymbol{k}_+\cdot\boldsymbol{r}} \end{aligned} \tag{7.2.1}$$

where the A_+ and B_+ terms represent the TM and TE components, respectively. Thus, the transverse components are:

$$\begin{aligned} \boldsymbol{E}_{T+}(x,z) &= \big[\hat{\mathbf{x}}A_+\cos\theta + \hat{\mathbf{y}}B_+\big]e^{-j(k_xx+k_zz)} \\ \boldsymbol{H}_{T+}(x,z) &= \frac{1}{\eta}\big[\hat{\mathbf{y}}A_+ - \hat{\mathbf{x}}B_+\cos\theta\big]e^{-j(k_xx+k_zz)} \end{aligned} \tag{7.2.2}$$

Similarly, the wave reflected back into the left medium will have the form:

$$\begin{aligned} \boldsymbol{E}_-(\boldsymbol{r}) &= \big[(\hat{\mathbf{x}}\cos\theta + \hat{\mathbf{z}}\sin\theta)A_- + \hat{\mathbf{y}}B_-\big]e^{-j\boldsymbol{k}_-\cdot\boldsymbol{r}} \\ \boldsymbol{H}_-(\boldsymbol{r}) &= \frac{1}{\eta}\big[-\hat{\mathbf{y}}A_- + (\hat{\mathbf{x}}\cos\theta + \hat{\mathbf{z}}\sin\theta)B_-\big]e^{-j\boldsymbol{k}_-\cdot\boldsymbol{r}} \end{aligned} \tag{7.2.3}$$

with corresponding transverse parts:

$$\begin{aligned} \boldsymbol{E}_{T-}(x,z) &= \big[\hat{\mathbf{x}}A_-\cos\theta + \hat{\mathbf{y}}B_-\big]e^{-j(k_xx-k_zz)} \\ \boldsymbol{H}_{T-}(x,z) &= \frac{1}{\eta}\big[-\hat{\mathbf{y}}A_- + \hat{\mathbf{x}}B_-\cos\theta\big]e^{-j(k_xx-k_zz)} \end{aligned} \tag{7.2.4}$$

Defining the transverse amplitudes and transverse impedances by:

$$\begin{aligned} A_{T\pm} &= A_\pm\cos\theta\,, \quad B_{T\pm} = B_\pm \\ \eta_{TM} &= \eta\cos\theta\,, \qquad \eta_{TE} = \frac{\eta}{\cos\theta} \end{aligned} \tag{7.2.5}$$

and noting that $A_{T\pm}/\eta_{TM} = A_\pm/\eta$ and $B_{T\pm}/\eta_{TE} = B_\pm\cos\theta/\eta$, we may write Eq. (7.2.2) in terms of the transverse quantities as follows:

$$\begin{aligned} \boldsymbol{E}_{T+}(x,z) &= \big[\hat{\mathbf{x}}A_{T+} + \hat{\mathbf{y}}B_{T+}\big]e^{-j(k_xx+k_zz)} \\ \boldsymbol{H}_{T+}(x,z) &= \Big[\hat{\mathbf{y}}\frac{A_{T+}}{\eta_{TM}} - \hat{\mathbf{x}}\frac{B_{T+}}{\eta_{TE}}\Big]e^{-j(k_xx+k_zz)} \end{aligned} \tag{7.2.6}$$

Similarly, Eq. (7.2.4) is expressed as:

$$\begin{aligned} \boldsymbol{E}_{T-}(x,z) &= \big[\hat{\mathbf{x}}A_{T-} + \hat{\mathbf{y}}B_{T-}\big]e^{-j(k_xx-k_zz)} \\ \boldsymbol{H}_{T-}(x,z) &= \Big[-\hat{\mathbf{y}}\frac{A_{T-}}{\eta_{TM}} + \hat{\mathbf{x}}\frac{B_{T-}}{\eta_{TE}}\Big]e^{-j(k_xx-k_zz)} \end{aligned} \tag{7.2.7}$$

Adding up Eqs. (7.2.6) and (7.2.7) and ignoring the common factor e^{-jk_xx}, we find for the net transverse fields on the left side:

$$\begin{aligned} \boldsymbol{E}_T(z) &= \hat{\mathbf{x}}E_{TM}(z) + \hat{\mathbf{y}}E_{TE}(z) \\ \boldsymbol{H}_T(z) &= \hat{\mathbf{y}}H_{TM}(z) - \hat{\mathbf{x}}H_{TE}(z) \end{aligned} \tag{7.2.8}$$

where the TM and TE components have the same structure provided one uses the appropriate transverse impedance:

$$\begin{aligned} E_{TM}(z) &= A_{T+}e^{-jk_zz} + A_{T-}e^{jk_zz} \\ H_{TM}(z) &= \frac{1}{\eta_{TM}}\big[A_{T+}e^{-jk_zz} - A_{T-}e^{jk_zz}\big] \\ E_{TE}(z) &= B_{T+}e^{-jk_zz} + B_{T-}e^{jk_zz} \\ H_{TE}(z) &= \frac{1}{\eta_{TE}}\big[B_{T+}e^{-jk_zz} - B_{T-}e^{jk_zz}\big] \end{aligned} \tag{7.2.9}$$

$$\tag{7.2.10}$$

We summarize these in the compact form, where E_T stands for either E_{TM} or E_{TE}:

$$\boxed{\begin{aligned} E_T(z) &= E_{T+}e^{-jk_z z} + E_{T-}e^{jk_z z} \\ H_T(z) &= \frac{1}{\eta_T}\left[E_{T+}e^{-jk_z z} - E_{T-}e^{jk_z z}\right] \end{aligned}} \tag{7.2.11}$$

The transverse impedance η_T stands for either η_{TM} or η_{TE}:

$$\boxed{\eta_T = \begin{cases} \eta\cos\theta\,, & \text{TM, parallel, p-polarization} \\ \dfrac{\eta}{\cos\theta}\,, & \text{TE, perpendicular, s-polarization} \end{cases}} \tag{7.2.12}$$

Because $\eta = \eta_o/n$, it is convenient to define also a *transverse refractive index* through the relationship $\eta_T = \eta_0/n_T$. Thus, we have:

$$\boxed{n_T = \begin{cases} \dfrac{n}{\cos\theta}\,, & \text{TM, parallel, p-polarization} \\ n\cos\theta\,, & \text{TE, perpendicular, s-polarization} \end{cases}} \tag{7.2.13}$$

For the right side of the interface, we obtain similar expressions:

$$\begin{aligned} E'_T(z) &= E'_{T+}e^{-jk'_z z} + E'_{T-}e^{jk'_z z} \\ H'_T(z) &= \frac{1}{\eta'_T}\left(E'_{T+}e^{-jk'_z z} - E'_{T-}e^{jk'_z z}\right) \end{aligned} \tag{7.2.14}$$

$$\eta'_T = \begin{cases} \eta'\cos\theta'\,, & \text{TM, parallel, p-polarization} \\ \dfrac{\eta'}{\cos\theta'}\,, & \text{TE, perpendicular, s-polarization} \end{cases} \tag{7.2.15}$$

$$n'_T = \begin{cases} \dfrac{n'}{\cos\theta'}\,, & \text{TM, parallel, p-polarization} \\ n'\cos\theta'\,, & \text{TE, perpendicular, s-polarization} \end{cases} \tag{7.2.16}$$

where $E'_{T\pm}$ stands for $A'_{T\pm} = A'_\pm\cos\theta'$ or $B'_{T\pm} = B'_\pm$.

For completeness, we give below the complete expressions for the fields on both sides of the interface obtained by adding Eqs. (7.2.1) and (7.2.3), with all the propagation factors restored. On the left side, we have:

$$\begin{aligned} \boldsymbol{E}(\boldsymbol{r}) &= \boldsymbol{E}_{TM}(\boldsymbol{r}) + \boldsymbol{E}_{TE}(\boldsymbol{r}) \\ \boldsymbol{H}(\boldsymbol{r}) &= \boldsymbol{H}_{TM}(\boldsymbol{r}) + \boldsymbol{H}_{TE}(\boldsymbol{r}) \end{aligned} \tag{7.2.17}$$

where

$$\begin{aligned} \boldsymbol{E}_{TM}(\boldsymbol{r}) &= (\hat{\mathbf{x}}\cos\theta - \hat{\mathbf{z}}\sin\theta)A_+e^{-j\boldsymbol{k}_+\cdot\boldsymbol{r}} + (\hat{\mathbf{x}}\cos\theta + \hat{\mathbf{z}}\sin\theta)A_-e^{-j\boldsymbol{k}_-\cdot\boldsymbol{r}} \\ \boldsymbol{H}_{TM}(\boldsymbol{r}) &= \hat{\mathbf{y}}\,\frac{1}{\eta}\left(A_+e^{-j\boldsymbol{k}_+\cdot\boldsymbol{r}} - A_-e^{-j\boldsymbol{k}_-\cdot\boldsymbol{r}}\right) \\ \boldsymbol{E}_{TE}(\boldsymbol{r}) &= \hat{\mathbf{y}}\left(B_+e^{-j\boldsymbol{k}_+\cdot\boldsymbol{r}} + B_-e^{-j\boldsymbol{k}_-\cdot\boldsymbol{r}}\right) \\ \boldsymbol{H}_{TE}(\boldsymbol{r}) &= \frac{1}{\eta}\left[-(\hat{\mathbf{x}}\cos\theta - \hat{\mathbf{z}}\sin\theta)B_+e^{-j\boldsymbol{k}_+\cdot\boldsymbol{r}} + (\hat{\mathbf{x}}\cos\theta + \hat{\mathbf{z}}\sin\theta)B_-e^{-j\boldsymbol{k}_-\cdot\boldsymbol{r}}\right] \end{aligned} \tag{7.2.18}$$

The transverse parts of these are the same as those given in Eqs. (7.2.9) and (7.2.10). On the right side of the interface, we have:

$$\begin{aligned} \boldsymbol{E}'(\boldsymbol{r}) &= \boldsymbol{E}'_{TM}(\boldsymbol{r}) + \boldsymbol{E}'_{TE}(\boldsymbol{r}) \\ \boldsymbol{H}'(\boldsymbol{r}) &= \boldsymbol{H}'_{TM}(\boldsymbol{r}) + \boldsymbol{H}'_{TE}(\boldsymbol{r}) \end{aligned} \tag{7.2.19}$$

$$\begin{aligned} \boldsymbol{E}'_{TM}(\boldsymbol{r}) &= (\hat{\mathbf{x}}\cos\theta' - \hat{\mathbf{z}}\sin\theta')A'_+e^{-j\boldsymbol{k}'_+\cdot\boldsymbol{r}} + (\hat{\mathbf{x}}\cos\theta' + \hat{\mathbf{z}}\sin\theta')A'_-e^{-j\boldsymbol{k}'_-\cdot\boldsymbol{r}} \\ \boldsymbol{H}'_{TM}(\boldsymbol{r}) &= \hat{\mathbf{y}}\,\frac{1}{\eta'}\left(A'_+e^{-j\boldsymbol{k}'_+\cdot\boldsymbol{r}} - A'_-e^{-j\boldsymbol{k}'_-\cdot\boldsymbol{r}}\right) \\ \boldsymbol{E}'_{TE}(\boldsymbol{r}) &= \hat{\mathbf{y}}\left(B'_+e^{-j\boldsymbol{k}'_+\cdot\boldsymbol{r}} + B'_-e^{-j\boldsymbol{k}'_-\cdot\boldsymbol{r}}\right) \\ \boldsymbol{H}'_{TE}(\boldsymbol{r}) &= \frac{1}{\eta'}\left[-(\hat{\mathbf{x}}\cos\theta' - \hat{\mathbf{z}}\sin\theta')B'_+e^{-j\boldsymbol{k}'_+\cdot\boldsymbol{r}} + (\hat{\mathbf{x}}\cos\theta' + \hat{\mathbf{z}}\sin\theta')B'_-e^{-j\boldsymbol{k}'_-\cdot\boldsymbol{r}}\right] \end{aligned} \tag{7.2.20}$$

7.3 Propagation and Matching of Transverse Fields

Eq. (7.2.11) has the identical form of Eq. (5.1.1) of the normal incidence case, but with the substitutions:

$$\boxed{\eta \to \eta_T\,, \quad e^{\pm jkz} \to e^{\pm jk_z z} = e^{\pm jkz\cos\theta}} \tag{7.3.1}$$

Every definition and concept of Chap. 5 translates into the oblique case. For example, we can define the *transverse wave impedance* at position z by:

$$Z_T(z) = \frac{E_T(z)}{H_T(z)} = \eta_T\,\frac{E_{T+}e^{-jk_z z} + E_{T-}e^{jk_z z}}{E_{T+}e^{-jk_z z} - E_{T-}e^{jk_z z}} \tag{7.3.2}$$

and the *transverse reflection coefficient* at position z:

$$\Gamma_T(z) = \frac{E_{T-}(z)}{E_{T+}(z)} = \frac{E_{T-}e^{jk_z z}}{E_{T+}e^{-jk_z z}} = \Gamma_T(0)\,e^{2jk_z z} \tag{7.3.3}$$

They are related as in Eq. (5.1.7):

$$Z_T(z) = \eta_T\,\frac{1+\Gamma_T(z)}{1-\Gamma_T(z)} \quad\Leftrightarrow\quad \Gamma_T(z) = \frac{Z_T(z)-\eta_T}{Z_T(z)+\eta_T} \tag{7.3.4}$$

The propagation matrices, Eqs. (5.1.11) and (5.1.13), relating the fields at two positions z_1, z_2 within the same medium, read now:

$$\begin{bmatrix} E_{T1+} \\ E_{T1-} \end{bmatrix} = \begin{bmatrix} e^{jk_z l} & 0 \\ 0 & e^{-jk_z l} \end{bmatrix} \begin{bmatrix} E_{T2+} \\ E_{T2-} \end{bmatrix} \qquad \text{(propagation matrix)} \tag{7.3.5}$$

$$\begin{bmatrix} E_{T1} \\ H_{T1} \end{bmatrix} = \begin{bmatrix} \cos k_z l & j\eta_T\sin k_z l \\ j\eta_T^{-1}\sin k_z l & \cos k_z l \end{bmatrix} \begin{bmatrix} E_{T2} \\ H_{T2} \end{bmatrix} \qquad \text{(propagation matrix)} \tag{7.3.6}$$

where $l = z_2 - z_1$. Similarly, the reflection coefficients and wave impedances propagate as:

$$\Gamma_{T1} = \Gamma_{T2} e^{-2jk_z l}\,, \qquad Z_{T1} = \eta_T \frac{Z_{T2} + j\eta_T \tan k_z l}{\eta_T + jZ_{T2}\tan k_z l} \tag{7.3.7}$$

The phase thickness $\delta = kl = 2\pi(nl)/\lambda$ of the normal incidence case, where λ is the free-space wavelength, is replaced now by:

$$\boxed{\delta_z = k_z l = kl\cos\theta = \frac{2\pi}{\lambda}\, nl\, \cos\theta} \tag{7.3.8}$$

At the interface $z = 0$, the boundary conditions for the tangential electric and magnetic fields give rise to the same conditions as Eqs. (5.2.1) and (5.2.2):

$$E_T = E'_T\,, \quad H_T = H'_T \tag{7.3.9}$$

and in terms of the forward/backward fields:

$$\begin{aligned} E_{T+} + E_{T-} &= E'_{T+} + E'_{T-} \\ \frac{1}{\eta_T}(E_{T+} - E_{T-}) &= \frac{1}{\eta'_T}(E'_{T+} - E'_{T-}) \end{aligned} \tag{7.3.10}$$

which can be solved to give the *matching matrix*:

$$\begin{bmatrix} E_{T+} \\ E_{T-} \end{bmatrix} = \frac{1}{\tau_T}\begin{bmatrix} 1 & \rho_T \\ \rho_T & 1 \end{bmatrix}\begin{bmatrix} E'_{T+} \\ E'_{T-} \end{bmatrix} \qquad \text{(matching matrix)} \tag{7.3.11}$$

where ρ_T, τ_T are transverse reflection coefficients, replacing Eq. (5.2.5):

$$\boxed{\begin{aligned} \rho_T &= \frac{\eta'_T - \eta_T}{\eta'_T + \eta_T} = \frac{n_T - n'_T}{n_T + n'_T} \\ \tau_T &= \frac{2\eta'_T}{\eta'_T + \eta_T} = \frac{2n_T}{n_T + n'_T} \end{aligned}} \qquad \text{(Fresnel coefficients)} \tag{7.3.12}$$

where $\tau_T = 1 + \rho_T$. We may also define the reflection coefficients from the right side of the interface: $\rho'_T = -\rho_T$ and $\tau'_T = 1 + \rho'_T = 1 - \rho_T$. Eqs. (7.3.12) are known as the *Fresnel* reflection and transmission coefficients.

The matching conditions for the transverse fields translate into corresponding matching conditions for the wave impedances and reflection responses:

$$Z_T = Z'_T \quad \Leftrightarrow \quad \Gamma_T = \frac{\rho_T + \Gamma'_T}{1 + \rho_T \Gamma'_T} \quad \Leftrightarrow \quad \Gamma'_T = \frac{\rho'_T + \Gamma_T}{1 + \rho'_T \Gamma_T} \tag{7.3.13}$$

If there is no left-incident wave from the right, that is, $E'_- = 0$, then, Eq. (7.3.11) takes the specialized form:

$$\begin{bmatrix} E_{T+} \\ E_{T-} \end{bmatrix} = \frac{1}{\tau_T}\begin{bmatrix} 1 & \rho_T \\ \rho_T & 1 \end{bmatrix}\begin{bmatrix} E'_{T+} \\ 0 \end{bmatrix} \tag{7.3.14}$$

which explains the meaning of the transverse reflection and transmission coefficients:

$$\rho_T = \frac{E_{T-}}{E_{T+}}\,, \quad \tau_T = \frac{E'_{T+}}{E_{T+}} \tag{7.3.15}$$

The relationship of these coefficients to the reflection and transmission coefficients of the *total* field amplitudes depends on the polarization. For TM, we have $E_{T\pm} = A_\pm \cos\theta$ and $E'_{T\pm} = A'_\pm \cos\theta'$, and for TE, $E_{T\pm} = B_\pm$ and $E'_{T\pm} = B'_\pm$. For both cases, it follows that the reflection coefficient ρ_T measures also the reflection of the total amplitudes, that is,

$$\rho_{TM} = \frac{A_- \cos\theta}{A_+ \cos\theta} = \frac{A_-}{A_+}\,, \qquad \rho_{TE} = \frac{B_-}{B_+}$$

whereas for the transmission coefficients, we have:

$$\tau_{TM} = \frac{A'_+ \cos\theta'}{A_+ \cos\theta} = \frac{\cos\theta'}{\cos\theta}\,\frac{A'_+}{A_+}\,, \qquad \tau_{TE} = \frac{B'_+}{B_+}$$

In addition to the boundary conditions of the transverse field components, there are also applicable boundary conditions for the longitudinal components. For example, in the TM case, the component E_z is normal to the surface and therefore, we must have the continuity condition $D_z = D'_z$, or $\epsilon E_z = \epsilon' E'_z$. Similarly, in the TE case, we must have $B_z = B'_z$. It can be verified that these conditions are automatically satisfied due to Snel's law (7.1.6).

The fields carry energy towards the z-direction, as well as the transverse x-direction. The energy flux along the z-direction must be conserved across the interface. The corresponding components of the Poynting vector are:

$$\mathcal{P}_z = \frac{1}{2}\,\mathrm{Re}\big[E_x H_y^* - E_y H_x^*\big]\,, \quad \mathcal{P}_x = \frac{1}{2}\,\mathrm{Re}\big[E_y H_z^* - E_z H_y^*\big]$$

For TM, we have $\mathcal{P}_z = \mathrm{Re}[E_x H_y^*]/2$ and for TE, $\mathcal{P}_z = -\mathrm{Re}[E_y H_x^*]/2$. Using the above equations for the fields, we find that $\mathcal{P}_z$ is given by the *same* expression for both TM and TE polarizations:

$$\mathcal{P}_z = \frac{\cos\theta}{2\eta}\big(|A_+|^2 - |A_-|^2\big), \quad \text{or,} \quad \frac{\cos\theta}{2\eta}\big(|B_+|^2 - |B_-|^2\big) \tag{7.3.16}$$

Using the appropriate definitions for $E_{T\pm}$ and η_T, Eq. (7.3.16) can be written in terms of the transverse components for either polarization:

$$\mathcal{P}_z = \frac{1}{2\eta_T}\big(|E_{T+}|^2 - |E_{T-}|^2\big) \tag{7.3.17}$$

As in the normal incidence case, the structure of the matching matrix (7.3.11) implies that (7.3.17) is conserved across the interface.

7.4 Fresnel Reflection Coefficients

We look now at the specifics of the Fresnel coefficients (7.3.12) for the two polarization cases. Inserting the two possible definitions (7.2.13) for the transverse refractive indices, we can express ρ_T in terms of the incident and refracted angles:

$$\rho_{TM} = \frac{\dfrac{n}{\cos\theta} - \dfrac{n'}{\cos\theta'}}{\dfrac{n}{\cos\theta} + \dfrac{n'}{\cos\theta'}} = \frac{n\cos\theta' - n'\cos\theta}{n\cos\theta' + n'\cos\theta}$$
$$\rho_{TE} = \frac{n\cos\theta - n'\cos\theta'}{n\cos\theta + n'\cos\theta'} \tag{7.4.1}$$

We note that for normal incidence, $\theta = \theta' = 0$, they both reduce to the usual reflection coefficient $\rho = (n - n')/(n + n')$.† Using Snel's law, $n\sin\theta = n'\sin\theta'$, and some trigonometric identities, we may write Eqs. (7.4.1) in a number of equivalent ways. In terms of the angle of incidence only, we have:

$$\rho_{TM} = \frac{\sqrt{\left(\dfrac{n'}{n}\right)^2 - \sin^2\theta} - \left(\dfrac{n'}{n}\right)^2\cos\theta}{\sqrt{\left(\dfrac{n'}{n}\right)^2 - \sin^2\theta} + \left(\dfrac{n'}{n}\right)^2\cos\theta}$$
$$\rho_{TE} = \frac{\cos\theta - \sqrt{\left(\dfrac{n'}{n}\right)^2 - \sin^2\theta}}{\cos\theta + \sqrt{\left(\dfrac{n'}{n}\right)^2 - \sin^2\theta}} \tag{7.4.2}$$

Note that at *grazing angles* of incidence, $\theta \to 90^o$, the reflection coefficients tend to $\rho_{TM} \to 1$ and $\rho_{TE} \to -1$, *regardless* of the refractive indices n, n'. One consequence of this property is in wireless communications where the effect of the ground reflections causes the power of the propagating radio wave to attenuate with the *fourth* (instead of the second) power of the distance, thus, limiting the propagation range (see Example 22.3.5.)

We note also that Eqs. (7.4.1) and (7.4.2) remain valid when one or both of the media are lossy. For example, if the right medium is lossy with complex refractive index $n'_c = n'_r - jn'_i$, then, Snel's law, $n\sin\theta = n'_c\sin\theta'$, is still valid but with a complex-valued θ' and (7.4.2) remains the same with the replacement $n' \to n'_c$. The third way of expressing the ρs is in terms of θ, θ' only, without the n, n':

$$\rho_{TM} = \frac{\sin 2\theta' - \sin 2\theta}{\sin 2\theta' + \sin 2\theta} = \frac{\tan(\theta' - \theta)}{\tan(\theta' + \theta)}$$
$$\rho_{TE} = \frac{\sin(\theta' - \theta)}{\sin(\theta' + \theta)} \tag{7.4.3}$$

Fig. 7.4.1 shows the special case of an air-dielectric interface. If the incident wave is from the air side, then Eq. (7.4.2) gives with $n = 1$, $n' = n_d$, where n_d is the (possibly complex-valued) refractive index of the dielectric:

†Some references define ρ_{TM} with the opposite sign. Our convention was chosen because it has the expected limit at normal incidence.

$$\rho_{TM} = \frac{\sqrt{n_d^2 - \sin^2\theta} - n_d^2\cos\theta}{\sqrt{n_d^2 - \sin^2\theta} + n_d^2\cos\theta}, \quad \rho_{TE} = \frac{\cos\theta - \sqrt{n_d^2 - \sin^2\theta}}{\cos\theta + \sqrt{n_d^2 - \sin^2\theta}} \tag{7.4.4}$$

If the incident wave is from inside the dielectric, then we set $n = n_d$ and $n' = 1$:

$$\rho_{TM} = \frac{\sqrt{n_d^{-2} - \sin^2\theta} - n_d^{-2}\cos\theta}{\sqrt{n_d^{-2} - \sin^2\theta} + n_d^{-2}\cos\theta}, \quad \rho_{TE} = \frac{\cos\theta - \sqrt{n_d^{-2} - \sin^2\theta}}{\cos\theta + \sqrt{n_d^{-2} - \sin^2\theta}} \tag{7.4.5}$$

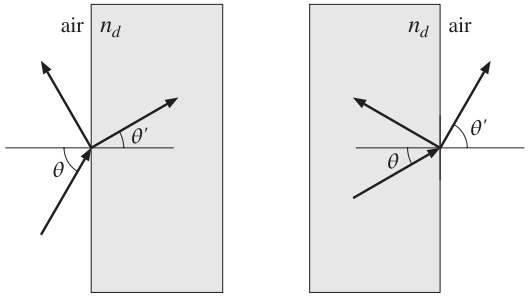

Fig. 7.4.1 Air-dielectric interfaces.

The MATLAB function `fresnel` calculates the expressions (7.4.2) for any range of values of θ. Its usage is as follows:

```
[rtm,rte] = fresnel(na,nb,theta);          % Fresnel reflection coefficients
```

7.5 Maximum Angle and Critical Angle

As the incident angle θ varies over $0 \le \theta \le 90^o$, the angle of refraction θ' will have a corresponding range of variation. It can be determined by solving for θ' from Snel's law, $n\sin\theta = n'\sin\theta'$:

$$\sin\theta' = \frac{n}{n'}\sin\theta \tag{7.5.1}$$

If $n < n'$ (we assume lossless dielectrics here,) then Eq. (7.5.1) implies that $\sin\theta' = (n/n')\sin\theta < \sin\theta$, or $\theta' < \theta$. Thus, if the incident wave is from a lighter to a denser medium, the refracted angle is always smaller than the incident angle. The maximum value of θ', denoted here by θ'_c, is obtained when θ has its maximum, $\theta = 90^o$:

$$\sin\theta'_c = \frac{n}{n'} \quad \text{(maximum angle of refraction)} \tag{7.5.2}$$

Thus, the angle ranges are $0 \le \theta \le 90^o$ and $0 \le \theta' \le \theta'_c$. Fig. 7.5.1 depicts this case, as well as the case $n > n'$.

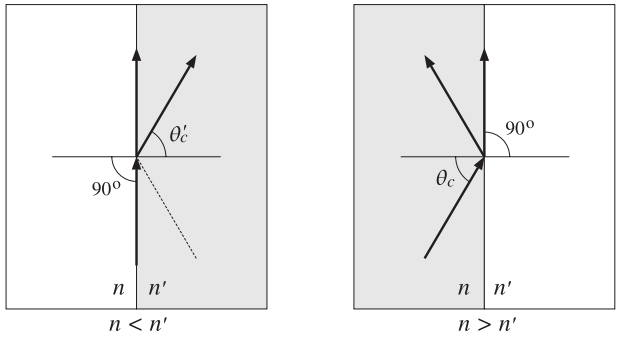

Fig. 7.5.1 Maximum angle of refraction and critical angle of incidence.

On the other hand, if $n > n'$, and the incident wave is from a denser onto a lighter medium, then $\sin\theta' = (n/n')\sin\theta > \sin\theta$, or $\theta' > \theta$. Therefore, θ' will reach the maximum value of 90^o before θ does. The corresponding maximum value of θ satisfies Snel's law, $n\sin\theta_c = n'\sin(\pi/2) = n'$, or,

$$\boxed{\sin\theta_c = \frac{n'}{n}} \qquad \text{(critical angle of incidence)} \tag{7.5.3}$$

This angle is called the *critical angle of incidence*. If the incident wave were from the right, θ_c would be the maximum angle of refraction according to the above discussion.

If $\theta \le \theta_c$, there is normal refraction into the lighter medium. But, if θ exceeds θ_c, the incident wave cannot be refracted and gets completely reflected back into the denser medium. This phenomenon is called *total internal reflection*. Because $n'/n = \sin\theta_c$, we may rewrite the reflection coefficients (7.4.2) in the form:

$$\rho_{TM} = \frac{\sqrt{\sin^2\theta_c - \sin^2\theta} - \sin^2\theta_c\cos\theta}{\sqrt{\sin^2\theta_c - \sin^2\theta} + \sin^2\theta_c\cos\theta}\,, \quad \rho_{TE} = \frac{\cos\theta - \sqrt{\sin^2\theta_c - \sin^2\theta}}{\cos\theta + \sqrt{\sin^2\theta_c - \sin^2\theta}}$$

When $\theta < \theta_c$, the reflection coefficients are real-valued. At $\theta = \theta_c$, they have the values, $\rho_{TM} = -1$ and $\rho_{TE} = 1$. And, when $\theta > \theta_c$, they become complex-valued with unit magnitude. Indeed, switching the sign under the square roots, we have in this case:

$$\rho_{TM} = \frac{-j\sqrt{\sin^2\theta - \sin^2\theta_c} - \sin^2\theta_c\cos\theta}{-j\sqrt{\sin^2\theta - \sin^2\theta_c} + \sin^2\theta_c\cos\theta}\,, \quad \rho_{TE} = \frac{\cos\theta + j\sqrt{\sin^2\theta - \sin^2\theta_c}}{\cos\theta - j\sqrt{\sin^2\theta - \sin^2\theta_c}}$$

where we used the evanescent definition of the square root as discussed in Eqs. (7.7.9) and (7.7.10), that is, we made the replacement

$$\sqrt{\sin^2\theta_c - \sin^2\theta} \longrightarrow -j\sqrt{\sin^2\theta - \sin^2\theta_c}\,, \quad \text{for } \theta \ge \theta_c$$

Both expressions for ρ_T are the ratios of a complex number and its conjugate, and therefore, they are unimodular, $|\rho_{TM}| = |\rho_{TE}| = 1$, for all values of $\theta > \theta_c$. The interface becomes a perfect mirror, with zero transmittance into the lighter medium.

When $\theta > \theta_c$, the fields on the right side of the interface are not zero, but do not propagate away to the right. Instead, they decay exponentially with the distance z. There is no transfer of power (on the average) to the right. To understand this behavior of the fields, we consider the solutions given in Eqs. (7.2.18) and (7.2.20), with no incident field from the right, that is, with $A'_- = B'_- = 0$.

The longitudinal wavenumber in the right medium, k'_z, can be expressed in terms of the angle of incidence θ as follows. We have from Eq. (7.1.7):

$$k_z^2 + k_x^2 = k^2 = n^2k_0^2$$

$$k_z'^2 + k_x'^2 = k'^2 = n'^2k_0^2$$

Because, $k'_x = k_x = k\sin\theta = nk_0\sin\theta$, we may solve for k'_z to get:

$$k_z'^2 = n'^2k_0^2 - k_x'^2 = n'^2k_0^2 - k_x^2 = n'^2k_0^2 - n^2k_0^2\sin^2\theta = k_0^2(n'^2 - n^2\sin^2\theta)$$

or, replacing $n' = n\sin\theta_c$, we find:

$$\boxed{k_z'^2 = n^2k_0^2(\sin^2\theta_c - \sin^2\theta)} \tag{7.5.4}$$

If $\theta \le \theta_c$, the wavenumber k'_z is real-valued and corresponds to ordinary propagating fields that represent the refracted wave. But if $\theta > \theta_c$, we have $k_z'^2 < 0$ and k'_z becomes pure imaginary, say $k'_z = -j\alpha'_z$. The z-dependence of the fields on the right of the interface will be:

$$e^{-jk'_z z} = e^{-\alpha'_z z}\,, \qquad \alpha'_z = nk_0\sqrt{\sin^2\theta - \sin^2\theta_c}$$

Such exponentially decaying fields are called *evanescent waves* because they are effectively confined to within a few multiples of the distance $z = 1/\alpha'_z$ (the penetration length) from the interface.

The maximum value of α'_z, or equivalently, the smallest penetration length $1/\alpha'_z$, is achieved when $\theta = 90^o$, resulting in:

$$\alpha'_{\max} = nk_0\sqrt{1 - \sin^2\theta_c} = nk_0\cos\theta_c = k_0\sqrt{n^2 - n'^2}$$

Inspecting Eqs. (7.2.20), we note that the factor $\cos\theta'$ becomes pure imaginary because $\cos^2\theta' = 1 - \sin^2\theta' = 1 - (n/n')^2\sin^2\theta = 1 - \sin^2\theta/\sin^2\theta_c \le 0$, for $\theta \ge \theta_c$. Therefore for either the TE or TM case, the transverse components E_T and H_T will have a 90^o phase difference, which will make the time-average power flow into the right medium zero: $\mathcal{P}_z = \mathrm{Re}(E_T H_T^*)/2 = 0$.

Example 7.5.1: Determine the maximum angle of refraction and critical angle of reflection for (a) an air-glass interface and (b) an air-water interface. The refractive indices of glass and water at optical frequencies are: $n_{\text{glass}} = 1.5$ and $n_{\text{water}} = 1.333$.

Solution: There is really only one angle to determine, because if $n = 1$ and $n' = n_{\text{glass}}$, then $\sin(\theta_c') = n/n' = 1/n_{\text{glass}}$, and if $n = n_{\text{glass}}$ and $n' = 1$, then, $\sin(\theta_c) = n'/n = 1/n_{\text{glass}}$. Thus, $\theta_c' = \theta_c$:

$$\theta_c = \text{asin}\left(\frac{1}{1.5}\right) = 41.8^\circ$$

For the air-water case, we have:

$$\theta_c = \text{asin}\left(\frac{1}{1.333}\right) = 48.6^\circ$$

The refractive index of water at radio frequencies and below is $n_{\text{water}} = 9$ approximately. The corresponding critical angle is $\theta_c = 6.4^\circ$. □

Example 7.5.2: *Prisms.* Glass prisms with 45° angles are widely used in optical instrumentation for bending light beams without the use of metallic mirrors. Fig. 7.5.2 shows two examples.

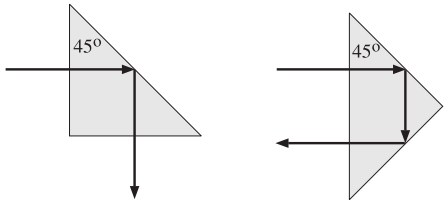

Fig. 7.5.2 Prisms using total internal reflection.

In both cases, the incident beam hits an internal prism side at an angle of 45°, which is greater than the air-glass critical angle of 41.8°. Thus, total internal reflection takes place and the prism side acts as a perfect mirror. □

Example 7.5.3: *Optical Manhole.* Because the air-water interface has $\theta_c = 48.6^\circ$, if we were to view a water surface from above the water, we could only see inside the water within the cone defined by the maximum angle of refraction.

Conversely, were we to view the surface of the water from underneath, we would see the air side only within the critical angle cone, as shown in Fig. 7.5.3. The angle subtended by this cone is $2\times 48.6 = 97.2^\circ$.

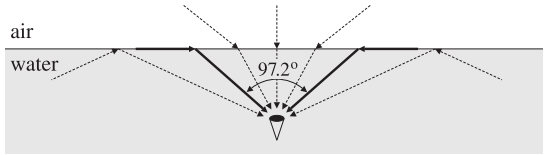

Fig. 7.5.3 Underwater view of the outside world.

The rays arriving from below the surface at an angle greater than θ_c get totally reflected. But because they are weak, the body of water outside the critical cone will appear dark. The critical cone is known as the "optical manhole" [50]. □

Example 7.5.4: *Apparent Depth.* Underwater objects viewed from the outside appear to be closer to the surface than they really are. The apparent depth of the object depends on our viewing angle. Fig. 7.5.4 shows the geometry of the incident and refracted rays.

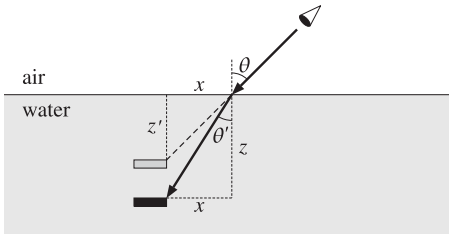

Fig. 7.5.4 Apparent depth of underwater object.

Let θ be the viewing angle and let z and z' be the actual and apparent depths. Our perceived depth corresponds to the extension of the incident ray at angle θ. From the figure, we have: $z = x\cot\theta'$ and $z' = x\cot\theta$. It follows that:

$$z' = \frac{\cot\theta}{\cot\theta'}\,z = \frac{\sin\theta'\cos\theta}{\sin\theta\cos\theta'}\,z$$

Using Snel's law $\sin\theta/\sin\theta' = n'/n = n_{\text{water}}$, we eventually find:

$$z' = \frac{\cos\theta}{\sqrt{n_{\text{water}}^2 - \sin^2\theta}}\,z$$

At normal incidence, we have $z' = z/n_{\text{water}} = z/1.333 = 0.75z$.

Reflection and refraction phenomena are very common in nature. They are responsible for the twinkling and aberration of stars, the flattening of the setting sun and moon, mirages, rainbows, and countless other natural phenomena. Four wonderful expositions of such effects are in Refs. [50–53]. See also the web page [1827]. □

Example 7.5.5: *Optical Fibers.* Total internal reflection is the mechanism by which light is guided along an optical fiber. Fig. 7.5.5 shows a step-index fiber with refractive index n_f surrounded by cladding material of index $n_c < n_f$.

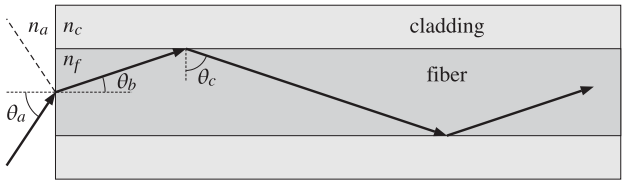

Fig. 7.5.5 Launching a beam into an optical fiber.

If the angle of incidence on the fiber-cladding interface is greater than the critical angle, then total internal reflection will take place. The figure shows a beam launched into the

fiber from the air side. The maximum angle of incidence θ_a must be made to correspond to the critical angle θ_c of the fiber-cladding interface. Using Snel's laws at the two interfaces, we have:

$$\sin\theta_a = \frac{n_f}{n_a}\sin\theta_b\,, \quad \sin\theta_c = \frac{n_c}{n_f}$$

Noting that $\theta_b = 90^o - \theta_c$, we find:

$$\sin\theta_a = \frac{n_f}{n_a}\cos\theta_c = \frac{n_f}{n_a}\sqrt{1-\sin^2\theta_c} = \frac{\sqrt{n_f^2 - n_c^2}}{n_a}$$

For example, with $n_a = 1$, $n_f = 1.49$, and $n_c = 1.48$, we find $\theta_c = 83.4^o$ and $\theta_a = 9.9^o$. The angle θ_a is called the *acceptance angle*, and the quantity $NA = \sqrt{n_f^2 - n_c^2}$, the *numerical aperture* of the fiber.

Besides its use in optical fibers, total internal reflection has several other applications [556–592], such as internal reflection spectroscopy, chemical and biological sensors, fingerprint identification, surface plasmon resonance, and high resolution microscopy. □

Example 7.5.6: *Fresnel Rhomb.* The Fresnel rhomb is a glass prism depicted in Fig. 7.5.6 that acts as a 90° retarder. It converts linear polarization into circular. Its advantage over the birefringent retarders discussed in Sec. 4.1 is that it is frequency-independent or achromatic.

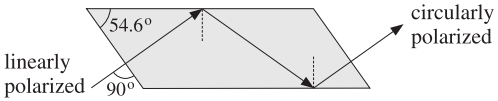

Fig. 7.5.6 Fresnel rhomb.

Assuming a refractive index $n = 1.51$, the critical angle is $\theta_c = 41.47^o$. The angle of the rhomb, $\theta = 54.6^o$, is also the angle of incidence on the internal side. This angle has been chosen such that, at each total internal reflection, the relative phase between the TE and TM polarizations changes by 45°, so that after two reflections it changes by 90°.

The angle of the rhomb can be determined as follows. For $\theta \geq \theta_c$, the reflection coefficients can be written as the unimodular complex numbers:

$$\rho_{TE} = \frac{1+jx}{1-jx}\,, \qquad \rho_{TM} = -\frac{1+jxn^2}{1-jxn^2}\,, \qquad x = \frac{\sqrt{\sin^2\theta - \sin^2\theta_c}}{\cos\theta} \tag{7.5.5}$$

where $\sin\theta_c = 1/n$. It follows that:

$$\rho_{TE} = e^{2j\psi_{TE}}\,, \quad \rho_{TM} = e^{j\pi + 2j\psi_{TM}}$$

where ψ_{TE}, ψ_{TM} are the phase angles of the numerators, that is,

$$\tan\psi_{TE} = x\,, \quad \tan\psi_{TM} = xn^2$$

The relative phase change between the TE and TM polarizations will be:

$$\frac{\rho_{TM}}{\rho_{TE}} = e^{2j\psi_{TM} - 2j\psi_{TE} + j\pi}$$

It is enough to require that $\psi_{TM} - \psi_{TE} = \pi/8$ because then, after two reflections, we will have a 90° change:

$$\frac{\rho_{TM}}{\rho_{TE}} = e^{j\pi/4 + j\pi} \quad \Rightarrow \quad \left(\frac{\rho_{TM}}{\rho_{TE}}\right)^2 = e^{j\pi/2 + 2j\pi} = e^{j\pi/2}$$

From the design condition $\psi_{TM} - \psi_{TE} = \pi/8$, we obtain the required value of x and then of θ. Using a trigonometric identity, we have:

$$\tan(\psi_{TM} - \psi_{TE}) = \frac{\tan\psi_{TM} - \tan\psi_{TE}}{1 + \tan\psi_{TM}\tan\psi_{TE}} = \frac{xn^2 - x}{1 + n^2x^2} = \tan\left(\frac{\pi}{8}\right)$$

This gives the quadratic equation for x:

$$x^2 - \frac{1}{\tan(\pi/8)}\left(1 - \frac{1}{n^2}\right)x + \frac{1}{n^2} = x^2 - \frac{\cos^2\theta_c}{\tan(\pi/8)}\,x + \sin^2\theta_c = 0 \tag{7.5.6}$$

Inserting the two solutions of (7.5.6) into Eq. (7.5.5), we may solve for $\sin\theta$, obtaining two possible solutions for θ:

$$\sin\theta = \sqrt{\frac{x^2 + \sin^2\theta_c}{x^2 + 1}} \tag{7.5.7}$$

We may also eliminate x and express the design condition directly in terms of θ:

$$\frac{\cos\theta\sqrt{\sin^2\theta - \sin^2\theta_c}}{\sin^2\theta} = \tan\left(\frac{\pi}{8}\right) \tag{7.5.8}$$

However, the two-step process is computationally more convenient. For $n = 1.51$, we find the two roots of Eq. (7.5.6): $x = 0.822$ and $x = 0.534$. Then, (7.5.7) gives the two values $\theta = 54.623^o$ and $\theta = 48.624^o$. The rhomb could just as easily be designed with the second value of θ.

For $n = 1.50$, we find the angles $\theta = 53.258^o$ and 50.229^o. For $n = 1.52$, we have $\theta = 55.458^o$ and 47.553^o. See Problem 7.5 for an equivalent approach. □

Example 7.5.7: *Goos-Hänchen Effect.* When a beam of light is reflected obliquely from a denser-to-rarer interface at an angle greater than the TIR angle, it suffers a lateral displacement, relative to the ordinary reflected ray, known as the Goos-Hänchen shift, as shown Fig. 7.5.7.

Let n, n' be the refractive indices of the two media with $n > n'$, and consider first the case of ordinary reflection at an incident angle $\theta_0 < \theta_c$. For a plane wave with a free-space wavenumber $k_0 = \omega/c_0$ and wavenumber components $k_x = k_0 n\sin\theta_0$, $k_z = k_0 n\cos\theta_0$, the corresponding incident, reflected, and transmitted transverse electric fields will be:

$$\begin{aligned} E_i(x,z) &= e^{-jk_x x}e^{-jk_z z} \\ E_r(x,z) &= \rho(k_x)e^{-jk_x x}e^{+jk_z z} \\ E_t(x,z) &= \tau(k_x)e^{-jk_x x}e^{-jk'_z z}\,, \quad k'_z = \sqrt{k_0^2 n'^2 - k_x^2} \end{aligned}$$

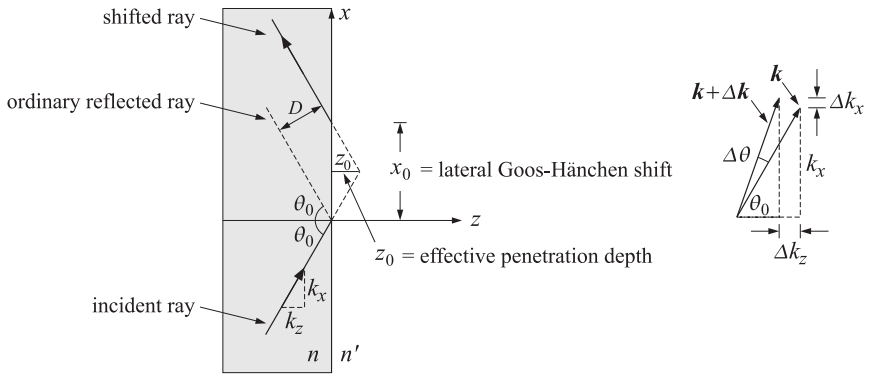

Fig. 7.5.7 Goos-Hänchen shift, with $n > n'$ and $\theta_0 > \theta_c$.

where $\rho(k_x)$ and $\tau(k_x) = 1 + \rho(k_x)$ are the transverse reflection and transmission coefficients, viewed as functions of k_x. For TE and TM polarizations, $\rho(k_x)$ is given by

$$\rho_{TE}(k_x) = \frac{k_z - k_z'}{k_z + k_z'}, \quad \rho_{TM}(k_x) = \frac{k_z' n^2 - k_z n'^2}{k_z' n^2 + k_z n'^2}$$

A beam can be made up by forming a linear combination of such plane waves having a small spread of angles about θ_0. For example, consider a second plane wave with wavenumber components $k_x + \Delta k_x$ and $k_z + \Delta k_z$. These must satisfy $(k_x + \Delta k_x)^2 + (k_z + \Delta k_z)^2 = k_x^2 + k_z^2 = k_0^2 n^2$, or to lowest order in Δk_x,

$$k_x \Delta k_x + k_z \Delta k_z = 0 \quad \Rightarrow \quad \Delta k_z = -\Delta k_x \frac{k_x}{k_z} = -\Delta k_x \tan\theta_0$$

Similarly, we have for the transmitted wavenumber $\Delta k_z' = -\Delta k_x \tan\theta_0'$, where θ_0' is given by Snel's law, $n \sin\theta_0 = n' \sin\theta_0'$. The incident, reflected, and transmitted fields will be given by the sum of the two plane waves:

$$\begin{aligned}
E_i(x,z) &= e^{-jk_x x} e^{-jk_z z} + e^{-j(k_x+\Delta k_x)x} e^{-j(k_z+\Delta k_z)z} \\
E_r(x,z) &= \rho(k_x) e^{-jk_x x} e^{+jk_z z} + \rho(k_x+\Delta k_x) e^{-j(k_x+\Delta k_x)x} e^{+j(k_z+\Delta k_z)z} \\
E_t(x,z) &= \tau(k_x) e^{-jk_x x} e^{-jk_z' z} + \tau(k_x+\Delta k_x) e^{-j(k_x+\Delta k_x)x} e^{-j(k_z'+\Delta k_z')z}
\end{aligned}$$

Replacing $\Delta k_z = -\Delta k_x \tan\theta_0$ and $\Delta k_z' = -\Delta k_x \tan\theta_0'$, we obtain:

$$\begin{aligned}
E_i(x,z) &= e^{-jk_x x} e^{-jk_z z} \left[1 + e^{-j\Delta k_x (x - z\tan\theta_0)}\right] \\
E_r(x,z) &= e^{-jk_x x} e^{+jk_z z} \left[\rho(k_x) + \rho(k_x+\Delta k_x) e^{-j\Delta k_x (x + z\tan\theta_0)}\right] \\
E_t(x,z) &= e^{-jk_x x} e^{-jk_z' z} \left[\tau(k_x) + \tau(k_x+\Delta k_x) e^{-j\Delta k_x (x - z\tan\theta_0')}\right]
\end{aligned} \tag{7.5.9}$$

The incidence angle of the second wave is $\theta_0 + \Delta\theta$, where $\Delta\theta$ is obtained by expanding $k_x + \Delta k_x = k_0 n \sin(\theta_0 + \Delta\theta)$ to first order, or, $\Delta k_x = k_0 n \cos\theta_0 \, \Delta\theta$. If we assume that $\theta_0 < \theta_c$, as well as $\theta_0 + \Delta\theta < \theta_c$, then $\rho(k_x)$ and $\rho(k_x + \Delta k_x)$ are both real-valued. It

follows that the two terms in the reflected wave $E_r(x,z)$ will differ by a small amplitude change and therefore we can set $\rho(k_x + \Delta k_x) \simeq \rho(k_x)$. Similarly, in the transmitted field we may set $\tau(k_x + \Delta k_x) \simeq \tau(k_x)$. Thus, when $\theta_0 < \theta_c$, Eq. (7.5.9) reads approximately,

$$\begin{aligned}
E_i(x,z) &= e^{-jk_x x} e^{-jk_z z} \left[1 + e^{-j\Delta k_x (x - z\tan\theta_0)}\right] \\
E_r(x,z) &= \rho(k_x) e^{-jk_x x} e^{+jk_z z} \left[1 + e^{-j\Delta k_x (x + z\tan\theta_0)}\right] \\
E_t(x,z) &= \tau(k_x) e^{-jk_x x} e^{-jk_z' z} \left[1 + e^{-j\Delta k_x (x - z\tan\theta_0')}\right]
\end{aligned} \tag{7.5.10}$$

Noting that $\left|1 + e^{-j\Delta k_x (x - z\tan\theta_0)}\right| \leq 2$, with equality achieved when $x - z\tan\theta_0 = 0$, it follows that the intensities of these waves are maximized along the ordinary geometric rays defined by the beam angles θ_0 and θ_0', that is, along the straight lines:

$$\begin{aligned}
&x - z\tan\theta_0 = 0, \quad \text{incident ray} \\
&x + z\tan\theta_0 = 0, \quad \text{reflected ray} \\
&x - z\tan\theta_0' = 0, \quad \text{transmitted ray}
\end{aligned} \tag{7.5.11}$$

On the other hand, if $\theta_0 > \theta_c$ and $\theta_0 + \Delta\theta > \theta_c$, the reflection coefficients become unimodular complex numbers, as in Eq. (7.5.5). Writing $\rho(k_x) = e^{j\phi(k_x)}$, Eq. (7.5.9) gives:

$$E_r(x,z) = e^{-jk_x x} e^{+jk_z z} \left[e^{j\phi(k_x)} + e^{j\phi(k_x+\Delta k_x)} e^{-j\Delta k_x (x + z\tan\theta_0)}\right] \tag{7.5.12}$$

Introducing the Taylor series expansion, $\phi(k_x + \Delta k_x) \simeq \phi(k_x) + \Delta k_x \, \phi'(k_x)$, we obtain:

$$E_r(x,z) = e^{j\phi(k_x)} e^{-jk_x x} e^{+jk_z z} \left[1 + e^{j\Delta k_x \phi'(k_x)} e^{-j\Delta k_x (x + z\tan\theta_0)}\right]$$

Setting $x_0 = \phi'(k_x)$, we have:

$$E_r(x,z) = e^{j\phi(k_x)} e^{-jk_x x} e^{+jk_z z} \left[1 + e^{-j\Delta k_x (x - x_0 + z\tan\theta_0)}\right] \tag{7.5.13}$$

This implies that the maximum intensity of the reflected beam will now be along the shifted ray defined by:

$$x - x_0 + z\tan\theta_0 = 0, \quad \text{shifted reflected ray} \tag{7.5.14}$$

Thus, the origin of the Goos-Hänchen shift can be traced to the relative phase shifts arising from the reflection coefficients in the plane-wave components making up the beam. The parallel displacement, denoted by D in Fig. 7.5.7, is related to x_0 by $D = x_0 \cos\theta_0$. Noting that $dk_x = k_0 n \cos\theta \, d\theta$, we obtain

$$\boxed{D = \cos\theta_0 \frac{d\phi}{dk_x} = \frac{1}{k_0 n} \frac{d\phi}{d\theta}\bigg|_{\theta_0}} \quad \text{(Goos-Hänchen shift)} \tag{7.5.15}$$

Using Eq. (7.5.5), we obtain the shifts for the TE and TM cases:

$$D_{TE} = \frac{2\sin\theta_0}{k_0 n \sqrt{\sin^2\theta_0 - \sin^2\theta_c}}, \quad D_{TM} = D_{TE} \cdot \frac{n'^2}{(n^2 + n'^2)\sin^2\theta_0 - n'^2} \tag{7.5.16}$$

These expressions are not valid near the critical angle $\theta_0 \simeq \theta_c$ because then the Taylor series expansion for $\phi(k_x)$ cannot be justified. Since geometrically, $z_0 = D/(2\sin\theta_0)$, it follows from (7.5.16) that the effective penetration depth into the n' medium is given by:

$$z_{TE} = \frac{1}{k_0 n \sqrt{\sin^2\theta_0 - \sin^2\theta_c}} = \frac{1}{\alpha_z'}, \quad z_{TM} = \frac{1}{\alpha_z'} \frac{n'^2}{(n^2 + n'^2)\sin^2\theta_0 - n'^2} \tag{7.5.17}$$

where $\alpha'_z = \sqrt{k_x^2 - k_0^2 n'^2} = k_0\sqrt{n^2\sin^2\theta_0 - n'^2} = k_0 n\sqrt{\sin^2\theta_0 - \sin^2\theta_c}$. These expressions are consistent with the field dependence $e^{-jk'_z z} = e^{-\alpha'_z z}$ inside the n' medium, which shows that the effective penetration length is of the order of $1/\alpha'_z$. □

7.6 Brewster Angle

The Brewster angle is that angle of incidence at which the TM Fresnel reflection coefficient vanishes, $\rho_{TM} = 0$. The TE coefficient ρ_{TE} cannot vanish for any angle θ, for non-magnetic materials. A scattering model of Brewster's law is discussed in [693]. Fig. 7.6.1 depicts the Brewster angles from either side of an interface.

The Brewster angle is also called the *polarizing* angle because if a mixture of TM and TE waves are incident on a dielectric interface at that angle, only the TE or perpendicularly polarized waves will be reflected. This is not necessarily a good method of generating polarized waves because even though ρ_{TE} is non-zero, it may be too small to provide a useful amount of reflected power. Better polarization methods are based on using (a) multilayer structures with alternating low/high refractive indices and (b) birefringent and dichroic materials, such as calcite and polaroids.

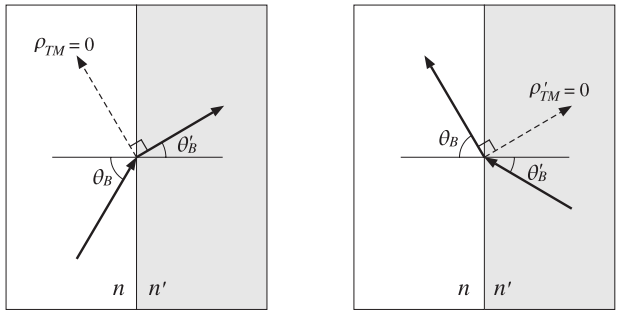

Fig. 7.6.1 Brewster angles.

The Brewster angle θ_B is determined by the condition, $\rho_{TM} = 0$, in Eq. (7.4.2). Setting the numerator of that expression to zero, we have:

$$\sqrt{\left(\frac{n'}{n}\right)^2 - \sin^2\theta_B} = \left(\frac{n'}{n}\right)^2 \cos\theta_B \tag{7.6.1}$$

After some algebra, we obtain the alternative expressions:

$$\boxed{\sin\theta_B = \frac{n'}{\sqrt{n^2+n'^2}}} \quad\Leftrightarrow\quad \boxed{\tan\theta_B = \frac{n'}{n}} \qquad \text{(Brewster angle)} \tag{7.6.2}$$

Similarly, the Brewster angle θ'_B from the other side of the interface is:

$$\boxed{\sin\theta'_B = \frac{n}{\sqrt{n^2+n'^2}}} \quad\Leftrightarrow\quad \boxed{\tan\theta'_B = \frac{n}{n'}} \qquad \text{(Brewster angle)} \tag{7.6.3}$$

The angle θ'_B is related to θ_B by Snel's law, $n'\sin\theta'_B = n\sin\theta_B$, and corresponds to zero reflection from that side, $\rho'_{TM} = -\rho_{TM} = 0$. A consequence of Eq. (7.6.2) is that $\theta_B = 90^o - \theta'_B$, or, $\theta_B + \theta'_B = 90^o$. Indeed,

$$\frac{\sin\theta_B}{\cos\theta_B} = \tan\theta_B = \frac{n'}{n} = \frac{\sin\theta_B}{\sin\theta'_B}$$

which implies $\cos\theta_B = \sin\theta'_B$, or $\theta_B = 90^o - \theta'_B$. The same conclusion can be reached immediately from Eq. (7.4.3). Because, $\theta'_B - \theta_B \neq 0$, the only way for the ratio of the two tangents to vanish is for the denominator to be infinity, that is, $\tan(\theta'_B + \theta_B) = \infty$, or, $\theta_B + \theta'_B = 90^o$.

As shown in Fig. 7.6.1, the angle of the refracted ray with the would-be reflected ray is 90^o. Indeed, this angle is $180^o - (\theta'_B + \theta_B) = 180^o - 90^o = 90^o$.

The TE reflection coefficient at θ_B can be calculated very simply by using Eq. (7.6.1) into (7.4.2). After canceling a common factor of $\cos\theta_B$, we find:

$$\rho_{TE}(\theta_B) = \frac{1 - \left(\frac{n'}{n}\right)^2}{1 + \left(\frac{n'}{n}\right)^2} = \frac{n^2 - n'^2}{n^2 + n'^2} \tag{7.6.4}$$

Example 7.6.1: *Brewster angles for water.* The Brewster angles from the air and the water sides of an air-water interface are:

$$\theta_B = \text{atan}\left(\frac{1.333}{1}\right) = 53.1^o\,, \quad \theta'_B = \text{atan}\left(\frac{1}{1.333}\right) = 36.9^o$$

We note that $\theta_B + \theta'_B = 90^o$. At RF, the refractive index is $n_{\text{water}} = 9$ and we find $\theta_B = 83.7^o$ and $\theta'_B = 6.3^o$. We also find $\rho_{TE}(\theta_B) = -0.2798$ and $|\rho_{TE}(\theta_B)|^2 = 0.0783/$ Thus, for TE waves, only 7.83% of the incident power gets reflected at the Brewster angle. □

Example 7.6.2: *Brewster Angles for Glass.* The Brewster angles for the two sides of an air-glass interface are:

$$\theta_B = \text{atan}\left(\frac{1.5}{1}\right) = 56.3^o\,, \quad \theta'_B = \text{atan}\left(\frac{1}{1.5}\right) = 33.7^o$$

Fig. 7.6.2 shows the reflection coefficients $|\rho_{TM}(\theta)|, |\rho_{TE}(\theta)|$ as functions of the angle of incidence θ from the air side, calculated with the MATLAB function `fresnel`.

Both coefficients start at their normal-incidence value $|\rho| = |(1-1.5)/(1+1.5)| = 0.2$ and tend to unity at grazing angle $\theta = 90^o$. The TM coefficient vanishes at the Brewster angle $\theta_B = 56.3^o$.

The right graph in the figure depicts the reflection coefficients $|\rho'_{TM}(\theta')|, |\rho'_{TE}(\theta')|$ as functions of the incidence angle θ' from the glass side. Again, the TM coefficient vanishes at the Brewster angle $\theta'_B = 33.7^o$. The typical MATLAB code for generating this graph was:

```
na = 1; nb = 1.5;
[thb,thc]  = brewster(na,nb);          % calculate Brewster angle
th = linspace(0,90,901);               % equally-spaced angles at 0.1° intervals
[rte,rtm] = fresnel(na,nb,th);         % Fresnel reflection coefficients
plot(th,abs(rtm), th,abs(rte));
```

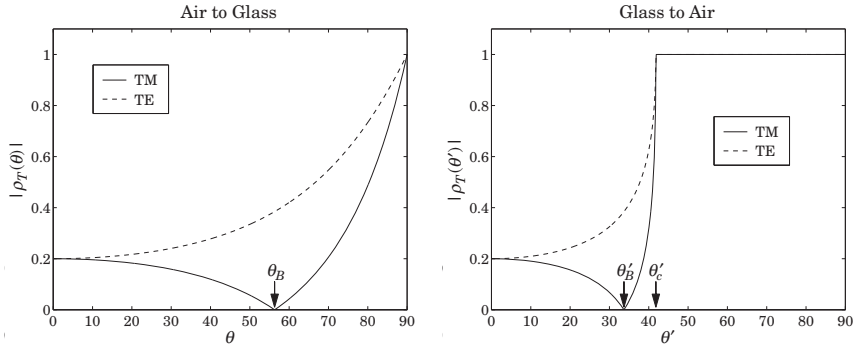

Fig. 7.6.2 TM and TE reflection coefficients versus angle of incidence.

The critical angle of reflection is in this case $\theta'_c = \text{asin}(1/1.5) = 41.8^\circ$. As soon as θ' exceeds θ'_c, both coefficients become complex-valued with unit magnitude.

The value of the TE reflection coefficient at the Brewster angle is $\rho_{TE} = -\rho'_{TE} = -0.38$, and the TE reflectance $|\rho_{TE}|^2 = 0.144$, or 14.4 percent. This is too small to be useful for generating TE polarized waves by reflection.

Two properties are evident from Fig. 7.6.2. One is that $|\rho_{TM}| \leq |\rho_{TE}|$ for all angles of incidence. The other is that $\theta'_B \leq \theta'_c$. Both properties can be proved in general. □

Example 7.6.3: *Lossy dielectrics.* The Brewster angle loses its meaning if one of the media is lossy. For example, assuming a complex refractive index for the dielectric, $n_d = n_r - jn_i$, we may still calculate the reflection coefficients from Eq. (7.4.4). It follows from Eq. (7.6.2) that the Brewster angle θ_B will be complex-valued.

Fig. 7.6.3 shows the TE and TM reflection coefficients versus the angle of incidence θ (from air) for the two cases $n_d = 1.50 - 0.15j$ and $n_d = 1.50 - 0.30j$ and compares them with the lossless case of $n_d = 1.5$. (The values for n_i were chosen only for plotting purposes and have no physical significance.)

The curves retain much of their lossless shape, with the TM coefficient having a minimum near the lossless Brewster angle. The larger the extinction coefficient n_i, the larger the deviation from the lossless case. In the next section, we discuss reflection from lossy media in more detail. □

7.7 Complex Waves

In this section, we discuss some examples of complex waves that appear in oblique incidence problems. We consider the cases of (a) total internal reflection, (b) reflection from and refraction into a lossy medium, (c) the Zenneck surface wave, and (d) surface plasmons. Further details may be found in [902–909] and [1293].

Because the wave numbers become complex-valued, e.g., $\boldsymbol{k} = \boldsymbol{\beta} - j\boldsymbol{\alpha}$, the angle of refraction and possibly the angle of incidence may become complex-valued. To avoid

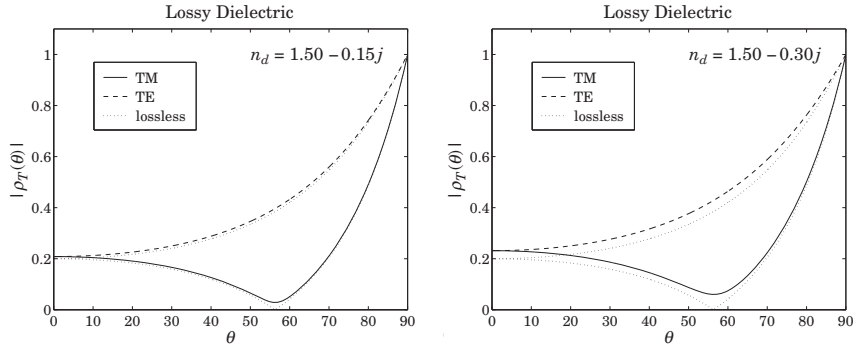

Fig. 7.6.3 TM and TE reflection coefficients for lossy dielectric.

unnecessary complex algebra, it proves convenient to recast impedances, reflection coefficients, and field expressions in terms of wavenumbers. This can be accomplished by making substitutions such as $\cos\theta = k_z/k$ and $\sin\theta = k_x/k$.

Using the relationships $k\eta = \omega\mu$ and $k/\eta = \omega\epsilon$, we may rewrite the TE and TM transverse impedances in the forms:

$$\eta_{TE} = \frac{\eta}{\cos\theta} = \frac{\eta k}{k_z} = \frac{\omega\mu}{k_z}, \qquad \eta_{TM} = \eta\cos\theta = \frac{\eta k_z}{k} = \frac{k_z}{\omega\epsilon} \tag{7.7.1}$$

We consider an interface geometry as shown in Fig. 7.1.1 and assume that there are no incident fields from the right of the interface. Snel's law implies that $k_x = k'_x$, where $k_x = k\sin\theta = \omega\sqrt{\mu_0\epsilon}\sin\theta$, if the incident angle is real-valued.

Assuming non-magnetic media from both sides of an interface ($\mu = \mu' = \mu_0$), the TE and TM transverse reflection coefficients will take the forms:

$$\rho_{TE} = \frac{\eta'_{TE} - \eta_{TE}}{\eta'_{TE} + \eta_{TE}} = \frac{k_z - k'_z}{k_z + k'_z}, \qquad \rho_{TM} = \frac{\eta'_{TM} - \eta_{TM}}{\eta'_{TM} + \eta_{TM}} = \frac{k'_z\epsilon - k_z\epsilon'}{k'_z\epsilon + k_z\epsilon'} \tag{7.7.2}$$

The corresponding transmission coefficients will be:

$$\tau_{TE} = 1 + \rho_{TE} = \frac{2k_z}{k_z + k'_z}, \qquad \tau_{TM} = 1 + \rho_{TM} = \frac{2k'_z\epsilon}{k'_z\epsilon + k_z\epsilon'} \tag{7.7.3}$$

We can now rewrite Eqs. (7.2.18) and (7.2.20) in terms of transverse amplitudes and transverse reflection and transmission coefficients. Defining $E_0 = A_+\cos\theta$ or $E_0 = B_+$ in the TM or TE cases and replacing $\tan\theta = k_x/k_z$, $\tan\theta' = k'_x/k'_z = k_x/k'_z$, we have for the TE case for the fields at the left and right sides of the interface:

$$\begin{aligned}
\boldsymbol{E}(\boldsymbol{r}) &= \hat{\mathbf{y}}\, E_0\left[e^{-jk_z z} + \rho_{TE}\, e^{jk_z z}\right] e^{-jk_x x} \\
\boldsymbol{H}(\boldsymbol{r}) &= \frac{E_0}{\eta_{TE}}\left[\left(-\hat{\mathbf{x}} + \frac{k_x}{k_z}\,\hat{\mathbf{z}}\right) e^{-jk_z z} + \rho_{TE}\left(\hat{\mathbf{x}} + \frac{k_x}{k_z}\,\hat{\mathbf{z}}\right) e^{jk_z z}\right] e^{-jk_x x} \\
\boldsymbol{E}'(\boldsymbol{r}) &= \hat{\mathbf{y}}\, \tau_{TE} E_0 e^{-jk'_z z} e^{-jk_x x} \\
\boldsymbol{H}'(\boldsymbol{r}) &= \frac{\tau_{TE} E_0}{\eta'_{TE}}\left(-\hat{\mathbf{x}} + \frac{k_x}{k'_z}\,\hat{\mathbf{z}}\right) e^{-jk'_z z} e^{-jk_x x}
\end{aligned} \qquad \text{(TE)} \qquad (7.7.4)$$

and for the TM case:

$$\begin{aligned}
\boldsymbol{E}(\boldsymbol{r}) &= E_0\left[\left(\hat{\mathbf{x}} - \frac{k_x}{k_z}\,\hat{\mathbf{z}}\right) e^{-jk_z z} + \rho_{TM}\left(\hat{\mathbf{x}} + \frac{k_x}{k_z}\,\hat{\mathbf{z}}\right) e^{jk_z z}\right] e^{-jk_x x} \\
\boldsymbol{H}(\boldsymbol{r}) &= \hat{\mathbf{y}}\,\frac{E_0}{\eta_{TM}}\left[e^{-jk_z z} - \rho_{TM}\, e^{jk_z z}\right] e^{-jk_x x} \\
\boldsymbol{E}'(\boldsymbol{r}) &= \tau_{TM} E_0\left(\hat{\mathbf{x}} - \frac{k_x}{k'_z}\,\hat{\mathbf{z}}\right) e^{-jk'_z z} e^{-jk_x x} \\
\boldsymbol{H}'(\boldsymbol{r}) &= \hat{\mathbf{y}}\,\frac{\tau_{TM} E_0}{\eta'_{TM}} e^{-jk'_z z} e^{-jk_x x}
\end{aligned} \qquad \text{(TM)} \qquad (7.7.5)$$

Equations (7.7.4) and (7.7.5) are dual to each other, as are Eqs. (7.7.1). They transform into each other under the duality transformation $\boldsymbol{E} \to \boldsymbol{H}$, $\boldsymbol{H} \to -\boldsymbol{E}$, $\epsilon \to \mu$, and $\mu \to \epsilon$. See Sec. 18.2 for more on the concept of duality.

In all of our complex-wave examples, the transmitted wave will be complex with $\boldsymbol{k}' = k_x\hat{\mathbf{x}} + k'_z\hat{\mathbf{z}} = \boldsymbol{\beta}' - j\boldsymbol{\alpha}' = (\beta_x - j\alpha_x)\hat{\mathbf{x}} + (\beta'_z - j\alpha'_z)\hat{\mathbf{z}}$. This must satisfy the constraint $\boldsymbol{k}' \cdot \boldsymbol{k}' = \omega^2\mu_0\epsilon'$. Thus, the space dependence of the transmitted fields will have the general form:

$$e^{-jk'_z z} e^{-jk_x x} = e^{-j(\beta'_z - j\alpha'_z)z} e^{-j(\beta_x - j\alpha_x)x} = e^{-(\alpha'_z z + \alpha_x x)} e^{-j(\beta'_z z + \beta_x x)} \qquad (7.7.6)$$

For the wave to attenuate at large distances into the right medium, it is required that $\alpha'_z > 0$. Except for the Zenneck-wave case, which has $\alpha_x > 0$, all other examples will have $\alpha_x = 0$, corresponding to a real-valued wavenumber $k'_x = k_x = \beta_x$. Fig. 7.7.1 shows the constant-amplitude and constant-phase planes within the transmitted medium defined, respectively, by:

$$\alpha'_z z + \alpha_x x = \text{const.}\,, \qquad \beta'_z z + \beta_x x = \text{const.} \qquad (7.7.7)$$

As shown in the figure, the corresponding angles ϕ and ψ that the vectors $\boldsymbol{\beta}'$ and $\boldsymbol{\alpha}'$ form with the z-axis are given by:

$$\tan\phi = \frac{\beta_x}{\beta'_z}\,, \qquad \tan\psi = \frac{\alpha_x}{\alpha'_z} \qquad (7.7.8)$$

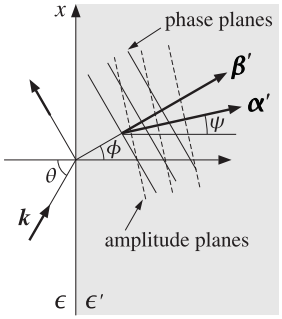

Fig. 7.7.1 Constant-phase and constant-amplitude planes for the transmitted wave.

The wave numbers k_z, k'_z are related to k_x through

$$k_z^2 = \omega^2\mu\epsilon - k_x^2\,, \quad k_z'^2 = \omega^2\mu\epsilon' - k_x^2$$

In calculating k_z and k'_z by taking square roots of the above expressions, it is necessary, in complex-waves problems, to get the correct signs of their imaginary parts, such that evanescent waves are described correctly. This leads us to define an "evanescent" square root as follows. Let $\epsilon = \epsilon_R - j\epsilon_I$ with $\epsilon_I > 0$ for an absorbing medium, then

$$k_z = \text{sqrte}\left(\omega^2\mu(\epsilon_R - j\epsilon_I) - k_x^2\right) = \begin{cases} \sqrt{\omega^2\mu(\epsilon_R - j\epsilon_I) - k_x^2}\,, & \text{if } \epsilon_I \neq 0 \\ -j\sqrt{k_x^2 - \omega^2\mu\epsilon_R}\,, & \text{if } \epsilon_I = 0 \end{cases} \qquad (7.7.9)$$

If $\epsilon_I = 0$ and $\omega^2\mu\epsilon_R - k_x^2 > 0$, then the two expressions give the same answer. But if $\epsilon_I = 0$ and $\omega^2\mu\epsilon_R - k_x^2 < 0$, then k_z is correctly calculated from the second expression. The MATLAB function `sqrte.m` implements the above definition. It is defined by

$$y = \text{sqrte}(z) = \begin{cases} -j\sqrt{|z|}\,, & \text{if } \text{Re}(z) < 0 \text{ and } \text{Im}(z) = 0 \\ \sqrt{z}\,, & \text{otherwise} \end{cases} \qquad \text{(evanescent SQRT)} \quad (7.7.10)$$

Some examples of the issues that arise in taking such square roots are elaborated in the next few sections.

7.8 Total Internal Reflection

We already discussed this case in Sec. 7.5. Here, we look at it from the point of view of complex-waves. Both media are assumed to be lossless, but with $\epsilon > \epsilon'$. The angle of incidence θ will be real, so that $k'_x = k_x = k\sin\theta$ and $k_z = k\cos\theta$, with $k = \omega\sqrt{\mu_0\epsilon}$. Setting $k'_z = \beta'_z - j\alpha'_z$, we have the constraint equation:

$$k_x'^2 + k_z'^2 = k'^2 \quad \Rightarrow \quad k_z'^2 = (\beta'_z - j\alpha'_z)^2 = \omega^2\mu_0\epsilon' - k_x^2 = \omega^2\mu_0(\epsilon' - \epsilon\sin^2\theta)$$

which separates into the real and imaginary parts:

$$\begin{aligned} \beta_z'^2 - \alpha_z'^2 &= \omega^2\mu_0(\epsilon' - \epsilon\sin^2\theta) = k^2(\sin^2\theta_c - \sin^2\theta) \\ \alpha_z'\beta_z' &= 0 \end{aligned} \tag{7.8.1}$$

where we set $\sin^2\theta_c = \epsilon'/\epsilon$ and $k^2 = \omega^2\mu_0\epsilon$. This has two solutions: (a) $\alpha_z' = 0$ and $\beta_z'^2 = k^2(\sin^2\theta_c - \sin^2\theta)$, valid when $\theta \le \theta_c$, and (b) $\beta_z' = 0$ and $\alpha_z'^2 = k^2(\sin^2\theta - \sin^2\theta_c)$, valid when $\theta \ge \theta_c$.

Case (a) corresponds to ordinary refraction into the right medium, and case (b), to total internal reflection. In the latter case, we have $k_z' = -j\alpha_z'$ and the TE and TM reflection coefficients (7.7.2) become unimodular complex numbers:

$$\rho_{TE} = \frac{k_z - k_z'}{k_z + k_z'} = \frac{k_z + j\alpha_z'}{k_z - j\alpha_z'}, \qquad \rho_{TM} = \frac{k_z'\epsilon - k_z\epsilon'}{k_z'\epsilon + k_z\epsilon'} = -\frac{k_z\epsilon' + j\alpha_z'\epsilon}{k_z\epsilon' - j\alpha_z'\epsilon} \tag{7.8.2}$$

The complete expressions for the fields are given by Eqs. (7.7.4) or (7.7.5). The propagation phase factor in the right medium will be in case (b):

$$e^{-jk_z'z}e^{-jk_xx} = e^{-\alpha_z'z}e^{-jk_xx}$$

Thus, the constant-phase planes are the constant-x planes ($\phi = 90^o$), or, the yz-planes. The constant-amplitude planes are the constant-z planes ($\psi = 0^o$), or, the xy-planes, as shown in Fig. 7.8.1.

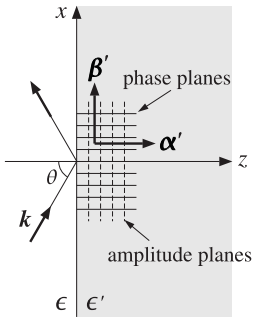

Fig. 7.8.1 Constant-phase and constant-amplitude planes for total internal reflection ($\theta \ge \theta_c$).

It follows from Eq. (7.8.2) that in case (b) the phases of the reflection coefficients are:

$$\begin{aligned} \rho_{TE} &= e^{2j\psi_{TE}}, \qquad \tan\psi_{TE} = \frac{\alpha_z'}{k_z} = \frac{\sqrt{k_x^2 - k_0^2n'^2}}{\sqrt{k_0^2n^2 - k_x^2}} = \frac{\sqrt{\sin^2\theta - \sin^2\theta_c}}{\cos\theta} \\ \rho_{TM} &= e^{j\pi + 2j\psi_{TM}}, \quad \tan\psi_{TM} = \frac{n^2\alpha_z'}{n'^2k_z} = \frac{n^2\sqrt{k_x^2 - k_0^2n'^2}}{n'^2\sqrt{k_0^2n^2 - k_x^2}} = \frac{n^2\sqrt{\sin^2\theta - \sin^2\theta_c}}{n'^2\cos\theta} \end{aligned} \tag{7.8.3}$$

where $k_0 = \omega\sqrt{\mu\epsilon_0}$ is the free-space wave number.

7.9 Oblique Incidence on a Lossy Medium

Here, we assume a lossless medium on the left side of the interface and a lossy one, such as a conductor, on the right. The effective dielectric constant ϵ' of the lossy medium is specified by its real and imaginary parts, as in Eq. (2.6.2):

$$\epsilon' = \epsilon_d' - j\left(\epsilon_d'' + \frac{\sigma}{\omega}\right) = \epsilon_R' - j\epsilon_I' \tag{7.9.1}$$

Equivalently, we may characterize the lossy medium by the real and imaginary parts of the wavenumber k', using Eq. (2.6.12):

$$k' = \beta' - j\alpha' = \omega\sqrt{\mu_0\epsilon'} = \omega\sqrt{\mu_0(\epsilon_R' - j\epsilon_I')} \tag{7.9.2}$$

In the left medium, the wavenumber is real with components $k_x = k\sin\theta$, $k_z = k\cos\theta$, with $k = \omega\sqrt{\mu_0\epsilon}$. In the lossy medium, the wavenumber is complex-valued with components $k_x' = k_x$ and $k_z' = \beta_z' - j\alpha_z'$. Using Eq. (7.9.2) in the condition $\boldsymbol{k}' \cdot \boldsymbol{k}' = k'^2$, we obtain:

$$k_x'^2 + k_z'^2 = k'^2 \quad \Rightarrow \quad k_x^2 + (\beta_z' - j\alpha_z')^2 = (\beta' - j\alpha')^2 = \omega^2\mu_0(\epsilon_R' - j\epsilon_I') \tag{7.9.3}$$

which separates into its real and imaginary parts:

$$\begin{aligned} \beta_z'^2 - \alpha_z'^2 &= \beta'^2 - \alpha'^2 - k_x^2 = \omega^2\mu_0\epsilon_R' - k_x^2 = \omega^2\mu_0(\epsilon_R' - \epsilon\sin^2\theta) \equiv D_R \\ 2\beta_z'\alpha_z' &= 2\beta'\alpha' = \omega^2\mu_0\epsilon_I' \equiv D_I \end{aligned} \tag{7.9.4}$$

where we replaced $k_x^2 = k^2\sin^2\theta = \omega^2\mu_0\epsilon\sin^2\theta$. The solutions of Eqs. (7.9.4) leading to a non-negative α_z' are:

$$\beta_z' = \left[\frac{\sqrt{D_R^2 + D_I^2} + D_R}{2}\right]^{1/2}, \quad \alpha_z' = \left[\frac{\sqrt{D_R^2 + D_I^2} - D_R}{2}\right]^{1/2} \tag{7.9.5}$$

For MATLAB implementation, it is simpler to solve Eq. (7.9.3) directly as a complex square root (but see also Eq. (7.9.10)):

$$k_z' = \beta_z' - j\alpha_z' = \sqrt{k'^2 - k_x^2} = \sqrt{\omega^2\mu_0(\epsilon_R' - j\epsilon_I') - k_x^2} = \sqrt{D_R - jD_I} \tag{7.9.6}$$

Eqs. (7.9.5) define completely the reflection coefficients (7.7.2) and the field solutions for both TE and TM waves given by Eqs. (7.7.4) and (7.7.5). Within the lossy medium the transmitted fields will have space-dependence:

$$e^{-jk_z'z}e^{-jk_xx} = e^{-\alpha_z'z}e^{-j(\beta_z'z + k_xx)}$$

The fields attenuate exponentially with distance z. The constant phase and amplitude planes are shown in Fig. 7.9.1.

For the reflected fields, the TE and TM reflection coefficients are given by Eqs. (7.7.2). If the incident wave is linearly polarized having both TE and TM components, the corresponding reflected wave will be elliptically polarized because the ratio ρ_{TM}/ρ_{TE} is now

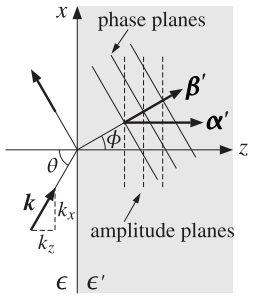

Fig. 7.9.1 Constant-phase and constant-amplitude planes for refracted wave.

complex-valued. Indeed, using the relationships $k_x^2+k_z^2 = \omega^2\mu_0\epsilon$ and $k_x^2+k_z'^2 = \omega^2\mu_0\epsilon'$ in ρ_{TM} of Eq. (7.7.2), it can be shown that (see Problem 7.5):

$$\frac{\rho_{TM}}{\rho_{TE}} = \frac{k_z k_z' - k_x^2}{k_z k_z' + k_x^2} = \frac{k_z' - k\sin\theta\tan\theta}{k_z' + k\sin\theta\tan\theta} = \frac{\beta_z' - j\alpha_z' - k\sin\theta\tan\theta}{\beta_z' - j\alpha_z' + k\sin\theta\tan\theta} \tag{7.9.7}$$

In the case of a lossless medium, $\epsilon' = \epsilon_R'$ and $\epsilon_I' = 0$, Eq. (7.9.5) gives:

$$\beta_z' = \sqrt{\frac{|D_R| + D_R}{2}}, \quad \alpha_z' = \sqrt{\frac{|D_R| - D_R}{2}} \tag{7.9.8}$$

If $\epsilon_R' > \epsilon$, then $D_R = \omega^2\mu_0(\epsilon_R' - \epsilon\sin^2\theta)$ is positive for all angles θ, and (7.9.8) gives the expected result $\beta_z' = \sqrt{D_R} = \omega\sqrt{\mu_0(\epsilon_R' - \epsilon\sin^2\theta)}$ and $\alpha_z' = 0$.

On the other hand, in the case of total internal reflection, that is, when $\epsilon_R' < \epsilon$, the quantity D_R is positive for angles $\theta < \theta_c$, and negative for $\theta > \theta_c$, where the critical angle is defined through $\epsilon_R' = \epsilon\sin^2\theta_c$ so that $D_R = \omega^2\mu_0(\sin^2\theta_c - \sin^2\theta)$. Eqs. (7.9.8) still give the right answers, that is, $\beta_z' = \sqrt{|D_R|}$ and $\alpha_z' = 0$, if $\theta \le \theta_c$, and $\beta_z' = 0$ and $\alpha_z' = \sqrt{|D_R|}$, if $\theta > \theta_c$.

For the case of a very good conductor, we have $\epsilon_I' \gg \epsilon_R'$, or $D_I \gg |D_R|$, and Eqs. (7.9.5) give $\beta_z' \simeq \alpha_z' \simeq \sqrt{D_I/2}$, or

$$\beta_z' \simeq \alpha_z' \simeq \beta' \simeq \alpha' \simeq \sqrt{\frac{\omega\mu_0\sigma}{2}}, \qquad \text{provided} \quad \frac{\sigma}{\omega\epsilon} \gg 1 \tag{7.9.9}$$

In this case, the angle of refraction ϕ for the phase vector $\boldsymbol{\beta}'$ becomes almost zero so that, regardless of the incidence angle θ, the phase planes are almost parallel to the constant-z amplitude planes. Using Eq. (7.9.9), we have:

$$\tan\phi = \frac{k_x}{\beta_z'} = \frac{\omega\sqrt{\mu_0\epsilon}\sin\theta}{\sqrt{\omega\mu_0\sigma/2}} = \sqrt{\frac{2\omega\epsilon}{\sigma}}\sin\theta$$

which is very small regardless of θ. For example, for copper ($\sigma = 5.7\times10^7$ S/m) at 10 GHz, and air on the left side ($\epsilon = \epsilon_0$), we find $\sqrt{2\omega\epsilon/\sigma} = 1.4\times10^{-4}$.

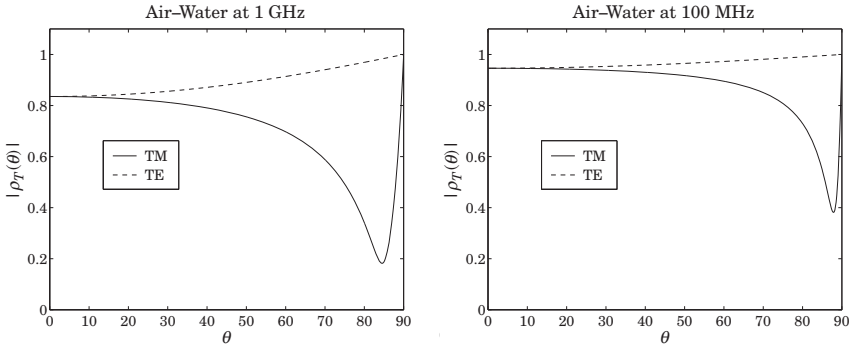

Fig. 7.9.2 TM and TE reflection coefficients for air-water interface.

Example 7.9.1: Fig. 7.9.2 shows the TM and TE reflection coefficients as functions of the incident angle θ, for an air-sea water interface at 100 MHz and 1 GHz. For the air side we have $\epsilon = \epsilon_0$ and for the water side: $\epsilon' = 81\epsilon_0 - j\sigma/\omega$, with $\sigma = 4$ S/m, which gives $\epsilon' = (81 - 71.9j)\epsilon_0$ at 1 GHz and $\epsilon' = (81 - 719j)\epsilon_0$ at 100 MHz.

At 1 GHz, we calculate $k' = \omega\sqrt{\mu_0\epsilon'} = \beta' - j\alpha' = 203.90 - 77.45j$ rad/m and $k' = \beta' - j\alpha' = 42.04 - 37.57j$ rad/m at 100 MHz. The following MATLAB code was used to carry out the calculations, using the formulation of this section:

```
ep0 = 8.854e-12; mu0 = 4*pi*1e-7;
sigma = 4; f = 1e9; w = 2*pi*f;
ep1 = ep0; ep2 = 81*ep0 - j*sigma/w;

k1 = w*sqrt(mu0*ep1); k2 = w*sqrt(mu0*ep2);                % Eq. (7.9.2)

th = linspace(0,90,901); thr = pi*th/180;

k1x = k1*sin(thr); k1z = k1*cos(thr);
k2z = sqrt(w^2*mu0*ep2 - k1x.^2);                          % Eq. (7.9.6)

rte = abs((k1z - k2z)./(k1z + k2z));                       % Eq. (7.7.2)
rtm = abs((k2z*ep1 - k1z*ep2)./(k2z*ep1 + k1z*ep2));

plot(th,rtm, th,rte);
```

The TM reflection coefficient reaches a minimum at the pseudo-Brewster angles 84.5° and 87.9°, respectively for 1 GHz and 100 MHz.

The reflection coefficients ρ_{TM} and ρ_{TE} can just as well be calculated from Eq. (7.4.2), with $n = 1$ and $n' = \sqrt{\epsilon'/\epsilon_0}$, where for 1 GHz we have $n' = \sqrt{81 - 71.9j} = 9.73 - 3.69j$, and for 100 MHz, $n' = \sqrt{81 - 719j} = 20.06 - 17.92j$. □

In computing the complex square roots in Eq. (7.9.6), MATLAB usually gets the right answer, that is, $\beta_z' \ge 0$ and $\alpha_z' \ge 0$.

If $\epsilon_R' > \epsilon$, then $D_R = \omega^2\mu_0(\epsilon_R' - \epsilon\sin^2\theta)$ is positive for all angles θ, and (7.9.6) may be used without modification for any value of ϵ_I'.

If $\epsilon'_R < \epsilon$ and $\epsilon'_I > 0$, then Eq. (7.9.6) still gives the correct algebraic signs for any angle θ. But when $\epsilon'_I = 0$, that is, for a lossless medium, then $D_I = 0$ and $k'_z = \sqrt{D_R}$. For $\theta > \theta_c$ we have $D_R < 0$ and MATLAB gives $k'_z = \sqrt{D_R} = \sqrt{-|D_R|} = j\sqrt{|D_R|}$, which has the wrong sign for α'_z (we saw that Eqs. (7.9.5) work correctly in this case.)

In order to coax MATLAB to produce the right algebraic sign for α'_z in all cases, we may redefine Eq. (7.9.6) by using double conjugation:

$$k'_z = \beta'_z - j\alpha'_z = \left(\sqrt{(D_R - jD_I)^*}\right)^* = \begin{cases} -j\sqrt{|D_R|}\,, & \text{if } D_I = 0 \text{ and } D_R < 0 \\ \sqrt{D_R - jD_I}\,, & \text{otherwise} \end{cases} \tag{7.9.10}$$

One word of caution, however, is that current versions of MATLAB (ver. ≤ 7.0) may produce inconsistent results for (7.9.10) depending on whether D_I is a scalar or a vector passing through zero.† Compare, for example, the outputs from the statements:

```
DI = 0;    kz = conj(sqrt(conj(-1 - j*DI)));
DI = -1:1; kz = conj(sqrt(conj(-1 - j*DI)));
```

Note, however, that Eq. (7.9.10) does work correctly when D_I is a single scalar with D_R being a vector of values, e.g., arising from a vector of angles θ.

Another possible alternative calculation is to add a small negative imaginary part to the argument of the square root, for example with the MATLAB code:

```
kz = sqrt(DR-j*DI-j*realmin);
```

where `realmin` is MATLAB's smallest positive floating point number (typically, equal to 2.2251×10^{-308}). This works well for all cases. Yet, a third alternative is to use Eq. (7.9.6) and then reverse the signs whenever $D_I = 0$ and $D_R < 0$, for example:

```
kz = sqrt(DR-j*DI);
kz(DI==0 & DR<0) = -kz(DI==0 & DR<0);
```

Next, we discuss briefly the energy flux into the lossy medium. It is given by the z-component of the Poynting vector, $\mathcal{P}_z = \frac{1}{2}\hat{\mathbf{z}} \cdot \mathrm{Re}(\boldsymbol{E} \times \boldsymbol{H}^*)$. For the TE case of Eq. (7.7.4), we find at the two sides of the interface:

$$\mathcal{P}_z = \frac{|E_0|^2}{2\omega\mu_0} k_z (1 - |\rho_{TE}|^2)\,, \quad \mathcal{P}'_z = \frac{|E_0|^2}{2\omega\mu_0} \beta'_z |\tau_{TE}|^2 e^{-2\alpha'_z z} \tag{7.9.11}$$

where we replaced $\eta_{TE} = \omega\mu_0/k_z$ and $\eta'_{TE} = \omega\mu_0/k'_z$. Thus, the transmitted power attenuates with distance as the wave propagates into the lossy medium.

The two expressions match at the interface, expressing energy conservation, that is, at $z = 0$, we have $\mathcal{P}_z = \mathcal{P}'_z$, which follows from the condition (see Problem 7.7):

$$k_z (1 - |\rho_{TE}|^2) = \beta'_z |\tau_{TE}|^2 \tag{7.9.12}$$

Because the net energy flow is to the right in the transmitted medium, we must have $\beta'_z \geq 0$. Because also $k_z > 0$, then Eq. (7.9.12) implies that $|\rho_{TE}| \leq 1$. For the case of

† this has been fixed in versions > v7.0.

total internal reflection, we have $\beta'_z = 0$, which gives $|\rho_{TE}| = 1$. Similar conclusions can be reached for the TM case of Eq. (7.7.5). The matching condition at the interface is now:

$$\frac{\epsilon}{k_z}(1 - |\rho_{TM}|^2) = \mathrm{Re}\left(\frac{\epsilon'}{k'_z}\right)|\tau_{TM}|^2 = \frac{\epsilon'_R \beta'_z + \epsilon'_I \alpha'_z}{|k'_z|^2}|\tau_{TM}|^2 \tag{7.9.13}$$

Using the constraint $\omega^2\mu_o\epsilon'_I = 2\beta'_z\alpha'_z$, it follows that the right-hand side will again be proportional to β'_z (with a positive proportionality coefficient.) Thus, the non-negative sign of β'_z implies that $|\rho_{TM}| \leq 1$.

7.10 Zenneck Surface Wave

For a lossy medium ϵ', the TM reflection coefficient cannot vanish for any real incident angle θ because the Brewster angle is complex valued: $\tan\theta_B = \sqrt{\epsilon'/\epsilon} = \sqrt{(\epsilon'_R - j\epsilon'_I)/\epsilon}$.

However, ρ_{TM} can vanish if we allow a complex-valued θ, or equivalently, a complex-valued incident wavevector $\boldsymbol{k} = \boldsymbol{\beta} - j\boldsymbol{\alpha}$, even though the left medium is lossless. This leads to the so-called Zenneck surface wave [32,902,903,909,1293].

The corresponding constant phase and amplitude planes in both media are shown in Fig. 7.10.1. On the lossless side, the vectors $\boldsymbol{\beta}$ and $\boldsymbol{\alpha}$ are necessarily orthogonal to each other, as discussed in Sec. 2.11.

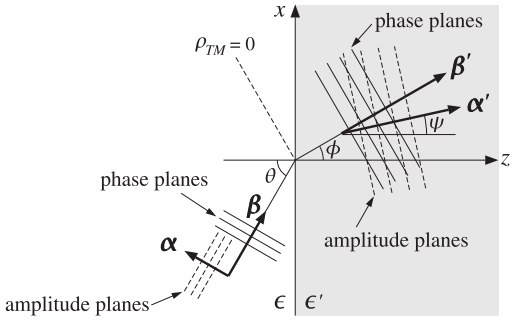

Fig. 7.10.1 Constant-phase and constant-amplitude planes for the Zenneck wave.

We note that the TE reflection coefficient can never vanish (unless $\mu \neq \mu'$) because this would require that $k'_z = k_z$, which together with Snel's law $k'_x = k_x$, would imply that $\boldsymbol{k} = \boldsymbol{k}'$, which is impossible for distinct media.

For the TM case, the fields are given by Eq. (7.7.5) with $\rho_{TM} = 0$ and $\tau_{TM} = 1$. The condition $\rho_{TM} = 0$ requires that $k'_z\epsilon = k_z\epsilon'$, which may be written in the equivalent form $k'_z k^2 = k_z k'^2$. Together with $k_x^2 + k_z^2 = k^2$ and $k_x^2 + k_z'^2 = k'^2$, we have three equations in the three complex unknowns k_x, k_z, k'_z. The solution is easily found to be:

$$k_x = \frac{kk'}{\sqrt{k^2 + k'^2}}\,, \quad k_z = \frac{k^2}{\sqrt{k^2 + k'^2}}\,, \quad k'_z = \frac{k'^2}{\sqrt{k^2 + k'^2}} \tag{7.10.1}$$

where $k = \omega\sqrt{\mu_0\epsilon}$ and $k' = \beta' - j\alpha' = \omega\sqrt{\mu_0\epsilon'}$. These may be written in the form:

$$k_x = \omega\sqrt{\mu_0}\sqrt{\frac{\epsilon\epsilon'}{\epsilon+\epsilon'}}\,, \quad k_z = \omega\sqrt{\mu_0}\,\frac{\epsilon}{\sqrt{\epsilon+\epsilon'}}\,, \quad k'_z = \omega\sqrt{\mu_0}\,\frac{\epsilon'}{\sqrt{\epsilon+\epsilon'}} \tag{7.10.2}$$

Using $k'_x = k_x$, the space-dependence of the fields at the two sides is as follows:

$$e^{-j(k_x x + k_z z)} = e^{-(\alpha_x x + \alpha_z z)}\, e^{-j(\beta_x x + \beta_z z)}\,, \quad \text{for } z \le 0$$

$$e^{-j(k'_x x + k'_z z)} = e^{-(\alpha_x x + \alpha'_z z)}\, e^{-j(\beta_x x + \beta'_z z)}\,, \quad \text{for } z \ge 0$$

Thus, in order for the fields not to grow exponentially with distance and to be confined near the interface surface, it is required that:

$$\alpha_x > 0\,, \quad \alpha_z < 0\,, \quad \alpha'_z > 0 \tag{7.10.3}$$

These conditions are guaranteed with the sign choices of Eq. (7.10.2). This can be verified by writing

$$\epsilon' = |\epsilon'|e^{-j\delta}$$

$$\epsilon + \epsilon' = |\epsilon + \epsilon'|e^{-j\delta_1}$$

$$\frac{\epsilon'}{\epsilon+\epsilon'} = \left|\frac{\epsilon'}{\epsilon+\epsilon'}\right| e^{-j(\delta-\delta_1)}$$

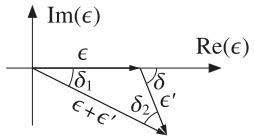

and noting that $\delta_2 = \delta - \delta_1 > 0$, as follows by inspecting the triangle formed by the three vectors ϵ, ϵ', and $\epsilon + \epsilon'$. Then, the phase angles of k_x, k_z, k'_z are $-\delta_2/2$, $\delta_1/2$, and $-(\delta_2 + \delta_1/2)$, respectively, thus, implying the condition (7.10.3). In drawing this triangle, we made the implicit assumption that $\epsilon'_R > 0$, which is valid for typical lossy dielectrics. In the next section, we discuss surface plasmons for which $\epsilon'_R < 0$.

Although the Zenneck wave attenuates both along the x- and z-directions, the attenuation constant along x tends to be much smaller than that along z. For example, in the weakly lossy approximation, we may write $\epsilon' = \epsilon'_R(1 - j\tau)$, where $\tau = \epsilon'_I/\epsilon'_R \ll 1$ is the loss tangent of ϵ'. Then, we have the following first-order approximations in τ:

$$\sqrt{\epsilon'} = \sqrt{\epsilon'_R}\left(1 - j\frac{\tau}{2}\right), \quad \frac{1}{\sqrt{\epsilon+\epsilon'}} = \frac{1}{\sqrt{\epsilon+\epsilon'_R}}\left(1 + j\frac{\tau}{2}\frac{\epsilon'_R}{\epsilon+\epsilon'_R}\right)$$

These lead to the first-order approximations for k_x and k_z:

$$k_x = \omega\sqrt{\mu_0}\sqrt{\frac{\epsilon\epsilon'_R}{\epsilon+\epsilon'_R}}\left(1 - j\frac{\tau}{2}\frac{\epsilon}{\epsilon+\epsilon'_R}\right), \qquad k_z = \omega\sqrt{\mu_0}\,\frac{\epsilon}{\sqrt{\epsilon+\epsilon'_R}}\left(1 + j\frac{\tau}{2}\frac{\epsilon'_R}{\epsilon+\epsilon'_R}\right)$$

It follows that:

$$\alpha_x = \omega\sqrt{\mu_0}\sqrt{\frac{\epsilon\epsilon'_R}{\epsilon+\epsilon'_R}}\,\frac{\tau}{2}\,\frac{\epsilon}{\epsilon+\epsilon'_R}\,, \quad \alpha_z = -\omega\sqrt{\mu_0}\,\frac{\epsilon}{\sqrt{\epsilon+\epsilon'_R}}\,\frac{\tau}{2}\,\frac{\epsilon'_R}{\epsilon+\epsilon'_R} \quad \Rightarrow \quad \frac{\alpha_x}{|\alpha_z|} = \sqrt{\frac{\epsilon}{\epsilon'_R}}$$

Typically, $\epsilon'_R > \epsilon$, implying that $\alpha_x < |\alpha_z|$. For example, for an air-water interface we have at microwave frequencies $\epsilon'_R/\epsilon = 81$, and for an air-ground interface, $\epsilon'_R/\epsilon = 6$.

If both media are lossless, then both $\boldsymbol{k}$ and $\boldsymbol{k}'$ are real and Eqs. (7.10.1) yield the usual Brewster angle formulas, that is,

$$\tan\theta_B = \frac{k_x}{k_z} = \frac{k'}{k} = \frac{\sqrt{\epsilon'}}{\sqrt{\epsilon}}\,, \quad \tan\theta'_B = \frac{k_x}{k'_z} = \frac{k}{k'} = \frac{\sqrt{\epsilon}}{\sqrt{\epsilon'}}$$

Example 7.10.1: For the data of the air-water interface of Example 7.9.1, we calculate the following Zenneck wavenumbers at 1 GHz and 100 MHz using Eq. (7.10.2):

f = 1 GHz	f = 100 MHz
$k_x = \beta_x - j\alpha_x = 20.89 - 0.064j$	$k_x = \beta_x - j\alpha_x = 2.1 - 0.001j$
$k_z = \beta_z - j\alpha_z = 1.88 + 0.71j$	$k_z = \beta_z - j\alpha_z = 0.06 + 0.05j$
$k'_z = \beta'_z - j\alpha'_z = 202.97 - 77.80j$	$k'_z = \beta'_z - j\alpha'_z = 42.01 - 37.59j$

The units are in rads/m. As required, α_x is negative. We observe that $\alpha_x \ll |\alpha_z|$ and that the attenuations are much more severe within the lossy medium. □

7.11 Surface Plasmons

Consider an interface between two non-magnetic semi-infinite media ϵ_1 and ϵ_2, as shown in Fig. 7.11.1 The wavevectors $\boldsymbol{k}_1 = \hat{\mathbf{x}}k_x + \hat{\mathbf{z}}k_{z1}$ and $\boldsymbol{k}_2 = \hat{\mathbf{x}}k_x + \hat{\mathbf{z}}k_{z2}$ at the two sides must have a common k_x component, as required by Snel's law, and their z-components must satisfy:

$$k_{z1}^2 = k_0^2\varepsilon_1 - k_x^2\,, \quad k_{z2}^2 = k_0^2\varepsilon_2 - k_x^2 \tag{7.11.1}$$

where we defined the *relative* dielectric constants $\varepsilon_1 = \epsilon_1/\epsilon_0$, $\varepsilon_2 = \epsilon_2/\epsilon_0$, and the free-space wavenumber $k_0 = \omega\sqrt{\mu_0\epsilon_0} = \omega/c_0$. The TM reflection coefficient is given by:

$$\rho_{TM} = \frac{k_{z2}\varepsilon_1 - k_{z1}\varepsilon_2}{k_{z2}\varepsilon_1 + k_{z1}\varepsilon_2}$$

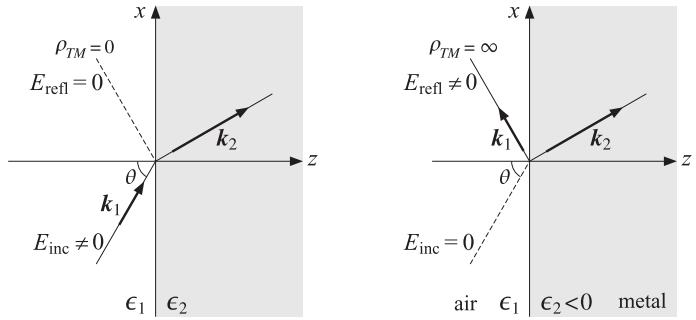

Fig. 7.11.1 Brewster-Zenneck ($\rho_{TM} = 0$) and surface plasmon ($\rho_{TM} = \infty$) cases.

Both the Brewster case for lossless dielectrics and the Zenneck case were characterized by the condition $\rho_{TM} = 0$, or, $k_{z2}\varepsilon_1 = k_{z1}\varepsilon_2$. This condition together with Eqs. (7.11.1) leads to the solution (7.10.2), which is the same in both cases:

$$k_x = k_0\sqrt{\frac{\varepsilon_1\varepsilon_2}{\varepsilon_1+\varepsilon_2}}\,,\quad k_{z1} = \frac{k_0\varepsilon_1}{\sqrt{\varepsilon_1+\varepsilon_2}}\,,\quad k_{z2} = \frac{k_0\varepsilon_2}{\sqrt{\varepsilon_1+\varepsilon_2}} \tag{7.11.2}$$

Surface plasmons or polaritons are waves that are propagating along the interface and attenuate exponentially perpendicularly to the interface in both media. They are characterized by a *pole* of the reflection coefficient, that is, $\rho_{TM} = \infty$. For such waves to exist, it is necessary to have the conditions:

$$\varepsilon_1\varepsilon_2 < 0 \quad\text{and}\quad \varepsilon_1+\varepsilon_2 < 0 \tag{7.11.3}$$

at least for the real-parts of these quantities, assuming their imaginary parts are small. If the left medium is an ordinary lossless dielectric $\varepsilon_1 > 0$, such as air, then we must have $\varepsilon_2 < 0$ and more strongly $\varepsilon_2 < -\varepsilon_1$. Conductors, such as silver and gold, have this property for frequencies typically up to ultraviolet. Indeed, using the simple conductivity model (1.12.3), we have for the dielectric constant of a metal:

$$\epsilon(\omega) = \epsilon_0 + \frac{\sigma}{j\omega} = \epsilon_0 + \frac{\epsilon_0\omega_p^2}{j\omega(j\omega+\gamma)} \quad\Rightarrow\quad \varepsilon(\omega) = 1 - \frac{\omega_p^2}{\omega^2 - j\omega\gamma} \tag{7.11.4}$$

Ignoring the imaginary part for the moment, we have

$$\varepsilon(\omega) = 1 - \frac{\omega_p^2}{\omega^2}$$

which is negative for $\omega < \omega_p$. The plasma frequency is of the order of 1000–2000 THz, and falls in the ultraviolet range. Thus, the condition (7.11.3) is easily met for optical frequencies. If $\varepsilon_1 = 1$, then, the condition $\varepsilon_2 < -\varepsilon_1$ requires further that

$$\varepsilon_2 = 1 - \frac{\omega_p^2}{\omega^2} < -1 \quad\Rightarrow\quad \omega < \frac{\omega_p}{\sqrt{2}}$$

and more generally, $\omega < \omega_p/\sqrt{1+\varepsilon_1}$. The condition $\rho_{TM} = \infty$ means that there is only a "reflected" wave, while the incident field is zero. Indeed, it follows from $E_{\text{refl}} = \rho_{TM}E_{\text{inc}}$, or $E_{\text{inc}} = E_{\text{refl}}/\rho_{TM}$, that E_{inc} will tend to zero for finite E_{refl} and $\rho_{TM} \to \infty$.

The condition $\rho_{TM} = \infty$ is equivalent to the vanishing of the denominator of ρ_{TM}, that is, $k_{z2}\varepsilon_1 = -k_{z1}\varepsilon_2$, which together with Eqs. (7.11.1) leads to a similar solution as (7.10.2), but with a change in sign for k_{z2}:

$$k_x = k_0\sqrt{\frac{\varepsilon_1\varepsilon_2}{\varepsilon_1+\varepsilon_2}}\,,\quad k_{z1} = \frac{k_0\varepsilon_1}{\sqrt{\varepsilon_1+\varepsilon_2}}\,,\quad k_{z2} = -\frac{k_0\varepsilon_2}{\sqrt{\varepsilon_1+\varepsilon_2}} \tag{7.11.5}$$

The fields at the two sides of the interface are given by Eqs. (7.7.5) by taking the limit $\rho_{TM} \to \infty$ and $\tau_{TM} = 1 + \rho_{TM} \to \infty$, which effectively amounts to keeping only the terms that involve ρ_{TM}. The fields have a z-dependence $e^{jk_{z1}z}$ on the left and $e^{-jk_{z2}z}$ on the right, and a common x-dependence e^{-jk_xx}:

$$\begin{aligned} \boldsymbol{E}_1 &= E_0\left(\hat{\mathbf{x}} + \frac{k_x}{k_{z1}}\hat{\mathbf{z}}\right)e^{jk_{z1}z}\,e^{-jk_xx} \\ \boldsymbol{H}_1 &= -\hat{\mathbf{y}}\,E_0\,\frac{\omega\epsilon_1}{k_{z1}}\,e^{jk_{z1}z}\,e^{-jk_xx} \end{aligned} \qquad \begin{aligned} \boldsymbol{E}_2 &= E_0\left(\hat{\mathbf{x}} - \frac{k_x}{k_{z2}}\hat{\mathbf{z}}\right)e^{-jk_{z2}z}\,e^{-jk_xx} \\ \boldsymbol{H}_2 &= \hat{\mathbf{y}}\,E_0\,\frac{\omega\epsilon_2}{k_{z2}}\,e^{-jk_{z2}z}\,e^{-jk_xx} \end{aligned} \tag{7.11.6}$$

It can be verified easily that these are solutions of Maxwell's equations provided that Eqs. (7.11.1) are satisfied. The boundary conditions are also satisfied. Indeed, the E_x components are the same from both sides, and the conditions $\varepsilon_1E_{z1} = \varepsilon_2E_{z2}$ and $H_{y1} = H_{y2}$ are both equivalent to the pole condition $k_{z2}\varepsilon_1 = -k_{z1}\varepsilon_2$.

The conditions (7.11.3) guarantee that k_x is real and k_{z1}, k_{z_2}, pure imaginary. Setting $\varepsilon_2 = -\varepsilon_{2r}$ with $\varepsilon_{2r} > \varepsilon_1$, we have $\sqrt{\varepsilon_1+\varepsilon_2} = \sqrt{\varepsilon_1-\varepsilon_{2r}} = j\sqrt{\varepsilon_{2r}-\varepsilon_1}$, and $\sqrt{\varepsilon_1\varepsilon_2} = \sqrt{-\varepsilon_1\varepsilon_{2r}} = j\sqrt{\varepsilon_1\varepsilon_{2r}}$. Then, Eqs. (7.11.5) read

$$k_x = k_0\sqrt{\frac{\varepsilon_1\varepsilon_{2r}}{\varepsilon_{2r}-\varepsilon_1}}\,,\quad k_{z1} = -j\,\frac{k_0\varepsilon_1}{\sqrt{\varepsilon_{2r}-\varepsilon_1}}\,,\quad k_{z2} = -j\,\frac{k_0\varepsilon_{2r}}{\sqrt{\varepsilon_{2r}-\varepsilon_1}} \tag{7.11.7}$$

Setting $k_{z1} = -j\alpha_{z1}$ and $k_{z2} = -j\alpha_{z2}$, with both αs positive, the z-dependence at both sides of the interface at $z = 0$ will be:

$$e^{jk_{z1}z} = e^{\alpha_{z1}z} \quad\Big|\quad e^{-jk_{z2}z} = e^{-\alpha_{z2}z}$$

that is, exponentially decaying for both $z < 0$ and $z > 0$. Inserting $\varepsilon_{2r} = \omega_p^2/\omega^2 - 1$ into k_x gives the so-called plasmon dispersion relationship, For example, if $\varepsilon_1 = 1$,

$$k_x^2 = \frac{\omega^2}{c_0^2}\,\frac{\omega_p^2-\omega^2}{\omega_p^2-2\omega^2}$$

Defining the normalized variables $\bar{\omega} = \omega/\omega_p$ and $\bar{k} = k_x/k_p$, where $k_p = \omega_p/c_0$, we may rewrite the above relationship as,

$$\bar{k}^2 = \bar{\omega}^2\,\frac{1-\bar{\omega}^2}{1-2\bar{\omega}^2}$$

with solution

$$\bar{\omega} = \sqrt{\bar{k}^2 + \frac{1}{2} - \sqrt{\bar{k}^4 + \frac{1}{4}}} \tag{7.11.8}$$

It is depicted in Fig. 7.11.2. In the large k_x limit, it converges to the horizontal line $\omega = \omega_p/\sqrt{2}$. For small k_x, it becomes the dispersion relationship in vacuum, $\omega = c_0k_x$, which is also depicted in this figure.

Because the curve stays to the right of the vacuum line $\omega = c_0k_x$, that is, $k_x > \omega/c_0$, such surface plasmon waves cannot be excited by an impinging plane wave on the interface. However, they can be excited with the help of frustrated total internal reflection, which increases k_x beyond its vacuum value and can match the value of Eq. (7.11.7) resulting into a so-called surface plasmon resonance. We discuss this further in Sec. 8.5.

In fact, the excitation of such plasmon resonance can only take place if the metal side is slightly lossy, that is, when $\varepsilon_2 = -\varepsilon_{2r} - j\varepsilon_{2i}$, with $0 < \varepsilon_{2i} \ll \varepsilon_{2r}$. In this case, the wavenumber k_x acquires a small imaginary part which causes the gradual attenuation of the wave along the surface, and similarly, k_{z1}, k_{z2}, acquire small real parts. Replacing ε_{2r} by $\varepsilon_{2r} + j\varepsilon_{2i}$ in (7.11.7), we now have:

$$k_x = k_0\sqrt{\frac{\varepsilon_1(\varepsilon_{2r}+j\varepsilon_{2i})}{\varepsilon_{2r}+j\varepsilon_{2i}-\varepsilon_1}}\,,\quad k_{z1} = \frac{-jk_0\varepsilon_1}{\sqrt{\varepsilon_{2r}+j\varepsilon_{2i}-\varepsilon_1}}\,,\quad k_{z2} = \frac{-jk_0(\varepsilon_{2r}+j\varepsilon_{2i})}{\sqrt{\varepsilon_{2r}+j\varepsilon_{2i}-\varepsilon_1}} \tag{7.11.9}$$

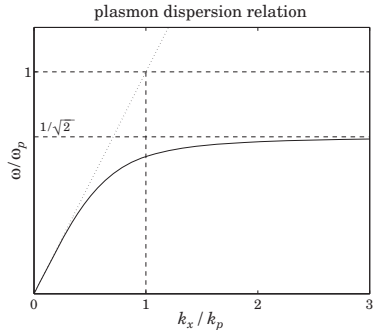

Fig. 7.11.2 Surface plasmon dispersion relationship.

Expanding k_x to first-order in ε_{2i}, we obtain the approximations:

$$k_x = \beta_x - j\alpha_x\,, \quad \beta_x = k_0\sqrt{\frac{\varepsilon_1\varepsilon_{2r}}{\varepsilon_{2r}-\varepsilon_1}}\,, \quad \alpha_x = k_0\left(\frac{\varepsilon_1\varepsilon_{2r}}{\varepsilon_{2r}-\varepsilon_1}\right)^{3/2}\frac{\varepsilon_{2i}}{2\varepsilon_{2r}^2} \tag{7.11.10}$$

Example 7.11.1: Using the value $\varepsilon_2 = -16 - 0.5j$ for silver at $\lambda_0 = 632$ nm, and air $\varepsilon_1 = 1$, we have $k_0 = 2\pi/\lambda_0 = 9.94$ rad/μm and Eqs. (7.11.9) give the following values for the wavenumbers and the corresponding effective propagation length and penetration depths:

$$k_x = \beta_x - j\alpha_x = 10.27 - 0.0107j \text{ rad}/\mu\text{m}, \qquad \delta_x = \frac{1}{\alpha_x} = 93.6\ \mu\text{m}$$

$$k_{z1} = \beta_{z1} - j\alpha_{z1} = -0.043 - 2.57j \text{ rad}/\mu\text{m}, \qquad \delta_{z1} = \frac{1}{\alpha_{z1}} = 390 \text{ nm}$$

$$k_{z2} = \beta_{z2} - j\alpha_{z2} = 0.601 - 41.12j \text{ rad}/\mu\text{m}, \qquad \delta_{z2} = \frac{1}{\alpha_{z2}} = 24 \text{ nm}$$

Thus, the fields extend more into the dielectric than the metal, but at either side they are confined to distances that are less than their free-space wavelength. □

Surface plasmons, and the emerging field of "plasmonics," are currently active areas of study [593–631] holding promise for the development of nanophotonic devices and circuits that take advantage of the fact that plasmons are confined to smaller spaces than their free-space wavelength and can propagate at decent distances in the nanoscale regime (i.e., tens of μm compared to nm scales.) They are also currently used in chemical and biological sensor technologies, and have other potential medical applications, such as cancer treatments.

7.12 Oblique Reflection from a Moving Boundary

In Sec. 5.8 we discussed reflection and transmission from a moving interface at normal incidence. Here, we present the oblique incidence case. The dielectric medium is

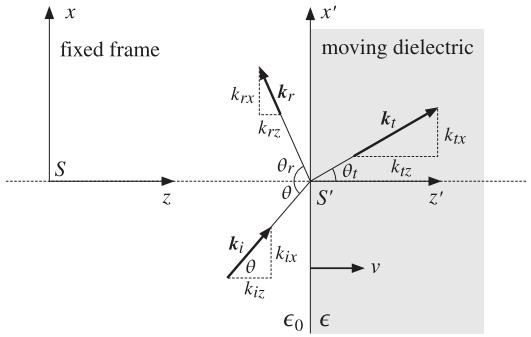

Fig. 7.12.1 Oblique reflection from a moving boundary.

assumed to be moving with velocity v perpendicularly to the interface, that is, in the z-direction as shown in Fig. 7.12.1. Other geometries may be found in [474–492].

Let S and S' be the stationary and the moving coordinate frames, whose coordinates $\{t,x,y,z\}$ and $\{t',x',y',z'\}$ are related by the Lorentz transformation of Eq. (K.1) of Appendix K.

We assume a TE plane wave of frequency ω incident obliquely at the moving interface at an angle θ, as measured in the stationary coordinate frame S. Let ω_r, ω_t be the Doppler-shifted frequencies, and θ_r, θ_t, the angles of the reflected and transmitted waves. Because of the motion, these angles no longer satisfy the usual Snel laws of reflection and refraction—however, the do satisfy modified versions of these laws.

In the moving frame S' with respect to which the dielectric is at rest, we have an ordinary TE oblique incidence problem, solved for example by Eq. (7.7.4), and therefore, all three frequencies will be the same, $\omega' = \omega'_r = \omega'_t$, and the corresponding angles $\theta', \theta'_r, \theta'_t$ will satisfy the ordinary Snel laws: $\theta'_r = \theta'$ and $\sin\theta' = n\sin\theta'_t$, where $n = \sqrt{\epsilon/\epsilon_0}$ and the left medium is assumed to be free space.

The electric field has only a y-component and will have the following form at the left and right sides of the interface, in the frame S and in the frame S':

$$\begin{aligned} E_y &= E_i e^{j\phi_i} + E_r e^{j\phi_r}\,, \qquad E_y = E_t e^{j\phi_t} \\ E'_y &= E'_i e^{j\phi'_i} + E'_r e^{j\phi'_r}\,, \qquad E'_y = E'_t e^{j\phi'_t} \end{aligned} \tag{7.12.1}$$

where $E'_r = \rho_{TE}E'_i$ and $E'_t = \tau_{TE}E'_i$, and from Eq. (7.7.2),

$$\rho_{TE} = \frac{k'_{iz} - k'_{tz}}{k'_{iz} + k'_{tz}} = \frac{\cos\theta' - n\cos\theta'_t}{\cos\theta' + n\cos\theta'_t}\,, \quad \tau_{TE} = 1 + \rho_{TE} = \frac{2\cos\theta'}{\cos\theta' + n\cos\theta'_t} \tag{7.12.2}$$

The propagation phases are Lorentz invariant in the two frames and are given by:

$$\begin{aligned} \phi_i &= \omega t - k_{iz}z - k_{ix}x = \omega' t' - k'_{iz}z' - k'_{ix}x' = \phi'_i \\ \phi_r &= \omega_r t + k_{rz}z - k_{rx}x = \omega' t' + k'_{rz}z' - k'_{rx}x' = \phi'_r \\ \phi_t &= \omega_t t - k_{tz}z - k_{tx}x = \omega' t' - k'_{tz}z' - k'_{tx}x' = \phi'_t \end{aligned} \tag{7.12.3}$$

with incident, reflected, and transmitted wavenumbers given in the frame S' by:

$$\begin{aligned} k'_{iz} &= k'_{rz} = k'_i \cos\theta' \,, \quad k'_{tz} = k'_t \cos\theta'_t \\ k'_{ix} &= k'_{rx} = k'_i \sin\theta' \,, \quad k'_{tx} = k'_t \sin\theta'_t \end{aligned} \tag{7.12.4}$$

where $k'_i = k'_r = \omega'/c$ and $k'_t = \omega'\sqrt{\epsilon\mu_0} = n\omega'/c$. The relationships between the primed and unprimed frequencies and wavenumbers are obtained by applying the Lorentz transformation (K.14) to the four-vectors $(\omega/c, k_{ix}, 0, k_{iz})$, $(\omega_r, k_{rx}, 0, -k_{rz})$, and $(\omega_t/c, k_{tx}, 0, k_{tz})$:

$$\begin{aligned} \omega &= \gamma(\omega' + \beta c k'_{iz}) = \omega'\gamma(1 + \beta\cos\theta') \\ k_{iz} &= \gamma(k'_{iz} + \frac{\beta}{c}\omega') = \frac{\omega'}{c}\gamma(\cos\theta' + \beta) \\ \omega_r &= \gamma(\omega' - \beta c k'_{rz}) = \omega'\gamma(1 - \beta\cos\theta') \\ -k_{rz} &= \gamma(-k'_{rz} + \frac{\beta}{c}\omega') = -\frac{\omega'}{c}\gamma(\cos\theta' - \beta) \\ \omega_t &= \gamma(\omega' + \beta c k'_{tz}) = \omega'\gamma(1 + \beta n\cos\theta'_t) \\ k_{tz} &= \gamma(k'_{tz} + \frac{\beta}{c}\omega') = \frac{\omega'}{c}\gamma(n\cos\theta'_t + \beta) \end{aligned} \tag{7.12.5}$$

where $\beta = v/c$ and $\gamma = 1/\sqrt{1-\beta^2}$. Combining Snel's laws for the system S' with the invariance of the x-components of the wavevector under the Lorentz transformation (K.14), we have also:

$$\begin{aligned} &k_{ix} = k_{rx} = k_{tx} = k'_{ix} = k'_{rx} = k'_{tx} \\ &k_i \sin\theta = k_r \sin\theta_r = k_t \sin\theta_t = \frac{\omega'}{c}\sin\theta' = \frac{\omega'}{c}\sin\theta'_r = n\frac{\omega'}{c}\sin\theta'_t \end{aligned} \tag{7.12.6}$$

Because the incident and reflected waves are propagating in free space, their wavenumbers will be $k_i = \omega/c$ and $k_r = \omega_r/c$. This also follows from the invariance of the scalar $(\omega/c)^2 - k^2$ under Lorentz transformations. Indeed, because $k'_i = k'_r = \omega'/c$ in the S' system, we will have:

$$\frac{\omega^2}{c^2} - k_i^2 = \frac{\omega'^2}{c^2} - k_i'^2 = 0 \,, \quad \frac{\omega_r^2}{c^2} - k_r^2 = \frac{\omega'^2}{c^2} - k_r'^2 = 0$$

For the transmitted wavenumber k_t, we find from Eqs. (7.12.5) and (7.12.6):

$$k_t = \sqrt{k_{tz}^2 + k_{tx}^2} = \frac{\omega'}{c}\sqrt{\gamma^2(n\cos\theta'_t + \beta)^2 + n^2\sin^2\theta'_t} \tag{7.12.7}$$

Setting $v_t = \omega_t/k_t = c/n_t$, we obtain the "effective" refractive index n_t within the moving dielectric medium:

$$n_t = \frac{c}{v_t} = \frac{ck_t}{\omega_t} = \frac{\sqrt{\gamma^2(n\cos\theta'_t + \beta)^2 + n^2\sin^2\theta'_t}}{\gamma(1 + \beta n\cos\theta'_t)} \tag{7.12.8}$$

At normal incidence, this is equivalent to Eq. (5.8.6). Replacing $k_i = \omega/c$, $k_r = \omega_r/c$, and $k_t = \omega_t n_t/c$ in Eq. (7.12.6), we obtain the generalization of Snel's laws:

$$\omega\sin\theta = \omega_r\sin\theta_r = \omega_t n_t \sin\theta_t = \omega'\sin\theta' = \omega'\sin\theta'_r = \omega' n\sin\theta'_t \tag{7.12.9}$$

For a stationary interface, all the frequency factors drop out and we obtain the ordinary Snel laws. The reflected and transmitted frequencies are θ-dependent and are obtained from (7.12.5) by eliminating ω':

$$\omega_r = \omega\frac{1 - \beta\cos\theta'}{1 + \beta\cos\theta'} \,, \quad \omega_t = \omega\frac{1 + \beta n\cos\theta'_t}{1 + \beta\cos\theta'} \tag{7.12.10}$$

Replacing $k_{iz} = k_i\cos\theta = (\omega/c)\cos\theta$ and $k_{rz} = k_r\cos\theta_r = (\omega_r/c)\cos\theta_r$ in Eq. (7.12.5), we obtain the relationship of the angles θ, θ_r to the angle θ':

$$\cos\theta = \frac{\cos\theta' + \beta}{1 + \beta\cos\theta'} \,, \quad \cos\theta_r = \frac{\cos\theta' - \beta}{1 - \beta\cos\theta'} \tag{7.12.11}$$

which can also be written as:

$$\cos\theta' = \frac{\cos\theta - \beta}{1 - \beta\cos\theta} = \frac{\cos\theta_r + \beta}{1 + \beta\cos\theta_r} \tag{7.12.12}$$

Solving for θ_r in terms of θ, we obtain:

$$\boxed{\cos\theta_r = \frac{(1+\beta^2)\cos\theta - 2\beta}{1 - 2\beta\cos\theta + \beta^2}} \tag{7.12.13}$$

Inserting $\cos\theta'$ in Eq. (7.12.10), we find the reflected frequency in terms of θ:

$$\boxed{\omega_r = \omega\frac{1 - 2\beta\cos\theta + \beta^2}{1 - \beta^2}} \tag{7.12.14}$$

Eqs. (7.12.13) and (7.12.14) were originally derived by Einstein in his 1905 paper on special relativity [474]. The quantity $n\cos\theta'_t$ can also be written in terms of θ. Using Snel's law and Eq. (7.12.12), we have:

$$n\cos\theta'_t = \sqrt{n^2 - \sin^2\theta'} = \sqrt{n^2 - 1 + \cos^2\theta'} = \sqrt{n^2 - 1 + \left(\frac{\cos\theta - \beta}{1 - \beta\cos\theta}\right)^2} \,, \quad \text{or,}$$

$$n\cos\theta'_t = \frac{\sqrt{(n^2-1)(1-\beta\cos\theta)^2 + (\cos\theta - \beta)^2}}{1 - \beta\cos\theta} \equiv \frac{Q}{1 - \beta\cos\theta} \tag{7.12.15}$$

Using (7.12.15) and the identity $(1 + \beta\cos\theta')(1 - \beta\cos\theta) = 1 - \beta^2$, we find for the transmitted frequency:

$$\omega_t = \omega\frac{1 + \beta n\cos\theta'_t}{1 + \beta\cos\theta'} = \omega\frac{1 - \beta\cos\theta + \beta Q}{1 - \beta^2} \tag{7.12.16}$$

The TE reflection coefficient (7.12.2) may also be expressed in terms of θ:

$$\rho_{TE} = \frac{\cos\theta' - n\cos\theta'_t}{\cos\theta' + n\cos\theta'_t} = \frac{\cos\theta - \beta - Q}{\cos\theta - \beta + Q} \tag{7.12.17}$$

Next, we determine the reflected and transmitted fields in the frame S. The simplest approach is to apply the Lorentz transformation (K.30) separately to the incident, reflected, and transmitted waves. In the S' frame, a plane wave propagating along the unit vector $\hat{\mathbf{k}}'$ has magnetic field:

$$\boldsymbol{H}' = \frac{1}{\eta}\hat{\mathbf{k}}'\times\boldsymbol{E}' \quad\Rightarrow\quad c\boldsymbol{B}' = c\mu_0\boldsymbol{H}' = \frac{\eta_0}{\eta}\hat{\mathbf{k}}'\times\boldsymbol{E}' = n\hat{\mathbf{k}}'\times\boldsymbol{E}' \tag{7.12.18}$$

where $n = 1$ for the incident and reflected waves. Because we assumed a TE wave and the motion is along the z-direction, the electric field will be perpendicular to the velocity, that is, $\boldsymbol{\beta}\cdot\boldsymbol{E}' = 0$. Using the BAC-CAB rule, Eq. (K.30) then gives:

$$\begin{aligned}\boldsymbol{E} = \boldsymbol{E}_\perp &= \gamma(\boldsymbol{E}'_\perp - \boldsymbol{\beta}\times c\boldsymbol{B}'_\perp) = \gamma(\boldsymbol{E}' - \boldsymbol{\beta}\times c\boldsymbol{B}') = \gamma\big(\boldsymbol{E}' - \boldsymbol{\beta}\times(n\hat{\mathbf{k}}'\times\boldsymbol{E}')\big)\\ &= \gamma(\boldsymbol{E}' - n(\boldsymbol{\beta}\cdot\boldsymbol{E}')\hat{\mathbf{k}}' + n(\boldsymbol{\beta}\cdot\hat{\mathbf{k}}')\boldsymbol{E}') = \gamma\boldsymbol{E}'(1+n\boldsymbol{\beta}\cdot\hat{\mathbf{k}}')\end{aligned} \tag{7.12.19}$$

Applying this result to the incident, reflected, and transmitted fields, we find:

$$\begin{aligned}E_i &= \gamma E'_i(1+\beta\cos\theta')\\ E_r &= \gamma E'_r(1-\beta\cos\theta') = \gamma\rho_{TE}E'_i(1-\beta\cos\theta')\\ E_t &= \gamma E'_t(1+n\beta\cos\theta'_t) = \gamma\tau_{TE}E'_i(1+n\beta\cos\theta'_t)\end{aligned} \tag{7.12.20}$$

It follows that the reflection and transmission coefficients will be:

$$\frac{E_r}{E_i} = \rho_{TE}\frac{1-\beta\cos\theta'}{1+\beta\cos\theta'} = \rho_{TE}\frac{\omega_r}{\omega}\,,\quad \frac{E_t}{E_i} = \tau_{TE}\frac{1+n\beta\cos\theta'_t}{1+\beta\cos\theta'} = \tau_{TE}\frac{\omega_t}{\omega} \tag{7.12.21}$$

The case of a perfect mirror corresponds to $\rho_{TE} = -1$ and $\tau_{TE} = 0$. To be interpretable as a reflection angle, θ_r must be in the range $0 \le \theta_r \le 90^o$, or, $\cos\theta_r > 0$. This requires that the numerator of (7.12.13) be positive, or,

$$(1+\beta^2)\cos\theta - 2\beta \ge 0 \quad\Leftrightarrow\quad \cos\theta \ge \frac{2\beta}{1+\beta^2} \quad\Leftrightarrow\quad \theta \le \operatorname{acos}\Big(\frac{2\beta}{1+\beta^2}\Big) \tag{7.12.22}$$

Because $2\beta/(1+\beta^2) > \beta$, (7.12.22) also implies that $\cos\theta > \beta$, or, $v < c_z = c\cos\theta$. Thus, the z-component of the phase velocity of the incident wave can catch up with the receding interface. At the maximum allowed θ, the angle θ_r reaches 90^o. In the above, we assumed that $\beta > 0$. For negative β, there are no restrictions on the range of θ.

7.13 Geometrical Optics

Geometrical optics and the concepts of wavefronts and rays can be derived from Maxwell's equations in the short-wavelength or high-frequency limit.

We saw in Chap. 2 that a uniform plane wave propagating in a lossless isotropic dielectric in the direction of a wave vector $\boldsymbol{k} = k\hat{\mathbf{k}} = nk_0\hat{\mathbf{k}}$ is given by:

$$\boldsymbol{E}(\boldsymbol{r}) = \boldsymbol{E}_0\, e^{-jnk_0\hat{\mathbf{k}}\cdot\boldsymbol{r}}\,,\quad \boldsymbol{H}(\boldsymbol{r}) = \boldsymbol{H}_0\, e^{-jnk_0\hat{\mathbf{k}}\cdot\boldsymbol{r}}\,,\qquad \hat{\mathbf{k}}\cdot\boldsymbol{E}_0 = 0\,,\quad \boldsymbol{H}_0 = \frac{n}{\eta_0}\hat{\mathbf{k}}\times\boldsymbol{E}_0 \tag{7.13.1}$$

where n is the refractive index of the medium $n = \sqrt{\epsilon/\epsilon_0}$, k_0 and η_0 are the free-space wavenumber and impedance, and $\hat{\mathbf{k}}$, the unit-vector in the direction of propagation.

The wavefronts are defined to be the constant-phase plane surfaces $S(\boldsymbol{r}) = \text{const.}$, where $S(\boldsymbol{r}) = n\hat{\mathbf{k}}\cdot\boldsymbol{r}$. The perpendiculars to the wavefronts are the optical rays.

In an inhomogeneous medium with a space-dependent refractive index $n(\boldsymbol{r})$, the wavefronts and their perpendicular rays become curved, and can be derived by considering the high-frequency limit of Maxwell's equations. By analogy with Eqs. (7.13.1), we look for solutions of the form:

$$\boldsymbol{E}(\boldsymbol{r}) = \boldsymbol{E}_0(\boldsymbol{r})\, e^{-jk_0S(\boldsymbol{r})}\,,\quad \boldsymbol{H}(\boldsymbol{r}) = \boldsymbol{H}_0(\boldsymbol{r})\, e^{-jk_0S(\boldsymbol{r})} \tag{7.13.2}$$

where we will assume that k_0 is large and that $\boldsymbol{E}_0, \boldsymbol{H}_0$ are slowly-varying functions of $\boldsymbol{r}$. This means that their space-derivatives are small compared to k_0 or to $1/\lambda$. For example, $|\nabla\times\boldsymbol{E}_0| \ll k_0$.

Inserting these expressions into Maxwell's equations and assuming $\mu = \mu_0$ and $\epsilon = n^2\epsilon_0$, we obtain:

$$\begin{aligned}\nabla\times\boldsymbol{E} &= e^{-jk_0S}\big(\nabla\times\boldsymbol{E}_0 - jk_0\nabla S\times\boldsymbol{E}_0\big) = -j\omega\mu_0\boldsymbol{H}_0\, e^{-jk_0S}\\ \nabla\times\boldsymbol{H} &= e^{-jk_0S}\big(\nabla\times\boldsymbol{H}_0 - jk_0\nabla S\times\boldsymbol{H}_0\big) = jn^2\omega\epsilon_0\boldsymbol{E}_0\, e^{-jk_0S}\end{aligned}$$

Assuming $|\nabla\times\boldsymbol{E}_0| \ll |k_0\nabla S\times\boldsymbol{E}_0|$, and similarly for $\boldsymbol{H}_0$, and dropping the common phase factor e^{-jk_0S}, we obtain the high-frequency approximations:

$$\begin{aligned}-jk_0\nabla S\times\boldsymbol{E}_0 &= -j\omega\mu_0\boldsymbol{H}_0\\ -jk_0\nabla S\times\boldsymbol{H}_0 &= jn^2\omega\epsilon_0\boldsymbol{E}_0\end{aligned}$$

Replacing $k_0 = \omega\sqrt{\mu_0\epsilon_0}$, and defining the vector $\hat{\mathbf{k}} = \dfrac{1}{n}\nabla S$, we find:

$$\boxed{\boldsymbol{H}_0 = \frac{n}{\eta_0}\hat{\mathbf{k}}\times\boldsymbol{E}_0\,,\quad \boldsymbol{E}_0 = -\frac{\eta_0}{n}\hat{\mathbf{k}}\times\boldsymbol{H}_0} \tag{7.13.3}$$

These imply the transversality conditions $\hat{\mathbf{k}}\cdot\boldsymbol{E}_0 = \hat{\mathbf{k}}\cdot\boldsymbol{H}_0 = 0$. The consistency of the equations (7.13.3) requires that $\hat{\mathbf{k}}$ be a *unit vector*. Indeed, using the BAC-CAB rule, we have:

$$\hat{\mathbf{k}}\times(\hat{\mathbf{k}}\times\boldsymbol{E}_0) = \hat{\mathbf{k}}(\hat{\mathbf{k}}\cdot\boldsymbol{E}_0) - \boldsymbol{E}_0(\hat{\mathbf{k}}\cdot\hat{\mathbf{k}}) = -\boldsymbol{E}_0(\hat{\mathbf{k}}\cdot\hat{\mathbf{k}}) = \frac{\eta_0}{n}\hat{\mathbf{k}}\times\boldsymbol{H}_0 = -\boldsymbol{E}_0$$

Thus, we obtain the unit-vector condition, known as the *eikonal equation*:

$$\hat{\mathbf{k}}\cdot\hat{\mathbf{k}} = 1 \quad\Rightarrow\quad |\nabla S|^2 = n^2 \qquad \text{(eikonal equation)} \tag{7.13.4}$$

This equation determines the wavefront phase function $S(\boldsymbol{r})$. The rays are the perpendiculars to the constant-phase surfaces $S(\boldsymbol{r}) = \text{const.}$, so that they are in the direction of ∇S or $\hat{\mathbf{k}}$. Fig. 7.13.1 depicts these wavefronts and rays.

The ray passing through a point $\boldsymbol{r}$ on the surface $S(\boldsymbol{r}) = S_A$, will move ahead by a distance $d\boldsymbol{r}$ in the direction of the gradient ∇S. The length of $d\boldsymbol{r}$ is $dl = (d\boldsymbol{r}\cdot d\boldsymbol{r})^{1/2}$.

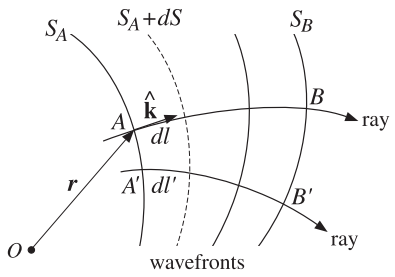

Fig. 7.13.1 Wavefront surfaces and rays.

The vector $d\boldsymbol{r}/dl$ is a unit vector in the direction of ∇S and, therefore, it must be equal to $\hat{\mathbf{k}}$. Thus, we obtain the defining equation for the rays:

$$\frac{d\boldsymbol{r}}{dl} = \hat{\mathbf{k}} \quad \Rightarrow \quad \frac{d\boldsymbol{r}}{dl} = \frac{1}{n}\nabla S \quad \Rightarrow \quad \boxed{n\frac{d\boldsymbol{r}}{dl} = \nabla S} \tag{7.13.5}$$

The eikonal equation determines S, which in turn determines the rays. The ray equation can be expressed directly in terms of the refractive index by eliminating S. Indeed, differentiating (7.13.5), we have:

$$\frac{d}{dl}\left(n\frac{d\boldsymbol{r}}{dl}\right) = \frac{d}{dl}(\nabla S) = \left(\frac{d\boldsymbol{r}}{dl}\cdot\nabla\right)\nabla S = \frac{1}{n}(\nabla S\cdot\nabla)\nabla S$$

where, in differentiating along a ray, we used the expression for d/dl:

$$\frac{d}{dl} = \frac{d\boldsymbol{r}}{dl}\cdot\nabla \tag{7.13.6}$$

But, $\nabla(\nabla S\cdot\nabla S) = 2(\nabla S\cdot\nabla)\nabla S$, which follows from the differential identity Eq. (C.16) of the Appendix. Therefore,

$$\frac{d}{dl}\left(n\frac{d\boldsymbol{r}}{dl}\right) = \frac{1}{n}(\nabla S\cdot\nabla)\nabla S = \frac{1}{2n}\nabla(\nabla S\cdot\nabla S) = \frac{1}{2n}\nabla(n^2) = \frac{1}{2n}2n\nabla n\,, \quad \text{or,}$$

$$\boxed{\frac{d}{dl}\left(n\frac{d\boldsymbol{r}}{dl}\right) = \nabla n} \qquad \text{(ray equation)} \tag{7.13.7}$$

The vectors $\boldsymbol{E}_0, \boldsymbol{H}_0, \hat{\mathbf{k}}$ form a right-handed system as in the uniform plane-wave case. The energy density and flux are:

$$\begin{aligned} w_e &= \frac{1}{2}\mathrm{Re}\left[\frac{1}{2}\epsilon\,\boldsymbol{E}\cdot\boldsymbol{E}^*\right] = \frac{1}{4}\epsilon_0 n^2|\boldsymbol{E}_0|^2 \\ w_m &= \frac{1}{4}\mu_0|\boldsymbol{H}_0|^2 = \frac{1}{4}\mu_0\frac{n^2}{\eta_0^2}|\boldsymbol{E}_0|^2 = \frac{1}{4}\epsilon_0 n^2|\boldsymbol{E}_0|^2 = w_e \\ w &= w_e + w_m = \frac{1}{2}\epsilon_0 n^2|\boldsymbol{E}_0|^2 \\ \boldsymbol{\mathcal{P}} &= \frac{1}{2}\mathrm{Re}\left[\boldsymbol{E}\times\boldsymbol{H}^*\right] = \frac{n}{2\eta_0}\hat{\mathbf{k}}\,|\boldsymbol{E}_0|^2 \end{aligned} \tag{7.13.8}$$

Thus, the energy transport velocity is:

$$\boldsymbol{v} = \frac{\boldsymbol{\mathcal{P}}}{w} = \frac{c_0}{n}\hat{\mathbf{k}} \tag{7.13.9}$$

The velocity $\boldsymbol{v}$ depends on $\boldsymbol{r}$, because n and $\hat{\mathbf{k}}$ do.

7.14 Fermat's Principle

An infinitesimal movement by dl along a ray will change the wavefront phase function by $dS = ndl$. Indeed, using Eq. (7.13.6) and the eikonal equation we find:

$$\frac{dS}{dl} = \frac{d\boldsymbol{r}}{dl}\cdot\nabla S = \frac{1}{n}\nabla S\cdot\nabla S = \frac{1}{n}n^2 = n \tag{7.14.1}$$

Integrating *along a ray path* from a point A on wavefront $S(\boldsymbol{r}) = S_A$ to a point B on wavefront $S(\boldsymbol{r}) = S_B$, as shown in Fig. 7.13.1, gives rise to the net phase change:

$$\boxed{S_B - S_A = \int_A^B dS = \int_A^B ndl} \tag{7.14.2}$$

The right-hand side is recognized as the *optical path length* from A to B. It is proportional to the travel time of moving from A to B with the ray velocity $\boldsymbol{v}$ given by Eq. (7.13.9). Indeed, we have $dl = \boldsymbol{v}\cdot\hat{\mathbf{k}}\,dt = c_0\,dt/n$, or, $dS = ndl = c_0 dt$. Thus,

$$\boxed{S_B - S_A = \int_A^B ndl = c_0\int_{t_A}^{t_B} dt = c_0(t_B - t_A)} \tag{7.14.3}$$

Fermat's Principle states that among all possible paths connecting the two points A and B, the geometrical optics ray path is the one the *minimizes* the optical path length (7.14.3), or equivalently, the travel time between the two points. The solution to this minimization problem is the ray equation (7.13.7).

Any path connecting the points A and B may be specified parametrically by the curve $\boldsymbol{r}(\tau)$, where the parameter τ varies over an interval $\tau_A \le \tau \le \tau_B$. The length dl may be written as:

$$dl = (d\boldsymbol{r}\cdot d\boldsymbol{r})^{1/2} = (\dot{\boldsymbol{r}}\cdot\dot{\boldsymbol{r}})^{1/2}\,d\tau\,, \quad \text{where} \quad \dot{\boldsymbol{r}} = \frac{d\boldsymbol{r}}{d\tau} \tag{7.14.4}$$

Then, the functional to be minimized is:

$$\int_A^B ndl = \int_{\tau_A}^{\tau_B}\mathcal{L}(\boldsymbol{r},\dot{\boldsymbol{r}})\,d\tau\,, \quad \text{where} \quad \mathcal{L}(\boldsymbol{r},\dot{\boldsymbol{r}}) = n(\boldsymbol{r})(\dot{\boldsymbol{r}}\cdot\dot{\boldsymbol{r}})^{1/2} \tag{7.14.5}$$

The minimization of Eq. (7.14.5) may be viewed as a problem in variational calculus with Lagrangian function $\mathcal{L}$. Its solution is obtained from the Euler-Lagrange equations:

$$\frac{d}{d\tau}\left(\frac{\partial\mathcal{L}}{\partial\dot{\boldsymbol{r}}}\right) = \frac{\partial\mathcal{L}}{\partial\boldsymbol{r}} \tag{7.14.6}$$

See [868–870] for a review of such methods. The required partial derivatives are:

$$\frac{\partial \mathcal{L}}{\partial \boldsymbol{r}} = \frac{\partial n}{\partial \boldsymbol{r}} (\dot{\boldsymbol{r}} \cdot \dot{\boldsymbol{r}})^{1/2}, \quad \frac{\partial \mathcal{L}}{\partial \dot{\boldsymbol{r}}} = n\, \dot{\boldsymbol{r}} (\dot{\boldsymbol{r}} \cdot \dot{\boldsymbol{r}})^{-1/2} = n \frac{d\boldsymbol{r}}{d\tau} (\dot{\boldsymbol{r}} \cdot \dot{\boldsymbol{r}})^{-1/2}$$

The Euler-Lagrange equations are then:

$$\frac{d}{d\tau}\left(n \frac{d\boldsymbol{r}}{d\tau} (\dot{\boldsymbol{r}} \cdot \dot{\boldsymbol{r}})^{-1/2} \right) = \frac{\partial n}{\partial \boldsymbol{r}} (\dot{\boldsymbol{r}} \cdot \dot{\boldsymbol{r}})^{1/2} \quad \text{or,}$$

$$\boxed{(\dot{\boldsymbol{r}} \cdot \dot{\boldsymbol{r}})^{-1/2} \frac{d}{d\tau}\left(n \frac{d\boldsymbol{r}}{d\tau} (\dot{\boldsymbol{r}} \cdot \dot{\boldsymbol{r}})^{-1/2} \right) = \frac{\partial n}{\partial \boldsymbol{r}}} \tag{7.14.7}$$

Using $dl = (\dot{\boldsymbol{r}} \cdot \dot{\boldsymbol{r}})^{1/2} d\tau$, we may rewrite these in terms of the length variable dl, resulting in the same equations as (7.13.7), that is,

$$\frac{d}{dl}\left(n \frac{d\boldsymbol{r}}{dl} \right) = \frac{\partial n}{\partial \boldsymbol{r}} \tag{7.14.8}$$

A variation of Fermat's principle states that the phase change between two wavefront surfaces is *independent* of the choice of the ray path taken between the surfaces. Following a different ray between points A' and B', as shown in Fig. 7.13.1, gives the same value for the net phase change as between the points A and B:

$$\boxed{S_B - S_A = \int_A^B n dl = \int_{A'}^{B'} n dl'} \tag{7.14.9}$$

This form is useful for deriving the shapes of parabolic reflector and hyperbolic lens antennas discussed in Chap. 21.

It can also be used to derive Snel's law of reflection and refraction. Fig. 7.14.1 shows the three families of incident, reflected, and refracted plane wavefronts on a horizontal interface between media n_a and n_b, such that the incident, reflected, and refracted rays are perpendicular to their corresponding wavefronts.

For the reflection problem, we consider the ray paths between the wavefront surfaces A_0A_1 and A_1A_2'. Fermat's principle implies that the optical path length of the rays AOA', A_0A_0', and A_2A_2' will be the same. This gives the condition:

$$n_a(l_a + l_a') = n_a L = n_a L' \quad \Rightarrow \quad L = L'$$

where L and L' are the lengths of the rays A_0A_0 and A_2A_2'. It follows that the two triangles $A_0A_2A_2'$ and $A_0A_0'A_2'$ will be congruent. and therefore, their angles at the vertices A_0 and A_2' will be equal. Thus, $\theta_a = \theta_a'$.

For the refraction problem, we consider the ray paths AOB, A_0B_0, and A_1B_1 between the wavefronts A_0A_1 and B_0B_1. The equality of the optical lengths gives now:

$$n_a l_a + n_b l_b = n_b L_b = n_a L_a \quad \Rightarrow \quad \frac{L_a}{L_b} = \frac{n_b}{n_a}$$

But, the triangles $A_0A_1B_1$ and $A_0B_0B_1$ have a common base A_0B_1. Therefore,

$$\frac{L_a}{L_b} = \frac{\sin\theta_a}{\sin\theta_b}$$

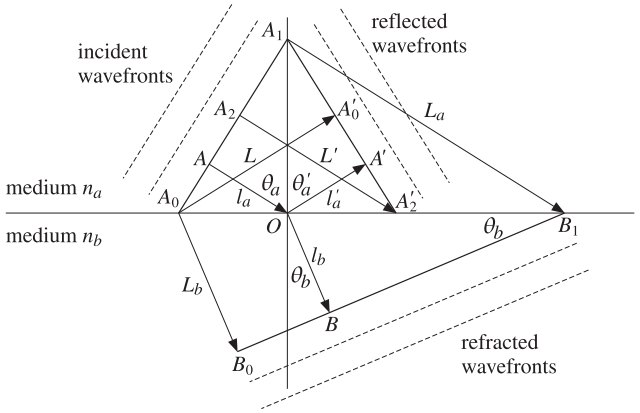

Fig. 7.14.1 Snel's laws of reflection and refraction.

Thus, we obtain Snel's law of refraction:

$$\frac{L_a}{L_b} = \frac{\sin\theta_a}{\sin\theta_b} = \frac{n_b}{n_a} \quad \Rightarrow \quad n_a \sin\theta_a = n_b \sin\theta_b$$

7.15 Ray Tracing

In this section, we apply Fermat's principle of least optical path to derive the ray curves in several integrable examples of inhomogeneous media.

As a special case of Eq. (7.14.8), we consider a stratified half-space $z \geq 0$, shown in Fig. 7.15.1, in which the refractive index is a function of z, but not of x.

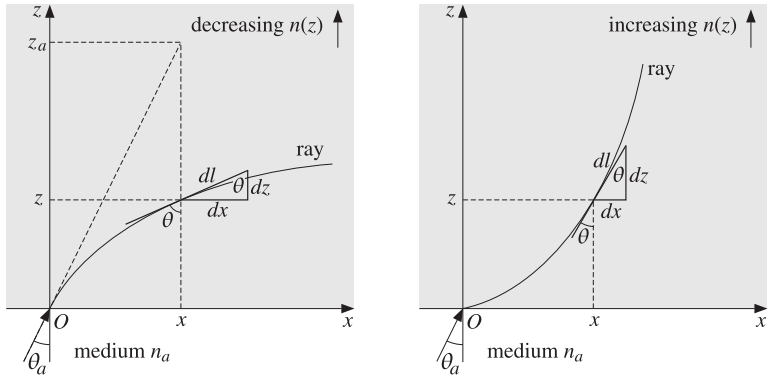

Fig. 7.15.1 Rays in an inhomogeneous medium.

Let θ be the angle formed by the tangent on the ray at point (x,z) and the vertical. Then, we have from the figure $dx = dl\sin\theta$ and $dz = dl\cos\theta$. Because $\partial n/\partial x = 0$, the ray equation (7.14.8) applied to the x-coordinate reads:

$$\frac{d}{dl}\left(n\frac{dx}{dl}\right) = 0 \quad \Rightarrow \quad n\frac{dx}{dl} = \text{const.} \quad \Rightarrow \quad n\sin\theta = \text{const.} \tag{7.15.1}$$

This is the generalization of Snel's law to an inhomogeneous medium. The constant may be determined by evaluating it at the entry point $z = 0$ and $x = 0$. We take the constant to be $n_a\sin\theta_a$. Thus, we write (7.15.2) as:

$$\boxed{n(z)\sin\theta(z) = n_a\sin\theta_a} \qquad \text{(generalized Snel's law)} \tag{7.15.2}$$

The z-component of the ray equation is, using $dz = dl\cos\theta$:

$$\frac{d}{dl}\left(n\frac{dz}{dl}\right) = \frac{dn}{dz} \quad \Rightarrow \quad \cos\theta\frac{d}{dz}(n\cos\theta) = \frac{dn}{dz} \tag{7.15.3}$$

This is a consequence of Eq. (7.15.2). To see this, we write:

$$n\cos\theta = \sqrt{n^2 - n^2\sin^2\theta} = \sqrt{n^2 - n_a^2\sin^2\theta_a} \tag{7.15.4}$$

Differentiating it with respect to z, we obtain Eq. (7.15.3). The ray in the left Fig. 7.15.1 is bending away from the z-axis with an increasing angle $\theta(z)$. This requires that $n(z)$ be a *decreasing* function of z. Conversely, if $n(z)$ is *increasing* as in the right figure, then $\theta(z)$ will be decreasing and the ray will curve towards the z-axis.

Thus, we obtain the rule that a ray always bends in the direction of increasing $n(z)$ and away from the direction of decreasing $n(z)$.

The constants n_a and θ_a may be taken to be the launch values at the origin, that is, $n(0)$ and $\theta(0)$. Alternatively, if there is a discontinuous change between the lower and upper half-spaces, we may take n_a, θ_a to be the refractive index and incident angle from below.

The ray curves can be determined by relating x and z. From Fig. 7.15.1, we have $dx = dz\tan\theta$, which in conjunction with Eqs. (7.15.2) and (7.15.4) gives:

$$\frac{dx}{dz} = \tan\theta = \frac{n\sin\theta}{n\cos\theta} = \frac{n_a\sin\theta_a}{\sqrt{n^2(z) - n_a^2\sin^2\theta_a}} \tag{7.15.5}$$

Integrating, we obtain:

$$\boxed{x = \int_0^z \frac{n_a\sin\theta_a}{\sqrt{n^2(z') - n_a^2\sin^2\theta_a}}\,dz'} \qquad \text{(ray curve)} \tag{7.15.6}$$

An object at the point (x,z) will appear to an observer sitting at the entry point O as though it is at the apparent location (x,z_a), as shown in Fig. 7.15.1. The apparent or virtual height will be $z_a = x\cot\theta_a$, which can be combined with Eq. (7.15.6) to give:

$$\boxed{z_a = \int_0^z \frac{n_a\cos\theta_a}{\sqrt{n^2(z') - n_a^2\sin^2\theta_a}}\,dz'} \qquad \text{(virtual height)} \tag{7.15.7}$$

The length z_a can be greater or less than z. For example, if the upper half-space is homogeneous with $n_b < n_a$, then $z_a > z$. If $n_b > n_a$, then $z_a < z$, as was the case in Example 7.5.4.

Next, we discuss a number of examples in which the integral (7.15.6) can be done explicitly to derive the ray curves.

Example 7.15.1: *Ionospheric Refraction.* Radio waves of frequencies typically in the range of about 4–40 MHz can be propagated at large distances such as 2000–4000 km by bouncing off the ionosphere. Fig. 7.15.2 depicts the case of a flat ground.

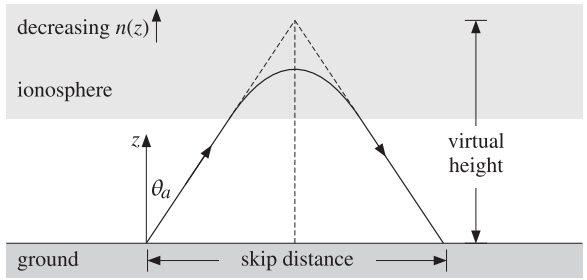

Fig. 7.15.2 Ionospheric refraction.

The atmosphere has a typical extent of 600 km and is divided in layers: the *troposphere* up to 10 km, the *stratosphere* at 10–50 km, and the *ionosphere* at 50–600 km. The ionosphere is further divided in sublayers, such as the D, E, F_1, and F_2 layers at 50–100 km, 100–150 km, 150–250 km, and 250–400 km, respectively.

The ionosphere consists mostly of ionized nitrogen and oxygen at low pressure. The ionization is due to solar radiation and therefore it varies between night and day. We recall from Sec. 1.15 that a collisionless plasma has an effective refractive index:

$$n^2 = \frac{\epsilon(\omega)}{\epsilon_0} = 1 - \frac{\omega_p^2}{\omega^2}, \qquad \omega_p^2 = \frac{Ne^2}{\epsilon_0 m} \tag{7.15.8}$$

The electron density N varies with the time of day and with height. Typically, N increases through the D and E layers and reaches a maximum value in the F layer, and then decreases after that because, even though the solar radiation is more intense, there are fewer gas atoms to be ionized.

Thus, the ionosphere acts as a stratified medium in which $n(z)$ first decreases with height from its vacuum value of unity and then it increases back up to unity. We will indicate the dependence on height by rewriting Eq. (7.15.8) in the form:

$$n^2(z) = 1 - \frac{f_p^2(z)}{f^2}, \qquad f_p^2(z) = \frac{N(z)e^2}{4\pi^2\epsilon_0 m} \tag{7.15.9}$$

If the wave is launched straight up and its frequency f is larger than the largest f_p, then it will penetrate through the ionosphere and be lost. But, if there is a height such that $f = f_p(z)$, then at that height $n(z) = 0$ and the wave will be reflected back down.

If the wave is launched at an angle θ_a, then it follows from Snel's law that while the refractive index $n(z)$ is decreasing, the angle of refraction $\theta(z)$ will be increasing and the ray path will bend more and more away from z-axis as shown on the left of Fig. 7.15.1. Below the ionosphere, we may assume that the atmosphere has refractive index $n_a = 1$. Then, the angle $\theta(z)$ may be written as:

$$\sin^2\theta(z) = \frac{n_a^2 \sin^2\theta_a}{n^2(z)} = \frac{\sin^2\theta_a}{1 - \dfrac{f_p^2(z)}{f^2}} \tag{7.15.10}$$

Because $\sin\theta(z)$ is required to be less than unity, we obtain the restriction:

$$\sin^2\theta_a \le 1 - \frac{f_p^2(z)}{f^2} \quad \Rightarrow \quad f_p(z) \le f\cos\theta_a \tag{7.15.11}$$

If there is a height, say $z_{\max}$, at which this becomes an equality, $f_p(z_{\max}) = f\cos\theta_a$, then Eq. (7.15.10) would imply that $\sin\theta(z_{\max}) = 1$, or that $\theta(z_{\max}) = 90^\circ$. At that height, the ray is horizontal and it will proceed to bend downwards, effectively getting reflected from the ionosphere.

If f is so large that Eq. (7.15.11) is satisfied only as a strict inequality, then the wave will escape through all the layers of the ionosphere. Thus, there is a maximum frequency, the so called *maximum usable frequency* (MUF), that will guarantee a reflection. There is also a *lowest usable frequency* (LUF) below which there is too much absorption of the wave, such as in the D layer, to be reflected at sufficient strength for reception.

As an oversimplified, but analytically tractable, model of the ionosphere we assume that the electron density increases linearly with height, up to a maximal height $z_{\max}$. Thus, the quantities $f_p^2(z)$ and $n^2(z)$ will also depend linearly on height:

$$f_p^2(z) = f_{\max}^2 \frac{z}{z_{\max}}, \qquad n^2(z) = 1 - \frac{f_{\max}^2}{f^2}\frac{z}{z_{\max}}, \quad \text{for} \quad 0 \le z \le z_{\max} \tag{7.15.12}$$

Over the assumed height range $0 \le z \le z_{\max}$, the condition (7.15.11) must also be satisfied. This restricts further the range of z. We have:

$$f_p^2(z) = f_{\max}^2 \frac{z}{z_{\max}} \le f^2\cos^2\theta_a \quad \Rightarrow \quad \frac{z}{z_{\max}} \le \frac{f^2\cos^2\theta_a}{f_{\max}^2} \tag{7.15.13}$$

If the right-hand side is greater than unity, so that $f\cos\theta_a > f_{\max}$, then there is no height z at which (7.15.11) achieves an equality, and the wave will escape. But, if $f\cos\theta_a \le f_{\max}$, then there is height, say z_0, at which the ray bends horizontally, that is,

$$\frac{z_0}{z_{\max}} = \frac{f^2\cos^2\theta_a}{f_{\max}^2} \quad \Rightarrow \quad z_0 = \frac{z_{\max} f^2\cos^2\theta_a}{f_{\max}^2} \tag{7.15.14}$$

The condition $f\cos\theta_a \le f_{\max}$ can be written as $f \le f_{\text{MUF}}$, where the MUF is in this case, $f_{\text{MUF}} = f_{\max}/\cos\theta_a$. The integral (7.15.6) can be done explicitly resulting in:

$$x = \frac{2z_{\max}\sin^2\theta_a}{a^2}\left[\cos\theta_a - \sqrt{\cos^2\theta_a - a^2\frac{z}{z_{\max}}}\right] \tag{7.15.15}$$

where we defined $a = f_{\max}/f$. Solving for z in terms of x, we obtain:

$$z - z_0 = -\frac{1}{4F}(x - x_0)^2 \tag{7.15.16}$$

where

$$x_0 = \frac{2z_{\max}\sin\theta_a\cos\theta_a}{a^2}, \quad F = \frac{z_{\max}\sin^2\theta_a}{a^2}$$

Therefore, the ray follows a downward parabolic path with vertex at (x_0, z_0) and focal length F, as shown in Fig. 7.15.3. □

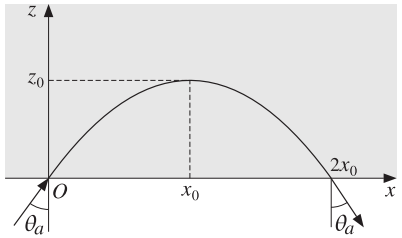

Fig. 7.15.3 Parabolic ray.

Example 7.15.2: *Mirages.* Temperature gradients can cause several types of mirage effects that are similar to ionospheric refraction. On a hot day, the ground is warmer than the air above it and therefore, the refractive index of the air is lower at the ground than a short distance above. (Normally, the air pressure causes the refractive index to be highest at the ground, decreasing with height.)

Because $n(z)$ decreases downwards, a horizontal ray from an object near the ground will initially be refracted downwards, but then it will bend upwards again and may arrive at an observer as though it were coming from below the ground, causing a mirage. Fig. 7.15.4 depicts a typical case. The ray path is like the ionospheric case, but inverted.

Such mirages are seen in the desert and on highways, which appear wet at far distances. Various types of mirages are discussed in [50–52,1827].

As a simple integrable model, we may assume that $n(z)$ increases linearly with height z, that is, $n(z) = n_0 + \kappa z$, where κ is the rate of increase per meter. For heights near the ground, this implies that $n^2(z)$ will also increase linearly:

$$\boxed{n(z) = n_0 + \kappa z} \quad \Rightarrow \quad \boxed{n^2(z) = n_0^2 + 2n_0\kappa z} \tag{7.15.17}$$

We consider a ray launched at a downward angle θ_a from an object with (x, z) coordinates $(0, h)$, as shown. Let $n_a^2 = n_0^2 + 2n_0\kappa h$ be the refractive index at the launch height. For convenience, we assume that the observer is also at height h. Because the ray will travel downward to points $z < h$, and then bend upwards, we integrate the ray equation over the limits $[z, h]$ and find:

$$x = \int_z^h \frac{n_a\sin\theta_a}{\sqrt{n^2(z') - n_a^2\sin^2\theta_a}}\,dz' = \frac{n_a\sin\theta_a}{n_0\kappa}\left[n_a\cos\theta_a - \sqrt{n_a^2\cos^2\theta_a + 2n_0\kappa(z-h)}\right]$$

where we used the approximation $n^2(z) = n_0^2 + 2n_0\kappa z$ in the integral. Solving for z in terms of x, we obtain the parabolic ray:

$$z = h + \frac{x(x-2x_0)}{4F}, \qquad x_0 = \frac{d}{2} = \frac{n_a^2 \sin\theta_a \cos\theta_a}{n_0\kappa}, \quad F = \frac{n_a^2 \sin^2\theta_a}{2n_0\kappa}$$

where d is the distance to the observer and F is the focal length. The apex of the parabola is at $x = x_0 = d/2$ at a height z_0 given by:

$$z_0 = h - \frac{x_0^2}{4F} \quad \Rightarrow \quad z - z_0 = \frac{1}{4F}(x - x_0)^2$$

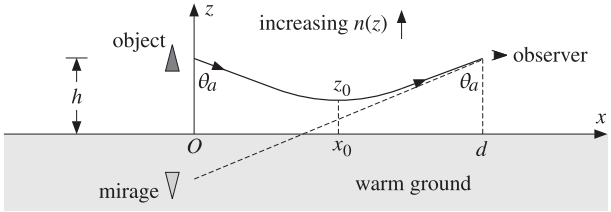

Fig. 7.15.4 Mirage due to a temperature gradient.

The launch angle that results in the ray being tangential to ground is obtained by setting the apex height to zero, $z_0 = 0$. This gives a condition that may be solved for θ_a:

$$x_0 = \sqrt{4Fh} \quad \Rightarrow \quad \sin\theta_a = \frac{n_0}{n_a} \quad \Rightarrow \quad F = \frac{n_0}{2\kappa} \quad \Rightarrow \quad \boxed{x_0 = \sqrt{\frac{2hn_0}{\kappa}}} \tag{7.15.18}$$

The corresponding $d = 2x_0$ is the maximum distance of the observer from the object for which a ray can just touch the ground. □

Example 7.15.3: *Atmospheric Refraction* [50–52]. Because of the compression of gravity, the density of the atmosphere† and its refractive index n are highest near the ground and decrease exponentially with height. A simplified model [721], which assumes a uniform temperature and constant acceleration of gravity, is as follows:

$$n(z) = 1 + (n_0 - 1)e^{-z/h_c} \tag{7.15.19}$$

The refractive index on the ground is approximately $n_0 = 1.0003$ (it also has some dependence on wavelength, which we ignore here.) The characteristic height h_c is given by $h_c = RT/Mg$, where R, T, M, g are the universal gas constant, temperature in absolute units, molecular mass of the atmosphere and acceleration of gravity:

$$R = 8.31\ \frac{\text{J}}{\text{K mole}}, \quad M = 0.029\ \frac{\text{kg}}{\text{mole}}, \quad g = 9.8\ \frac{\text{m}}{\text{s}^2}$$

For a temperature of $T = 303$K, or 30 °C, we find a height of $h_c = 8.86$ km. At a height of a few h_c, the refractive index becomes unity.

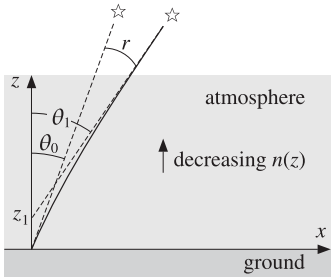

Fig. 7.15.5 Atmospheric refraction.

The bending of the light rays as they pass through the atmosphere cause the apparent displacement of a distant object, such as a star, the sun, or a geosynchronous satellite. Fig. 7.15.5 illustrates this effect. The object appears to be closer to the zenith.

The look-angle θ_0 at the ground and the true angle of the object θ_1 are related by Snel's law $n_1 \sin\theta_1 = n_0 \sin\theta_0$. But at large distances (many multiples of h_c), we have $n_1 = 1$. Therefore,

$$\sin\theta_1 = n_0 \sin\theta_0 \tag{7.15.20}$$

The refraction angle is $r = \theta_1 - \theta_0$. Assuming a small r, we may use the approximation $\sin(\theta_0 + r) = \sin\theta_0 + r\cos\theta_0$. Then, Eq. (7.15.20) gives the approximate expression:

$$r = (n_0 - 1)\tan\theta_0$$

The maximum viewing angle in this model is such that $n_0 \sin\theta_0 = \sin\theta_1 = 1$, corresponding to $\theta_1 = 90°$ and $\theta_0 = \text{asin}(1/n_0) = 88.6°$, for $n_0 = 1.0003$.

The model assumes a flat Earth. When the curvature of the Earth is taken into account, the total atmospheric refraction near the horizon, that is, near $\theta_0 = 90°$, is about 0.65° for a sea-level observer [50]. The setting sun subtends an angle of about 0.5°. Therefore, when it appears about to set and its lower edge is touching the horizon, it has already moved *below* the horizon.

The model of Eq. (7.15.19) may be integrated exactly. The ray curves are obtained from Eq. (7.15.6). Setting $n_a = n_0$, $\theta_a = \theta_0$ and using the definition (7.15.20), we obtain:

$$x = h_c \tan\theta_1 \left[\text{atanh}\left(\frac{A}{B}\right) - \text{atanh}\left(\frac{A_0}{B_0}\right)\right] = \tan\theta_1 \left[z + h_c \ln\left(\frac{A+B}{A_0+B_0}\right)\right] \tag{7.15.21}$$

where the quantities A, B, A_0, B_0 are defined as follows:

$$A = n(z) - \sin^2\theta_1, \qquad A_0 = n_0 - \sin^2\theta_1$$
$$B = \cos\theta_1\sqrt{n^2(z) - \sin^2\theta_1}, \qquad B_0 = \cos\theta_1\sqrt{n_0^2 - \sin^2\theta_1}$$

Thus, A_0, B_0 are the values of A, B at $z = 0$. It can be shown that $A > B$ and therefore, the hyperbolic arc-tangents will be complex-valued. However, the difference of the two atanh

† The troposphere and some of the stratosphere, consisting mostly of molecular nitrogen and oxygen.

terms is real and can be transformed into the second expression in (7.15.21) with the help of the result $A^2 - B^2 = (A_0^2 - B_0^2)e^{-2z/h_c}$.

In the limit of $z \gg h_c$, the quantities A, B tend to $A_1 = B_1 = \cos^2\theta_1$. and the ray equation becomes the *straight line* with a slope of $\tan\theta_1$:

$$x = (z + z_1)\tan\theta_1\,, \quad z_1 = h_c \ln\left(\frac{A_1 + B_1}{A_0 + B_0}\right) \tag{7.15.22}$$

This asymptotic line is depicted in Fig. 7.15.5, intercepting the z-axis at an angle of θ_1. □

Example 7.15.4: *Bouguer's Law.* The previous example assumed a flat Earth. For a spherical Earth in which the refractive index is a function of the radial distance r only, that is, $n(r)$, the ray tracing procedure must be modified.

Snel's law $n(z)\sin\theta(z) = n_0\sin\theta_0$ must be replaced by *Bouguer's law* [638], which states that the quantity $rn(r)\sin\theta$ remain constant:

$$\boxed{rn(r)\sin\theta(r) = r_0 n(r_0)\sin\theta_0} \qquad \text{(Bouguer's law)} \tag{7.15.23}$$

where $\theta(r)$ is the angle of the tangent to the ray and the radial vector. This law can be derived formally by considering the ray equations in spherical coordinates and assuming that $n(r)$ depends only on r [869].

A simpler derivation is to divide the atmosphere in equal-width spherical layers and assume that the refractive index is homogeneous in each layer. In Fig. 7.15.6, the layers are defined by the radial distances and refractive indices r_i, n_i, $i = 0, 1, 2, \ldots$.

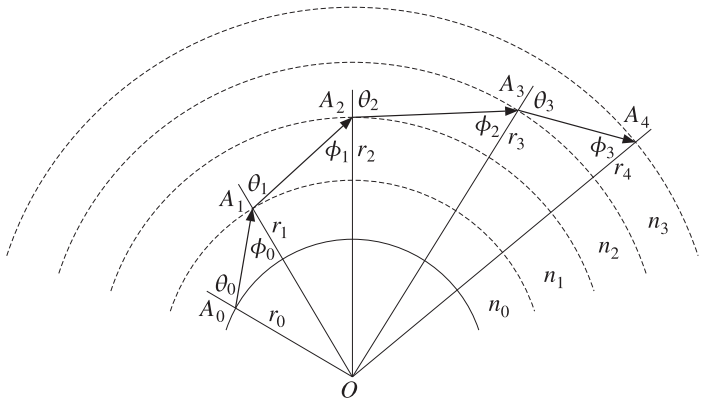

Fig. 7.15.6 Ray tracing in spherically stratified medium.

For sufficiently small layer widths, the ray segments between the points $A_0, A_1, A_2, \ldots$ are tangential to the radial circles. At the interface point A_3, Snel's law gives $n_2\sin\phi_2 = n_3\sin\theta_3$. On the other hand, from the triangle OA_2A_3, we have the law of sines:

$$\frac{r_2}{\sin\phi_2} = \frac{r_3}{\sin(\pi - \theta_2)} = \frac{r_3}{\sin\theta_2} \quad \Rightarrow \quad r_2\sin\theta_2 = r_3\sin\phi_2$$

Combining with Snel's law, we obtain:

$$r_2 n_2\sin\theta_2 = r_3 n_2\sin\phi_2 = r_3 n_3\sin\theta_3$$

Thus, the product $r_i n_i\sin\theta_i$ is the same for all $i = 0, 1, 2, \ldots$. Defining an effective refractive index by $n_{\text{eff}}(r) = n(r)r/r_0$, Bouguer's law may be written as Snel's law:

$$n_{\text{eff}}(r)\sin\theta(r) = n_0\sin\theta_0$$

where we have the initial value $n_{\text{eff}}(r_0) = n_0 r_0/r_0 = n_0$. □

Example 7.15.5: *Standard Atmosphere over Flat Earth.* For radiowave propagation over ground, the International Telecommunication Union (ITU) [877,878] defines a "standard" atmosphere with the values $n_0 = 1.000315$ and $h_c = 7.35$ km, in Eq. (7.15.19).

For heights of about one kilometer, such that $z \ll h_c$, we may linearize the exponential, $e^{-z/h_c} = 1 - z/h_c$, and obtain the refractive index for the standard atmosphere:

$$\boxed{n(z) = n_0 - \kappa z}\,, \qquad \kappa = \frac{n_0 - 1}{h_c} = \frac{315\times 10^{-6}}{7.35\times 10^3} = 4.2857\times 10^{-8}\ \text{m}^{-1} \tag{7.15.24}$$

This is similar to Eq. (7.15.17), with the replacement $\kappa \to -\kappa$. Therefore, we expect the rays to be parabolic bending downwards as in the case of the ionosphere. A typical ray between two antennas at height h and distance d is shown in Fig. 7.15.7.

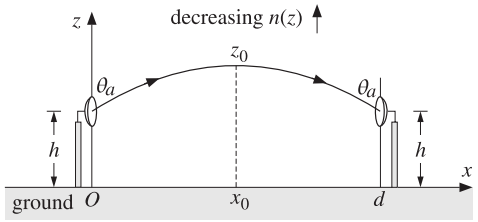

Fig. 7.15.7 Rays in standard atmosphere over a flat Earth.

Assuming an upward launch angle θ_a and defining the refractive index n_a at height h through $n_a^2 = n_0^2 - 2n_0\kappa h$, we obtain the ray equations by integrating over $[h, z]$:

$$x = \int_h^z \frac{n_a\sin\theta_a}{\sqrt{n^2(z') - n_a^2\sin^2\theta_a}}\,dz' = \frac{n_a\sin\theta_a}{n_0\kappa}\left[n_a\cos\theta_a - \sqrt{n_a^2\cos^2\theta_a - 2n_0\kappa(z-h)}\right]$$

where we used $n^2(z) = n_0^2 - 2n_0\kappa z$. Solving for z, we obtain the parabola:

$$z = h - \frac{x(x - 2x_0)}{4F}\,, \qquad x_0 = \frac{d}{2} = \frac{n_a^2\sin\theta_a\cos\theta_a}{n_0\kappa}\,, \quad F = \frac{n_a^2\sin^2\theta_a}{2n_0\kappa}$$

where d is the distance to the observer and F is the focal length. The apex of the parabola is at $x = x_0 = d/2$ at a height z_0 given by:

$$z_0 = h + \frac{x_0^2}{4F} \quad \Rightarrow \quad z - z_0 = -\frac{1}{4F}\,(x - x_0)^2$$

The minus sign in the right-hand side corresponds to a downward parabola with apex at the point (x_0, z_0). □

Example 7.15.6: *Standard Atmosphere over Spherical Earth.* We saw in Example 7.15.4 that in Bouguer's law the refractive index $n(r)$ may be replaced by an effective index $n_e(r) = n(r)\,r/r_0$. Applying this to the case of the Earth with $r_0 = R$ and $r = R + z$, where R is the Earth radius and z the height above the surface, we have $n_e(z) = n(z)\,(R+z)/R$, or,

$$n_e(z) = n(z)\left(1 + \frac{z}{R}\right) = (n_0 - \kappa z)\left(1 + \frac{z}{R}\right)$$

Thus, the spherical Earth introduces the factor $(1 + z/R)$, which increases with height and counteracts the decreasing $n(z)$. Keeping only linear terms in z, we find:

$$\boxed{n_e(z) = n_0 + \kappa_e z}, \qquad \kappa_e = \frac{n_0}{R} - \kappa \tag{7.15.25}$$

For the average Earth radius $R = 6370$ km and the ITU values of n_0 and κ given in Eq. (7.15.24), we find that the effective κ_e is *positive*:

$$\kappa_e = 1.1418 \times 10^{-7}\ \text{m}^{-1} \tag{7.15.26}$$

Making the approximation $n^2(z) = n_0^2 + 2n_0\kappa_e z$ will result in parabolic rays bending upwards as in Example 7.15.2.

Often, an equivalent Earth radius is defined by $\kappa_e = n_0/R_e$ so that the effective refractive index may be assumed to arise only from the curvature of the equivalent Earth:

$$n_e(z) = n_0 + \kappa_e z = n_0\left(1 + \frac{z}{R_e}\right)$$

In units of R, we have:

$$\boxed{\frac{R_e}{R} = \frac{n_0}{\kappa_e R} = \frac{n_0}{n_0 - \kappa R} = 1.3673} \tag{7.15.27}$$

which is usually replaced by $R_e = 4R/3$. In this model, the refractive index is assumed to be uniform above the surface of the equivalent Earth, $n(z) = n_0$.

The ray paths are determined by considering only the geometrical effect of the spherical surface. For example, to determine the maximum distance x_0 at which a ray from a transmitter at height h just grazes the ground, we may either use the results of Eq. (7.15.18), or consider a straight path that is tangential to the equivalent Earth, as shown in Fig. 7.15.8.

Setting $\kappa_e = n_0/R_e$ in Eq. (7.15.18), we obtain:

$$\boxed{x_0 = \sqrt{\frac{2n_0 h}{\kappa_e}} = \sqrt{2hR_e}} \tag{7.15.28}$$

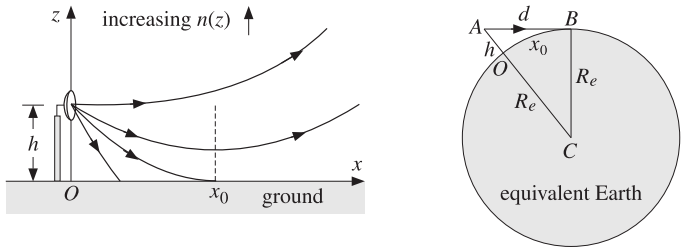

Fig. 7.15.8 Rays over a spherical Earth.

On the other hand, because $h \ll R_e$ the arc length $x_0 = (OB)$ may be taken to be a straight line in Fig. 7.15.8. Applying the Pythagorean theorem to the two orthogonal triangles OAB and CAB we find that:

$$x_0^2 + h^2 = d^2 = (h + R_e)^2 - R_e^2 = h^2 + 2hR_e \quad \Rightarrow \quad x_0^2 = 2hR_e$$

which is the same as Eq. (7.15.28). □

Example 7.15.7: *Graded-Index Optical Fibers.* In Example 7.5.5, we considered a step-index optical fiber in which the rays propagate by undergoing total internal reflection bouncing off the cladding walls. Here, we consider a graded-index fiber in which the refractive index of the core varies radially from the center value n_f to the cladding value n_c at the edge of the core. Fig. 7.15.9 shows the geometry.

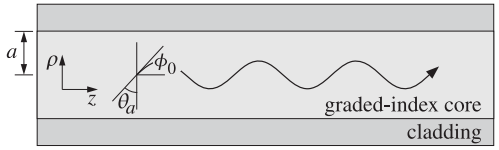

Fig. 7.15.9 Graded-index optical fiber.

As a simple model, we assume a parabolic dependence on the radial distance. We may write in cylindrical coordinates, where a is the radius of the core:

$$n^2(\rho) = n_f^2\left(1 - \Delta^2\,\frac{\rho^2}{a^2}\right), \qquad \Delta^2 = \frac{n_f^2 - n_c^2}{n_f^2} \tag{7.15.29}$$

Inserting this expression into Eq. (7.15.6), and changing variables from z, x to ρ, z, the integral can be done explicitly resulting in:

$$z = \frac{a\sin\theta_a}{\Delta}\ \text{asin}\left(\frac{\rho\Delta}{a\cos\theta_a}\right) \tag{7.15.30}$$

Inverting the arc-sine, we may solve for ρ in terms of z obtaining the following sinusoidal variation of the radial coordinate, where we also changed from the incident angle θ_a to the initial launch angle $\phi_0 = 90^\circ - \theta_a$:

$$\boxed{\rho = \frac{\tan\phi_0}{\kappa}\,\sin(\kappa z)}\,, \qquad \kappa = \frac{\Delta}{a\cos\phi_0} \tag{7.15.31}$$

For small launch angles ϕ_0, the oscillation frequency becomes independent of ϕ_0, that is, $\kappa = \Delta/(a\cos\phi_0) \simeq \Delta/a$. The rays described by Eq. (7.15.31) are meridional rays, that is, they lie on a plane through the fiber axis, such as the xz- or yz-plane.

There exist more general ray paths that have nontrivial azimuthal dependence and propagate in a helical fashion down the guide [871–876]. □

7.16 Snel's Law in Negative-Index Media

Consider the planar interface between a normal (i.e., positive-index) lossless medium ϵ, μ and a lossless negative-index medium [391] ϵ', μ' with negative permittivity and permeability, $\epsilon' < 0$ and $\mu' < 0$, and negative refractive index $n' = -\sqrt{\mu'\epsilon'/\mu_0\epsilon_0}$. The refractive index of the left medium is as usual $n = \sqrt{\mu\epsilon/\mu_0\epsilon_0}$. A TE or TM plane wave is incident on the interface at an angle θ, as shown in Fig. 7.16.1.

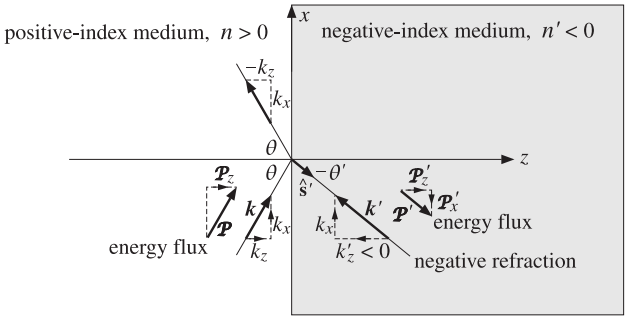

Fig. 7.16.1 Refraction into a negative-index medium.

Because $n' < 0$, Snel's law implies that the refracted ray will bend in the opposite direction (e.g., with a negative refraction angle) than in the normal refraction case. This follows from:

$$n\sin\theta = n'\sin\theta' = -|n'|\sin\theta' = |n'|\sin(-\theta') \tag{7.16.1}$$

As a result, the wave vector $\boldsymbol{k}'$ of the refracted wave will point *towards* the interface, instead of away from it. Its x-component matches that of the incident wave vector $\boldsymbol{k}$, that is, $k_x' = k_x$, which is equivalent to Snel's law (7.16.1), while its z-component points towards the interface or the negative z-direction in the above figure.

Formally, we have $\boldsymbol{k}' = k'\hat{\mathbf{s}}'$, where $\hat{\mathbf{s}}'$ is the unit vector in the direction of the refracted ray pointing away from the interface, and $k' = -\omega\sqrt{\mu'\epsilon'} = n'k_0$, with k_0 the free-space wavenumber $k_0 = \omega\sqrt{\mu_0\epsilon_0} = \omega/c_0$. As we see below, the energy flux Poynting vector $\boldsymbol{\mathcal{P}}'$ of the refracted wave is opposite $\boldsymbol{k}'$ and points in the direction of $\hat{\mathbf{s}}'$, and therefore, carries energy away from the interface. Thus, component-wise we have:

$$k_x' = n'k_0\sin\theta' = k_x = nk_0\sin\theta\,, \quad k_z' = n'k_0\cos\theta' = -|n'|k_0\cos\theta' < 0$$

The TE and TM wave solutions at both sides of the interface are still given by Eqs. (7.7.4) and (7.7.5), and reproduced below (with $e^{j\omega t}$ suppressed):

$$\boxed{\begin{aligned}
\boldsymbol{E}(\boldsymbol{r}) &= \hat{\mathbf{y}}\,E_0\left[e^{-jk_zz} + \rho_{TE}\,e^{jk_zz}\right]e^{-jk_xx}\\
\boldsymbol{H}(\boldsymbol{r}) &= \frac{E_0}{\eta_{TE}}\left[\left(-\hat{\mathbf{x}} + \frac{k_x}{k_z}\,\hat{\mathbf{z}}\right)e^{-jk_zz} + \rho_{TE}\left(\hat{\mathbf{x}} + \frac{k_x}{k_z}\,\hat{\mathbf{z}}\right)e^{jk_zz}\right]e^{-jk_xx}\\
\boldsymbol{E}'(\boldsymbol{r}) &= \hat{\mathbf{y}}\,\tau_{TE}E_0\,e^{-jk_z'z}e^{-jk_xx}\\
\boldsymbol{H}'(\boldsymbol{r}) &= \frac{\tau_{TE}E_0}{\eta_{TE}'}\left(-\hat{\mathbf{x}} + \frac{k_x}{k_z'}\,\hat{\mathbf{z}}\right)e^{-jk_z'z}e^{-jk_xx}
\end{aligned}} \quad \text{(TE)} \tag{7.16.2}$$

where, allowing for magnetic media, we have

$$\eta_{TE} = \frac{\omega\mu}{k_z}\,, \quad \eta_{TE}' = \frac{\omega\mu'}{k_z'}\,, \quad \rho_{TE} = \frac{\eta_{TE}' - \eta_{TE}}{\eta_{TE}' + \eta_{TE}} = \frac{k_z\mu' - k_z'\mu}{k_z\mu' + k_z'\mu}\,, \quad \tau_{TE} = 1 + \rho_{TE} \tag{7.16.3}$$

For the TM case we have:

$$\boxed{\begin{aligned}
\boldsymbol{E}(\boldsymbol{r}) &= E_0\left[\left(\hat{\mathbf{x}} - \frac{k_x}{k_z}\,\hat{\mathbf{z}}\right)e^{-jk_zz} + \rho_{TM}\left(\hat{\mathbf{x}} + \frac{k_x}{k_z}\,\hat{\mathbf{z}}\right)e^{jk_zz}\right]e^{-jk_xx}\\
\boldsymbol{H}(\boldsymbol{r}) &= \hat{\mathbf{y}}\,\frac{E_0}{\eta_{TM}}\left[e^{-jk_zz} - \rho_{TM}\,e^{jk_zz}\right]e^{-jk_xx}\\
\boldsymbol{E}'(\boldsymbol{r}) &= \tau_{TM}E_0\left(\hat{\mathbf{x}} - \frac{k_x}{k_z'}\,\hat{\mathbf{z}}\right)e^{-jk_z'z}e^{-jk_xx}\\
\boldsymbol{H}'(\boldsymbol{r}) &= \hat{\mathbf{y}}\,\frac{\tau_{TM}E_0}{\eta_{TM}'}e^{-jk_z'z}e^{-jk_xx}
\end{aligned}} \quad \text{(TM)} \tag{7.16.4}$$

with

$$\eta_{TM} = \frac{k_z}{\omega\epsilon}\,, \quad \eta_{TM}' = \frac{k_z'}{\omega\epsilon'}\,, \quad \rho_{TM} = \frac{\eta_{TM}' - \eta_{TM}}{\eta_{TM}' + \eta_{TM}} = \frac{k_z'\epsilon - k_z\epsilon'}{k_z'\epsilon + k_z\epsilon'}\,, \quad \tau_{TM} = 1 + \rho_{TM} \tag{7.16.5}$$

One can verify easily that in both cases the above expressions satisfy Maxwell's equations and the boundary conditions at the interface, provided that

$$\begin{aligned}
k_x^2 + k_z^2 &= \omega^2\mu\epsilon = n^2k_0^2\\
k_x^2 + k_z'^2 &= \omega^2\mu'\epsilon' = n'^2k_0^2
\end{aligned} \tag{7.16.6}$$

In fact, Eqs. (7.16.2)–(7.16.6) describe the most general case of arbitrary, homogeneous, isotropic, positive- or negative-index, and possibly lossy, media on the left and right and for either propagating or evanescent waves. We concentrate, next, on the case when the left medium is a positive-index lossless medium, $\mu > 0$ and $\epsilon > 0$, and the right one is lossless with $\mu' < 0$ and $\epsilon' < 0$, and consider a propagating incident wave with $k_x = nk_0\sin\theta$ and $k_z = nk_0\cos\theta$ and assume, for now, that $n \le |n'|$ to avoid evanescent waves into the right medium. The Poynting vector $\boldsymbol{\mathcal{P}}'$ in the right medium

can be calculated from Eqs. (7.16.2) and (7.16.4):

$$\begin{aligned}\text{(TE):}\quad \boldsymbol{\mathcal{P}}' &= \frac{1}{2}\,\text{Re}\,(\boldsymbol{E}'\times\boldsymbol{H}'^{*}) = \frac{1}{2}|\tau_{TE}|^2|E_0|^2\left[\hat{\mathbf{z}}\,\text{Re}\Big(\frac{k_z'}{\omega\mu'}\Big)+\hat{\mathbf{x}}\,\text{Re}\Big(\frac{k_x}{\omega\mu'}\Big)\right]\\ \text{(TM):}\quad \boldsymbol{\mathcal{P}}' &= \frac{1}{2}\,\text{Re}\,(\boldsymbol{E}'\times\boldsymbol{H}'^{*}) = \frac{1}{2}|\tau_{TM}|^2|E_0|^2\left[\hat{\mathbf{z}}\,\text{Re}\Big(\frac{\omega\epsilon'}{k_z'}\Big)+\hat{\mathbf{x}}\,\text{Re}\Big(\frac{\omega\epsilon' k_x}{|k_z'|^2}\Big)\right]\end{aligned} \tag{7.16.7}$$

Because $\mu' < 0$ and $\epsilon' < 0$, and k_z' is real, the requirement of positive energy flux away from the interface, $\mathcal{P}_z' > 0$, requires that $k_z' < 0$ in both cases. Similarly, because $k_x > 0$, the x-component of $\boldsymbol{\mathcal{P}}'$ will be negative, $\mathcal{P}_x' < 0$. Thus, the vector $\boldsymbol{\mathcal{P}}'$ has the direction shown in Fig. 7.16.1. We note also that the z-component is preserved across the interface, $\mathcal{P}_z = \mathcal{P}_z'$. This follows from the relationships:

$$\begin{aligned}\mathcal{P}_z &= \frac{1}{2}|E_0|^2\frac{k_z}{\omega\mu}\,(1-|\rho_{TE}|^2) = \frac{1}{2}|E_0|^2|\tau_{TE}|^2\,\text{Re}\Big(\frac{k_z'}{\omega\mu'}\Big) = \mathcal{P}_z'\\ \mathcal{P}_z &= \frac{1}{2}|E_0|^2\frac{\omega\epsilon}{k_z}\,(1-|\rho_{TM}|^2) = \frac{1}{2}|E_0|^2|\tau_{TM}|^2\,\text{Re}\Big(\frac{\omega\epsilon'}{k_z'}\Big) = \mathcal{P}_z'\end{aligned} \tag{7.16.8}$$

If $n > |n'|$, the possibility of total internal reflection arises. When $\sin\theta > |n'|/n$, then $k_z'^2 = n'^2k_0^2 - k_x^2 = k_0^2(n'^2 - n^2\sin^2\theta)$ is negative and k_z' becomes pure imaginary. In this case, the real-parts in the right-hand side of Eq. (7.16.8) are zero, showing that $|\rho_{TE}| = |\rho_{TM}| = 1$ and there is no (time-averaged) power flow into the right medium.

For magnetic media, including negative-index media, the Brewster angle may also exist for TE polarization, corresponding to $\rho_{TE} = 0$. This condition is equivalent to $k_z'\mu = k_z\mu'$. Similarly $\rho_{TM} = 0$ is equivalent to $k_z'\epsilon = k_z\epsilon'$. These two conditions imply the following relationship for the Brewster angles:

$$\begin{aligned}\rho_{TE} = 0 \quad&\Rightarrow\quad k_z'\mu = k_z\mu' \quad\Rightarrow\quad (\mu'^2-\mu^2)\sin^2\theta_B = \mu'^2 - \frac{\mu'\epsilon'}{\mu\epsilon}\,\mu^2\\ \rho_{TM} = 0 \quad&\Rightarrow\quad k_z'\epsilon = k_z\epsilon' \quad\Rightarrow\quad (\epsilon'^2-\epsilon^2)\sin^2\theta_B = \epsilon'^2 - \frac{\mu'\epsilon'}{\mu\epsilon}\,\epsilon^2\end{aligned} \tag{7.16.9}$$

Clearly, these may or may not have a solution, such that $0 < \sin^2\theta_B < 1$, depending on the relative values of the constitutive parameters. For non-magnetic media, $\mu = \mu' = \mu_0$, the TE case has no solution and the TM case reduces to the usual expression:

$$\sin^2\theta_B = \frac{\epsilon'^2-\epsilon'\epsilon}{\epsilon'^2-\epsilon^2} = \frac{\epsilon'}{\epsilon'+\epsilon} = \frac{n'^2}{n'^2+n^2}$$

Assuming that ϵ, μ and ϵ', μ' have the same sign (positive or negative), we may replace these quantities with their absolute values in Eq. (7.16.9). Defining the parameters $x = |\mu'/\mu|$ and $y = |\epsilon'/\epsilon|$, we may rewrite (7.16.9) in the form:

$$\begin{aligned}\text{TE case:}\quad &\Big(1-\frac{1}{x^2}\Big)\sin^2\theta_B = \Big(1-\frac{y}{x}\Big)\\ \text{TM case:}\quad &\Big(1-\frac{1}{y^2}\Big)\sin^2\theta_B = \Big(1-\frac{x}{y}\Big)\end{aligned} \tag{7.16.10}$$

with the TE and TM cases being obtained from each other by the duality transformations $x \to y$ and $y \to x$. It is straightforward to verify that the ranges of the x, y parameters for which a Brewster angle exists are as follows:

$$\begin{aligned}\text{TE case:}\quad &x > 1\,,\ \ y < x\,,\ \ y > \frac{1}{x}\,,\quad \text{or,}\quad x < 1\,,\ \ y > x\,,\ \ y < \frac{1}{x}\\ \text{TM case:}\quad &y > 1\,,\ \ x < y\,,\ \ y > \frac{1}{x}\,,\quad \text{or,}\quad y < 1\,,\ \ x > y\,,\ \ y < \frac{1}{x}\end{aligned} \tag{7.16.11}$$

These regions [697], which are bounded by the curves $y = x$ and $y = 1/x$, are shown in Fig. 7.16.2. We note, in particular, that the TE and TM regions are non-overlapping.

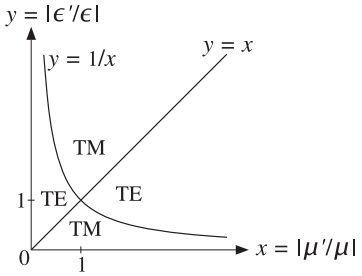

Fig. 7.16.2 Brewster angle regions.

The unusual property of Snel's law in negative-index media that the refracted ray bends in the opposite direction than in the normal case has been verified experimentally in artificial metamaterials constructed by arrays of wires and split-ring resonators [397], and by transmission line elements [430–432,452,465]. Another consequence of Snel's law is the possibility of a perfect lens [398] in the case $n' = -1$. We discuss this in Sec. 8.6.

7.17 Problems

7.1 The matching of the tangential components of the electric and magnetic fields resulted in Snel's laws and the matching matrix Eq. (7.3.11). In both the TE and TM polarization cases, show that the remaining boundary conditions $B_z = B_z'$ and $D_z = D_z'$ are also satisfied.

7.2 Show that the Fresnel coefficients (7.4.2) may be expressed in the forms:

$$\rho_{TM} = \frac{\sin 2\theta' - \sin 2\theta}{\sin 2\theta' + \sin 2\theta} = \frac{\tan(\theta'-\theta)}{\tan(\theta'+\theta)}\,,\qquad \rho_{TE} = \frac{\sin(\theta'-\theta)}{\sin(\theta'+\theta)}$$

7.3 Show that the refractive index ratio n'/n can be expressed in terms of the ratio $r = \rho_{TM}/\rho_{TE}$ and the incident angle θ by:

$$\frac{n'}{n} = \sin\theta\left[1+\Big(\frac{1+r}{1-r}\Big)^2\tan^2\theta\right]^{1/2}$$

This provides a convenient way of measuring the refractive index n' from measurements of the Fresnel coefficients [716]. It is valid also for complex n'.

7.4 It is desired to design a Fresnel rhomb such that the exiting ray will be elliptically polarized with relative phase difference ϕ between its TE and TM components. Let $\sin\theta_c = 1/n$ be the critical angle within the rhomb. Show that the rhomb angle replacing the 54.6° angle in Fig. 7.5.6 can be obtained from:

$$\sin^2\theta = \frac{\cos^2\theta_c \pm \sqrt{\cos^4\theta_c - 4\sin^2\theta_c \tan^2(\phi/4)}}{2\tan^2(\phi/4) + \cos^2\theta_c \pm \sqrt{\cos^4\theta_c - 4\sin^2\theta_c \tan^2(\phi/4)}}$$

Show ϕ is required to satisfy $\tan(\phi/4) \leq (n - n^{-1})/2$.

7.5 Show the relationship (7.9.7) for the ratio ρ_{TM}/ρ_{TE} by first proving and then using the following identities in the notation of Eq. (7.7.4):

$$(k'_z \pm k_z)(k_x^2 \pm k_z k'_z) = k^2 k'_z \pm k'^2 k_z$$

Using (7.9.7), show that when both media are lossless, the ratio ρ_{TM}/ρ_{TE} can be expressed directly in terms of the angles of incidence and refraction, θ and θ':

$$\frac{\rho_{TM}}{\rho_{TE}} = \frac{\cos(\theta + \theta')}{\cos(\theta - \theta')}$$

Using this result argue that $|\rho_{TM}| \leq |\rho_{TE}|$ at all angles θ. Argue also that $\theta_B + \theta'_B = 90°$, for the Brewster angles. Finally, show that for lossless media with $\epsilon > \epsilon'$, and angles of incidence $\theta \geq \theta_c$, where $\sin\theta_c = \sqrt{\epsilon'/\epsilon}$, we have:

$$\frac{\rho_{TM}}{\rho_{TE}} = \frac{j\sqrt{\sin^2\theta - \sin^2\theta_c} + \sin\theta\tan\theta}{j\sqrt{\sin^2\theta - \sin^2\theta_c} - \sin\theta\tan\theta}$$

Explain how this leads to the design equation (7.5.8) of the Fresnel rhomb.

7.6 Let the incident, reflected, and transmitted waves at an interface be:

$$\boldsymbol{E}_+(\boldsymbol{r}) = \boldsymbol{E}_+ e^{-j\boldsymbol{k}_+\cdot\boldsymbol{r}}, \quad \boldsymbol{E}_-(\boldsymbol{r}) = \boldsymbol{E}_- e^{-j\boldsymbol{k}_-\cdot\boldsymbol{r}}, \quad \boldsymbol{E}'(\boldsymbol{r}) = \boldsymbol{E}'_0 e^{-j\boldsymbol{k}'\cdot\boldsymbol{r}}$$

where $\boldsymbol{k}_\pm = k_x\hat{\mathbf{x}} \pm k_z\hat{\mathbf{z}}$ and $\boldsymbol{k}' = k_x\hat{\mathbf{x}} + k'_z\hat{\mathbf{z}}$. Show that the reflection and transmission coefficients defined in Eqs. (7.7.1)–(7.7.5) can be summarized compactly by the following vectorial relationships, which are valid for both the TE and TM cases:

$$\frac{\boldsymbol{k}_\pm \times (\boldsymbol{E}'_0 \times \boldsymbol{k}_\pm)}{k^2} = \frac{2k_z}{k_z \pm k'_z}\boldsymbol{E}_\pm$$

7.7 Using Eqs. (7.7.4), derive the expressions (7.9.11) for the Poynting vectors. Derive similar expressions for the TM case.

Using the definitions in Eqs. (7.3.12), show that if the left medium is lossless and the right one lossy, the following relationship holds:

$$\frac{1}{\eta_T}(1 - |\rho_T|^2) = \mathrm{Re}\left(\frac{1}{\eta'_T}\right)|\tau_T|^2$$

Then, show that Eqs. (7.9.12) and (7.9.13) are special cases of this result, specialized to the TE and TM cases.

7.8 A light ray enters a glass block from one side, suffers a total internal reflection from the top side, and exits from the opposite side, as shown below. The glass refractive index is $n = 1.5$.

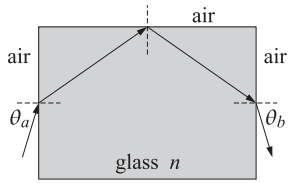

a. How is the exit angle θ_b related to the entry angle θ_a? Explain.

b. Show that all rays, regardless of the entry angle θ_a, will suffer total internal reflection at the top side.

c. Suppose that the glass block is replaced by another dielectric with refractive index n. What is the minimum value of n in order that all entering rays will suffer total internal reflection at the top side?

7.9 An underwater object is viewed from air at an angle θ through a glass plate, as shown below. Let $z = z_1 + z_2$ be the actual depth of the object from the air surface, where z_1 is the thickness of the glass plate, and let n_1, n_2 be the refractive indices of the glass and water. Show that the apparent depth of the object is given by:

$$z' = \frac{z_1\cos\theta}{\sqrt{n_1^2 - \sin^2\theta}} + \frac{z_2\cos\theta}{\sqrt{n_2^2 - \sin^2\theta}}$$

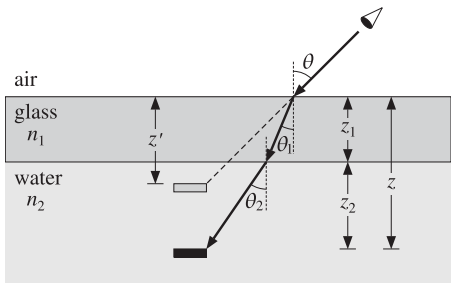

7.10 An underwater object is viewed from air at an angle θ through two glass plates of refractive indices n_1, n_2 and thicknesses z_1, z_2, as shown below. Let z_3 be the depth of the object within the water.

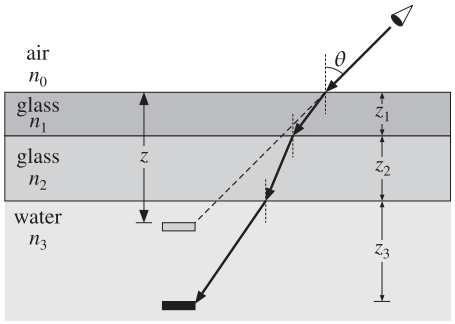

a. Express the apparent depth z of the object in terms of the quantities $\theta, n_0, n_1, n_2, n_3$ and z_1, z_2, z_3.

b. Generalize the results of the previous two problems to an arbitrary number of layers.

c. Consider also the continuous limit in which the body of water is inhomogeneous with a refractive index $n(z)$ given as a function of the depth z.

7.11 As shown below, light must be launched from air into an optical fiber at an angle $\theta \le \theta_a$ in order to propagate by total internal reflection.

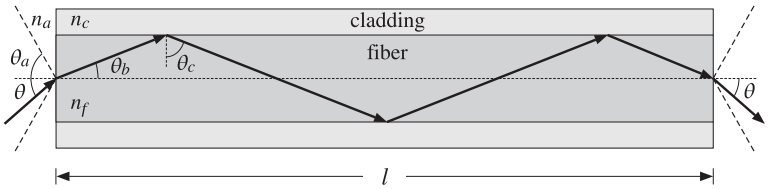

a. Show that the acceptance angle is given by:

$$\sin\theta_a = \frac{\sqrt{n_f^2 - n_c^2}}{n_a}$$

b. For a fiber of length l, show that the exiting ray, at the opposite end, is exiting at the same angle θ as the incidence angle.

c. Show that the propagation delay time through this fiber, for a ray entering at an angle θ, is given as follows, where $t_0 = l/c_0$:

$$t(\theta) = \frac{t_0 n_f^2}{\sqrt{n_f^2 - n_a^2 \sin^2\theta}}$$

d. What angles θ correspond to the maximum and minimum delay times? Show that the difference between the maximum and minimum delay times is given by:

$$\Delta t = t_{\max} - t_{\min} = \frac{t_0 n_f (n_f - n_c)}{n_c}$$

Such travel time delays cause "modal dispersion," that can limit the rate at which digital data may be transmitted (typically, the data rate must be $f_{\text{bps}} \le 1/(2\Delta t)$).

7.12 You are walking along the hallway in your classroom building wearing polaroid sunglasses and looking at the reflection of a light fixture on the waxed floor. Suddenly, at a distance d from the light fixture, the reflected image momentarily disappears. Show that the refractive index of the reflecting floor can be determined from the ratio of distances:

$$n = \frac{d}{h_1 + h_2}$$

where h_1 is your height and h_2 that of the light fixture. You may assume that light from the fixture is unpolarized, that is, a mixture of 50% TE and 50% TM, and that the polaroid sunglasses are designed to filter out horizontally polarized light. Explain your reasoning.[†]

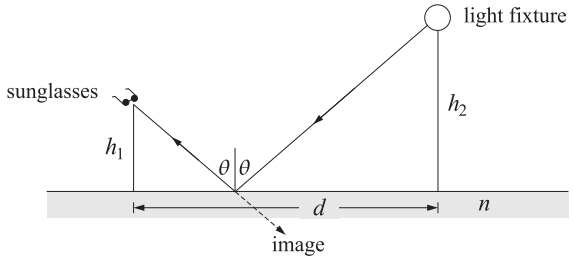

7.13 Prove the effective depth formulas (7.5.17) of the Goos-Hänchen effect by directly differentiating the reflection coefficient phases (7.8.3) with respect to k_x, noting that the lateral shift is $x_0 = 2d\psi/dk_x$ where ψ is either ψ_{TE} or ψ_{TM}.

7.14 First, prove Eq. (7.12.13) from Eqs. (7.12.11). Then, show the following relationships among the angles $\theta, \theta_r, \theta'$:

$$\frac{\tan(\theta/2)}{\tan(\theta'/2)} = \sqrt{\frac{1-\beta}{1+\beta}}, \quad \frac{\tan(\theta_r/2)}{\tan(\theta'/2)} = \sqrt{\frac{1+\beta}{1-\beta}}, \quad \frac{\tan(\theta_r/2)}{\tan(\theta/2)} = \frac{1-\beta}{1+\beta}$$

7.15 A TM plane wave is incident obliquely on a moving interface as shown in Fig. 7.12.1. Show that the Doppler-shifted frequencies of the reflected and transmitted waves are still given by Eqs. (7.12.14) and (7.12.16). Moreover, show that the Brewster angle is given by:

$$\cos\theta_B = \frac{1 + \beta\sqrt{n^2+1}}{\beta + \sqrt{n^2+1}}$$

[†] See, H. A. Smith, "Measuring Brewster's Angle Between Classes," *Physics Teacher*, Febr. 1979, p.109.